

Supplementary Information

Discovery of gargantulides B and C, new 52-membered macrolactones from *Amycolatopsis* sp. Complete absolute stereochemistry of the gargantulide family

Daniel Carretero-Molina,^{‡a} Francisco Javier Ortiz-López,*^{‡a} Tetiana Gren,^{‡b} Daniel Oves-Costales,^a Jesús Martín,^a Fernando Román-Hurtado,^a Tue Sparholt Jørgensen,^b Mercedes de la Cruz,^a Caridad Díaz,^a Francisca Vicente,^a Kai Blin,^b Fernando Reyes,^a Tilmann Weber*^b and Olga Genilloud*^a

^a Fundación MEDINA, Centro de Excelencia en Investigación de Medicamentos Innovadores en Andalucía, Avda. del Conocimiento 34, 18016 Armilla (Granada), Spain

^bThe Novo Nordisk Foundation Center for Biosustainability, Technical University of Denmark, Kemitorvet building 220, 2800 Kgs. Lyngby, Denmark

*Correspondence should be addressed to F.J.O-L (javier.ortiz@medinaandalucia.es), T.W. (tiwe@biosustain.dtu.dk) and O.G (olga.genilloud@medinaandalucia.es)

Table of Contents

Experimental section	3
General experimental procedures	3
Strain isolation, identification and fermentation.....	3
Isolation of gargantulides B (1) and C (2)	3
Characterization data of 1 and 2	4
Absolute configurations of the non-amino sugars present in 1 and 2	4
Genome sequence alignments	4
Antimicrobial bioassays.....	5
Supplementary data.....	6
Figure S1. Bioassay-guided isolation of gargantulides B (1) and C (2)	6
Figure S2. UV (DAD) and ESI-TOF spectrum of gargantulide B (1)	7-9
Figure S3. UV (DAD) and ESI-TOF spectrum of gargantulide C (2)	10-12
Table S1. ^1H NMR and ^{13}C NMR (CD_3OD) data of gargantulides B (1) and C (2)	13-15
Figure S4. 1D/2D NMR spectra of gargantulide B (1).....	16-27
Figure S5. 1D/2D NMR spectra of gargantulide C (1).....	28-39
Figure S6. Key COSY, TOCSY, HSQC-TOCSY and HMBC correlations observed for 2	40
Figure S7. LC-HRMS co-detection of gargantulides A (3), B (1) and C (2)	41
Table S2. antiSMAHS results	42
Table S3. Putative functions of genes in <i>gar</i> BGC	44
Table S4. Prediction of activity and stereochemistry of AT, KR, ER and DH domains from bioinformatics analysis. Stereochemical outcomes for gargantulides B and C.....	47
Figure S8. Extracted amino acid sequence alignments of AT, KR, DH and ER domains.....	48
Supplementary note: Biosynthesis of amino sugar maG	49
Table S5. Levels of identity and similarity of the putative <i>N</i> -Methyltransferase HUW46_03188 from CA-230715 to other known <i>N</i> -Methyltransferases	50
Table S6. Identified genes encoding for putative glucose-1-phosphate thymidyltransferase and dTDP-glucose 4,6-dehydratase in the genome of CA-230715	50
Figure S9. Proposed biosynthetic pathway for the unusual amino sugar 3,6-deoxy-3-methylamino glucose (maG)	50
Figure S10. Bioinformatics assignments of the absolute configurations for the gargantulides polyketide aglycon. Comparison with the absolute configurations previously reported for gargantulide A	51
Figure S11. Determination of the relative configuration of the C-55 to C-57 stereocluster for gargantulide B (1)	52
Figure S12. Determination of the relative configuration of the C-6–C-7 stereocluster for gargantulide B (1).	55
Figure S13. Determination of the relative configuration of the C-10–C-12 stereocluster for gargantulide B (1)	56
Figure S14. Determination of the relative configuration of the C-17(R)–C-18(R) stereocluster for gargantulide (1)	58
Figure S15. Determination of the absolute configuration of the non-amino sugars present in gargantulides B (1) and C (2)	59
Table S9. Antibacterial and antifungal activities of 1 and 2	61
Supplementary references	62

Experimental section

General experimental procedures: Optical rotations were measured on a Jasco P-2000 polarimeter. IR spectra were recorded with a JASCO FT/IR-4100 spectrometer equipped with a PIKE MIRacle single reflection ATR accessory. NMR spectra were recorded on a Bruker Avance III spectrometer (500 and 125 MHz for ¹H and ¹³C NMR, respectively) equipped with a 1.7 mm TCI MicroCryoProbe. Chemical shifts were reported in ppm using the signals of the residual solvents as internal reference (δ_{H} 3.31 and δ_{C} 49.1 for CD₃OD). LC-UV-LRMS analysis were performed on an Agilent 1100 single quadrupole LC-MS system as previously described.¹ ESI-TOF and MS/MS spectra were acquired using a Bruker maXis QTOF mass spectrometer coupled to an Agilent Rapid Resolution 1200 LC. The mass spectrometer was operated in positive ESI mode. The instrumental parameters were 4 kV capillary voltage, drying gas flow of 11 L min⁻¹ at 200 °C, and nebulizer pressure of 2.8 bar. TFA-Na cluster ions were used for mass calibration of the instrument prior to sample injection. Pre-run calibration was done by infusion with the same TFA-Na calibrant. Semi-preparative HPLC separation was performed on a Gilson GX-281 322H2 with a semi-preparative reversed-phase column (Waters XBridge Phenyl, 10 x 150 mm, 5 µm). Acetone used for extraction was analytical grade. Solvents employed for isolation were all HPLC grade. Chemical reagents and standards were purchased from Sigma-Aldrich.

Strain isolation, identification and fermentation: The strain CA-230715 was isolated from a soil sample collected at a waterlogged forest in Central African Republic. Initial similarity-based search with the 16S rDNA sequence (1318nt) against the EzBioCloud database indicated that the strain is closely related to *Amycolatopsis minnesotensis* 32U-2(T) (98.71% identity, 91.6% completeness).

A 250 mL fermentation of the producing microorganism was obtained as follows: a seed culture of the strain was obtained by inoculating one 150 x 25 mm tube containing 14 mL of seed-medium (soluble starch 20 g/L, glucose 10 g/L, NZ Amine Type E 5 g/L, meat extract 3 g/L, peptone 5 g/L, yeast extract 5 g/L, calcium carbonate 1 g/L, pH 7) with 0.7 mL of freshly thawed inoculum stock of CA-230715. The tube was incubated at 28 °C, 70% relative humidity and 220 rpm for 5 days. The fresh inoculum thus generated was employed to inoculate two 250 mL conical flasks each containing 125 mL of APM9 medium (glucose 50 g/L, soluble starch 12 g/L, soy flour 30 g/L, CoCl₂·6H₂O 2 mg/L, calcium carbonate 7 g/L, pH 7). The flasks were incubated at 28 °C, 70% relative humidity and 220 rpm during 13 days before harvesting.

Isolation of gargantulides B (1) and C (2): The 250 mL culture broth was extracted with an equal volume of acetone under continuous shaking at 220 rpm for 1h. The mycelial debris was discarded by centrifugation at 9000 rpm and the filtered supernatant/acetone mixture (ca. 0.5 L) was concentrated to 0.25 L under a nitrogen stream. The aqueous crude extract was loaded onto a Sepabeads® SP207ss resin column and eluted using acetone/methanol (1:1). The resulting organic extract was chromatographed by semipreparative reverse-phase HPLC (Waters XBridge Phenyl, 10 x 150 mm, 5 µm; 3.6 mL/min, UV detection at 210 and 280 nm) with a linear gradient of CH₃CN/H₂O/0.1% trifluoroacetic acid (TFA), from 15 to 28% CH₃CN (0.1% TFA) over 15 min followed by an isocratic step of 28% CH₃CN (0.1% TFA) over 19 min , to yield gargantulides B (1, 2.1 mg, rt 22 min) and C (2, 1.7 mg, rt 24.5min) as white amorphous powders.

Characterization data:

Gargantulide B (1): $[\alpha]^{25}_{\text{D}} -28.3$ (*c* 0.33, MeOH); IR (ATR) cm^{-1} : 3343, 2934, 1674, 1456, 1428, 1379, 1201, 1134, 1068, 1023; (+)-ESI-TOFMS *m/z* 2392.4804 [$\text{M}+\text{H}]^+$ (calcd. for $\text{C}_{116}\text{H}_{219}\text{N}_2\text{O}_{47}^+$, 2392.4808), 1197.2455 [$\text{M}+2\text{H}]^{2+}$ (calcd. for $\text{C}_{116}\text{H}_{220}\text{N}_2\text{O}_{47}^{2+}$, 1197.2455), 798.4995 [$\text{M}+3\text{H}]^{3+}$ (calcd. for $\text{C}_{116}\text{H}_{221}\text{N}_2\text{O}_{47}^{3+}$, 798.4994); ^1H and ^{13}C NMR data see Table S1.

Gargantulide C (2): $[\alpha]^{25}_{\text{D}} -20.5$ (*c* 0.33, MeOH); IR (ATR) cm^{-1} : 3342, 2935, 1674, 1456, 1425, 1379, 1201, 1135, 1067, 1024; (+)-ESI-TOFMS *m/z* 2230.4286 [$\text{M}+\text{H}]^+$ (calcd. for $\text{C}_{110}\text{H}_{209}\text{N}_2\text{O}_{42}^+$, 2230.4280), 1116.2170 [$\text{M}+2\text{H}]^{2+}$ (calcd. for $\text{C}_{110}\text{H}_{210}\text{N}_2\text{O}_{42}^{2+}$, 1116.2191), 744.4808 [$\text{M}+3\text{H}]^{3+}$ (calcd. for $\text{C}_{110}\text{H}_{211}\text{N}_2\text{O}_{42}^{3+}$, 744.4818); ^1H and ^{13}C NMR data see Table S1.

Determination of the absolute configurations of the non-amino sugars present in gargantulides B and C: Compounds **1** and **2** (400 μg each) were separately dissolved in 0.1 mL of 1 N HCl and heated at 85 °C for 3.5 h in a sealed vial. The crude hydrolysates were evaporated to dryness under a nitrogen stream and each residue was dissolved in 100 μL of pyridine containing 0.5 mg of L-cysteine methyl ester hydrochloride and heated at 60 °C for 1 h. A 100 μL solution of *o*-tolyl isothiocyanate (0.5 mg) in pyridine was added to the mixture, which was heated at 60 °C for 1 h. Standard monosaccharides (D-glucose, D-mannose and D-arabinose) were treated in the same manner with both L- and D- forms of cysteine methyl ester hydrochloride separately. The reaction mixtures (20 μL) were diluted with 50 μL of methanol and analyzed by ESI LC/MS on an Agilent 1100 single Quadrupole LC/MS. Separations were carried out on a Waters XBridge C18 column (4.6 \times 150 mm, 5 μm), maintained at 40 °C. A mixture of two solvents, A (10% CH_3CN , 90% H_2O) and B (90% CH_3CN , 10% H_2O), both containing 1.3 mM trifluoroacetic acid and 1.3 mM ammonium formate, was used as the mobile phase under a linear gradient elution mode (isocratic 15% B for 25 min, 15-100% B in 0.1 min and then isocratic 100% B for 5 min) at a flow rate of 1.0 mL/min. Retention times (min) for the derivatized standard monosaccharides (with both L- and D- forms of cysteine methyl ester hydrochloride) present in **1** and **2** were: D-glucose + L-Cys/*o*-TolyINCS: 17.05, D-glucose + D-Cys/*o*-TolyINCS: 15.70, D-mannose + L-Cys/*o*-TolyINCS: 10.14, D-mannose + D-Cys/*o*-TolyINCS: 17.22, D-arabinose + L-Cys/*o*-TolyINCS: 20.41, D-arabinose + D-Cys/*o*-TolyINCS: 18.99. Retention times (min) for the observed peaks in the HPLC trace of the L-Cys/*o*-TolyINCS derivatized hydrolysis product of **1** were: D-glucose + L-Cys/*o*-TolyINCS: 17.11, D-mannose + L-Cys/*o*-TolyINCS: 10.10, D-arabinose + L-Cys/*o*-TolyINCS: 20.48. Retention times (min) for the observed peaks in the HPLC trace of the L-Cys/*o*-TolyINCS derivatized hydrolysis product of **2** were: D-glucose + L-Cys/*o*-TolyINCS: 17.10, D-mannose + L-Cys/*o*-TolyINCS: 10.10, D-arabinose + L-Cys/*o*-TolyINCS: 20.56.

Genome sequence alignments: The sequences of AT, KR, DH and ER domains were manually extracted from the genome sequence of CA-230715 and analyzed using Geneious 9.1.8 software platform.² The catalytic regions and regions valuable for the prediction of stereochemistry were identified as described in previous works.³⁻⁶ Multiple sequence alignments were run using MUSCLE Alignment function⁷ of Geneious, set to 8 maximum iterations. As a comparison, domains manually extracted from the erythromycin cluster of *S. erythraea* NRRL2338 were used.

Antimicrobial bioassays: Compounds **1** and **2** were tested in antimicrobial assays against the growth of the gram-negative bacteria *E. coli* ATCC 25922, *A. baumannii* MB5973, *K. pneumoniae* ATCC 700603 and *P. aeruginosa* MB5919 and against the gram-positive bacteria methicillin-resistant *S. aureus* (MRSA) MB5393, methicillin-susceptible *S. aureus* (MSSA) and Van-A vancomycin-resistant *Enterococcus* (VRE) following previously described methodologies.⁸⁻¹⁰

Compounds **1** and **2** were also evaluated for their antifungal activity and spectrum against the filamentous fungus *Aspergillus fumigatus* ATCC46645 following previously described methodologies⁸ and the yeast *Candida albicans* ATCC64124 as follows: a thawed stock inoculum suspension from cryovials was streaked onto Sabouraud dextrose agar (SDA) plates and incubated at 37 °C overnight to obtain isolated colonies. The single colonies were inoculated into 20 mL of RPMI 1640 medium (Sigma) in 250 mL Erlenmeyer flasks and were adjusted at 0.25-0.28 ODU (612 nm) and then diluted 1:10 in order to obtain the inoculum for assay. The variation of the growth was quantified by measuring absorbance (OD612nm) using the plate reader EnVision® Multilabel (Perkin Elmer) with two readings, one at initial time and other after that the plate was incubated at 37 °C for 20 hours.

Each compound was serially diluted in DMSO with a dilution factor of 2 to provide 10 concentrations starting at 128 µg/mL for all the assays. The MIC was defined as the lowest concentration of compound that inhibited ≥ 95% of the growth of a microorganism after overnight incubation. The Genedata Screener software (Genedata, Inc., Basel, Switzerland) was used to process and analyze the data and also to calculate the RZ' factor, which predicts the robustness of an assay.¹¹ In all experiments performed in this work the RZ' factor obtained was between 0.76 and 0.93

Supplementary data

Figure S1. Bioassay-guided isolation of gargantulides B (**1**) and C (**2**). Semipreparative HPLC-UV chromatogram (blue trace: 210 nm; orange trace: 280 nm)

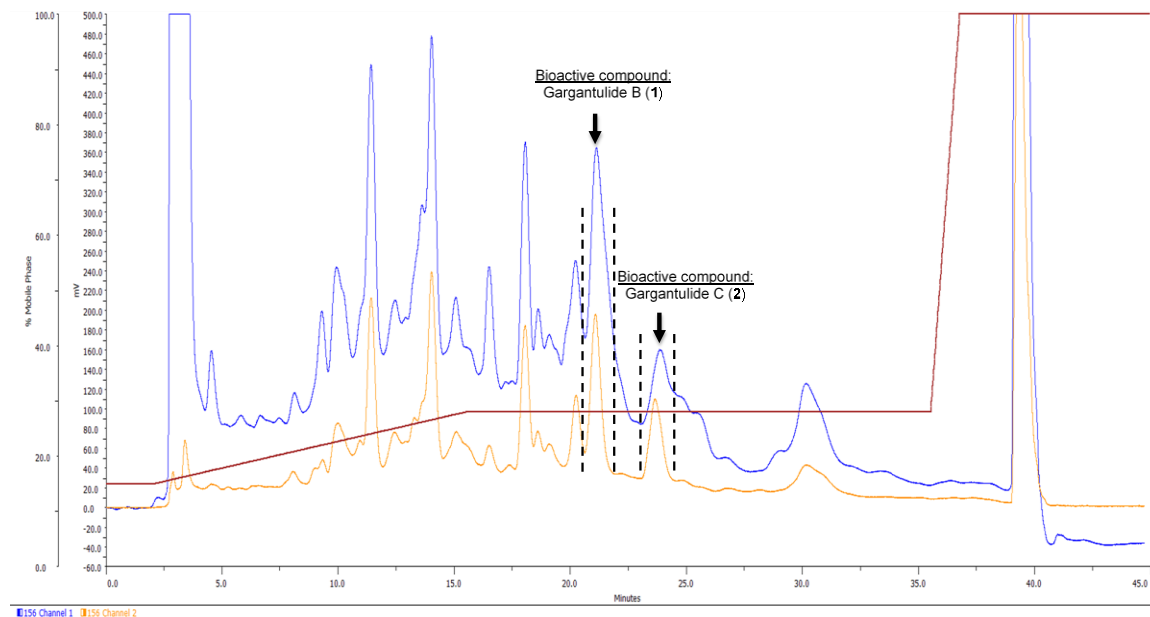
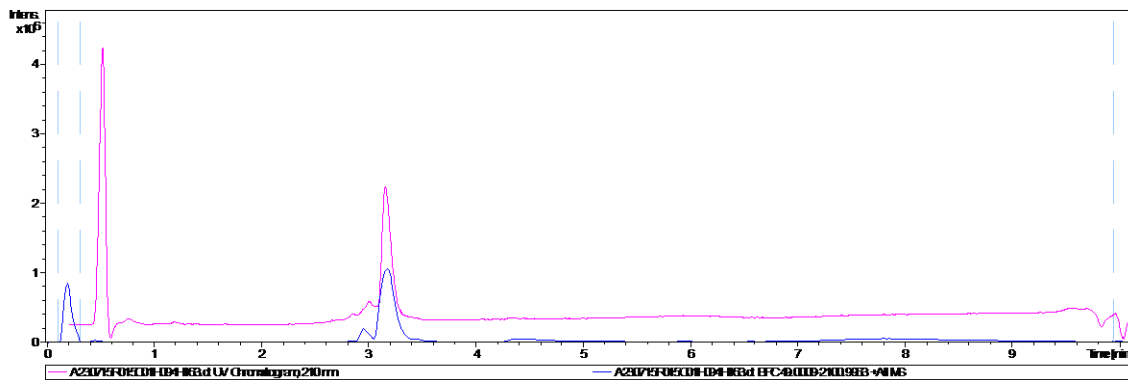
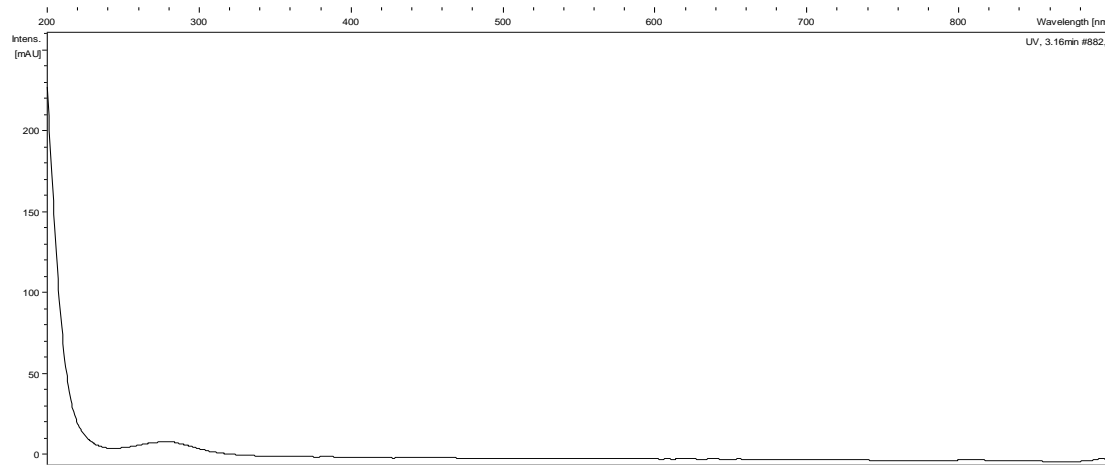


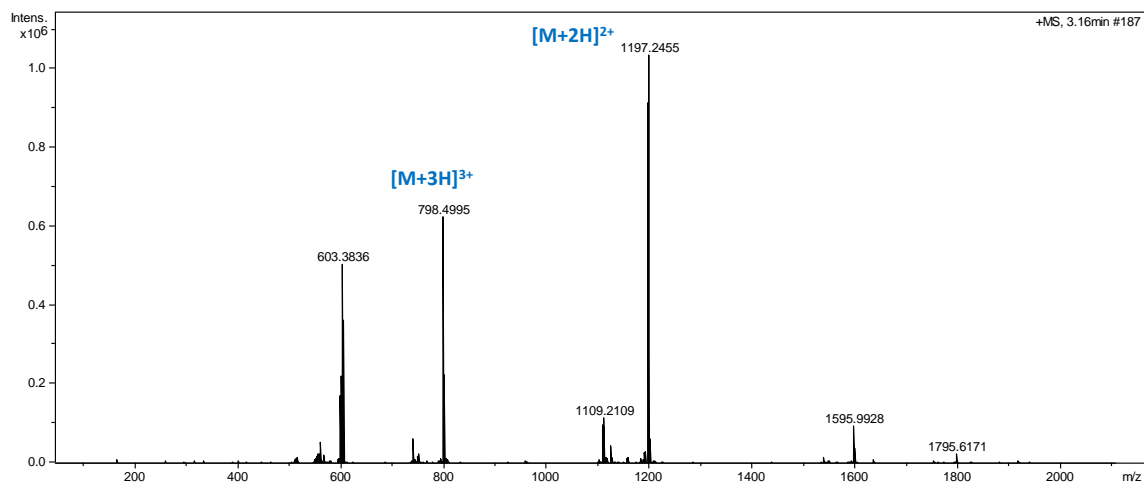
Figure S2. UV (DAD) and ESI(+) -TOF spectrum of gargantulide B (**1**)



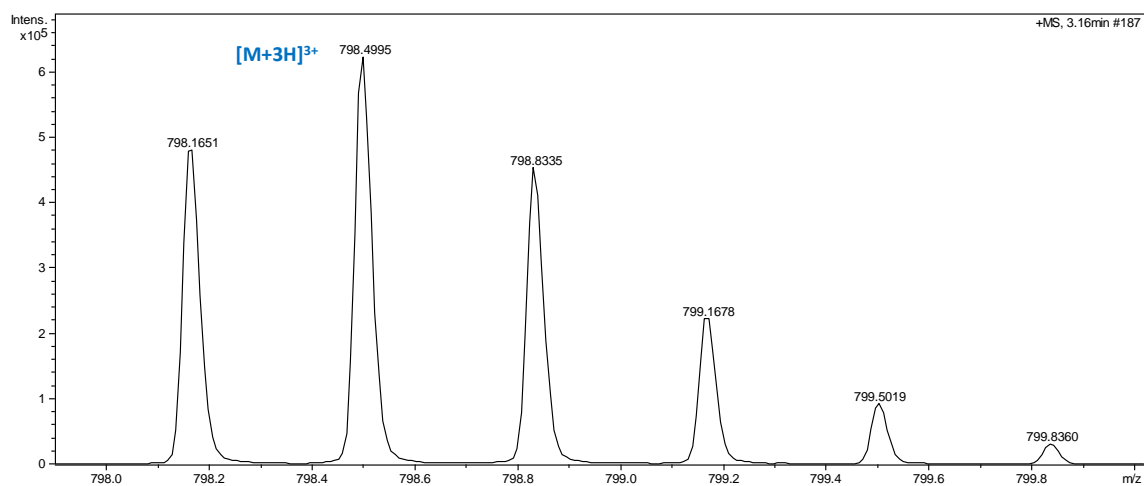
a) LC-UV-HRMS chromatogram (UV 210 nm: pink trace; MS+: blue trace) for **1**



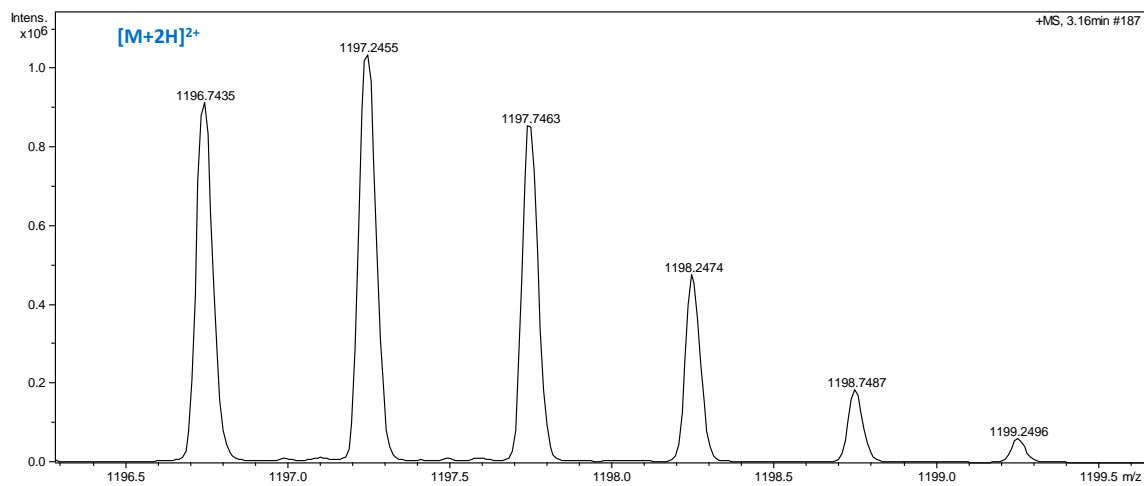
b) UV spectrum of **1**



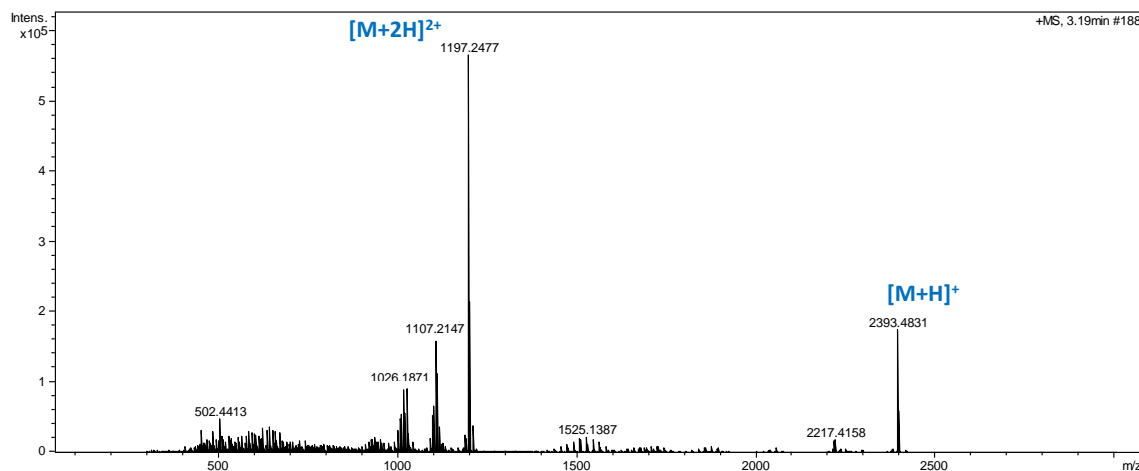
c) HRESIMS(+)TOF spectra (ISCID 0 eV) of **1** (overview)



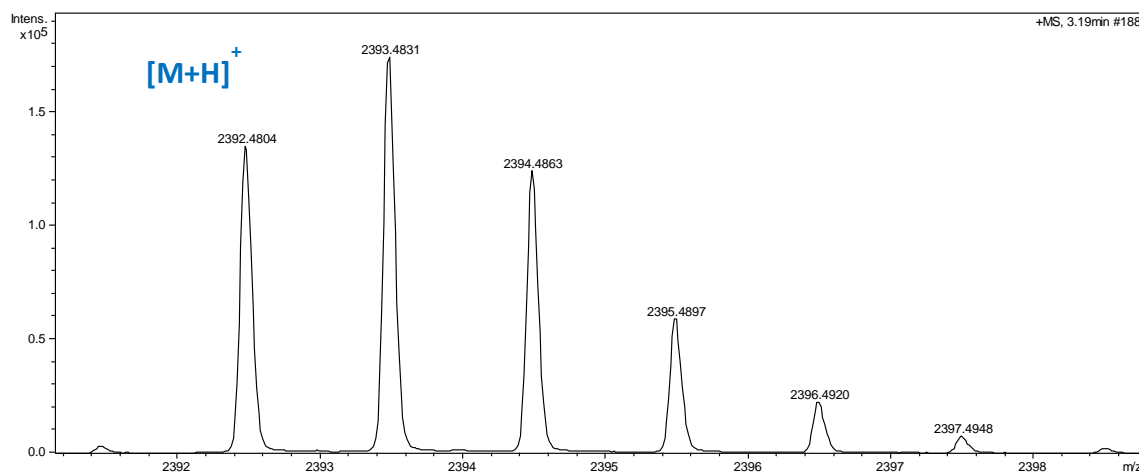
d) HRESIMS(+)TOF spectra (ISCID 0 eV) of **1**. Triply-charged adducts (zoom in region)



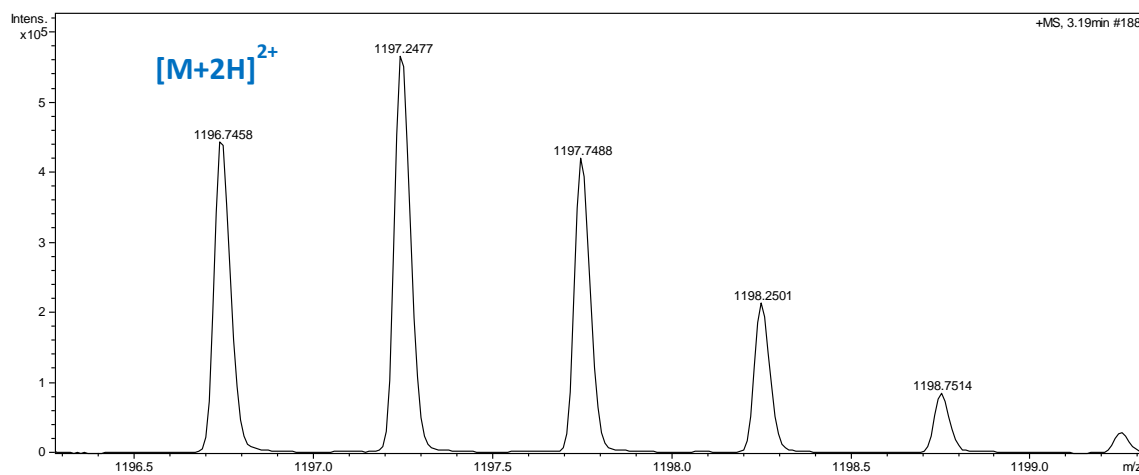
e) HRESIMS(+)TOF spectra (ISCID 0 eV) of **1**. Doubly-charged adducts (zoom in region)



f) . HRESIMS(+) -TOF spectra (ISCID 75 eV) of **1** (overview)

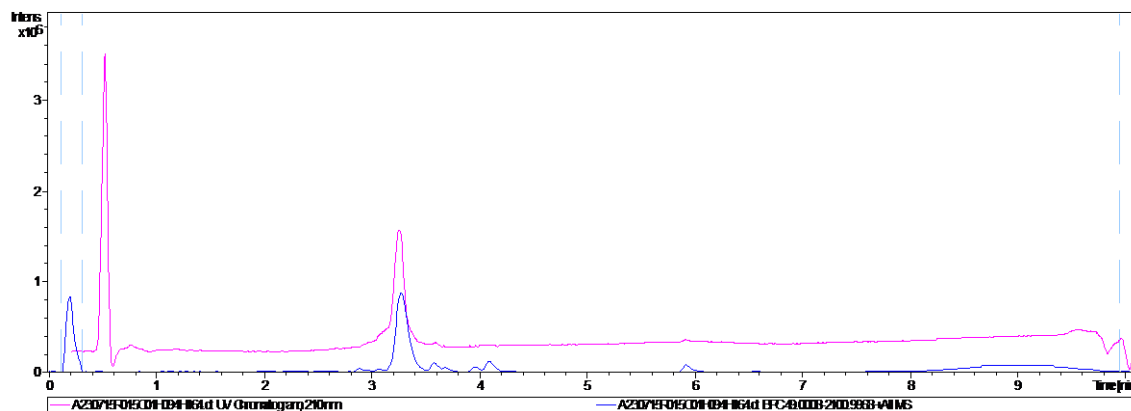


g) HRESIMS(+) -TOF spectra (ISCID 75 eV) of **1**. $[M+H]^+$ adduct (zoom in region)

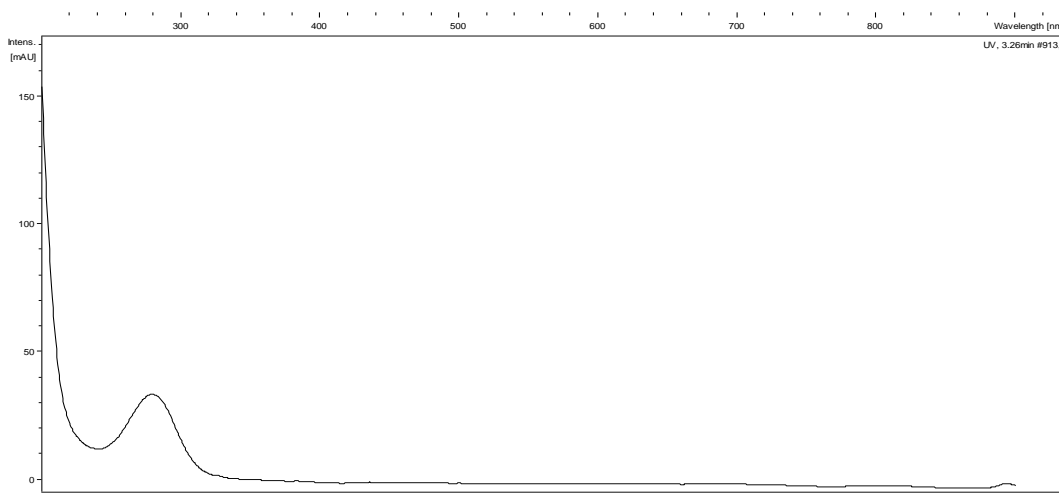


h) HRESIMS(+) -TOF spectra (ISCID 75 eV) of **1**. $[M+2H]^{2+}$ adduct (zoom in region)

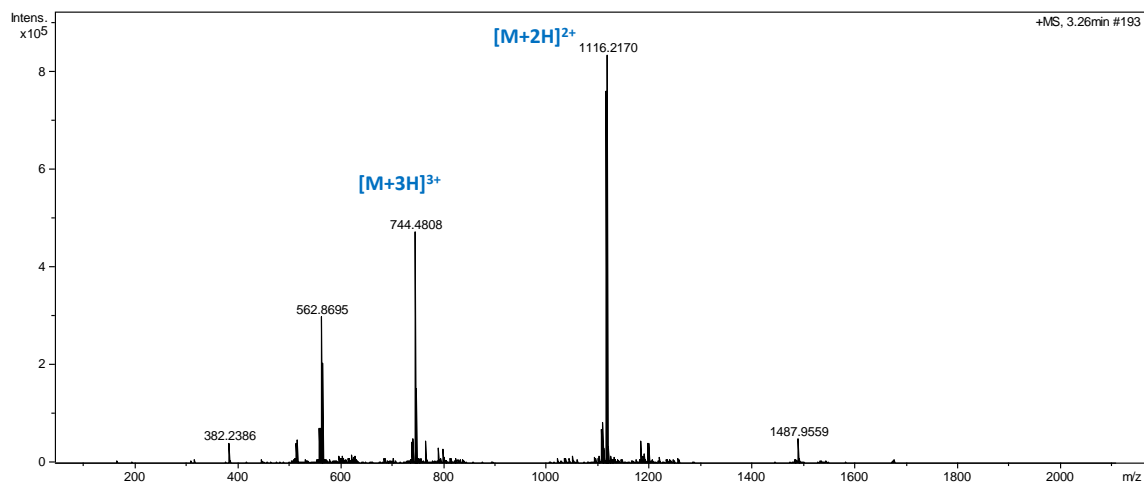
Figure S3. UV (DAD) and ESI(+) -TOF spectrum of gargantulide C (**2**)



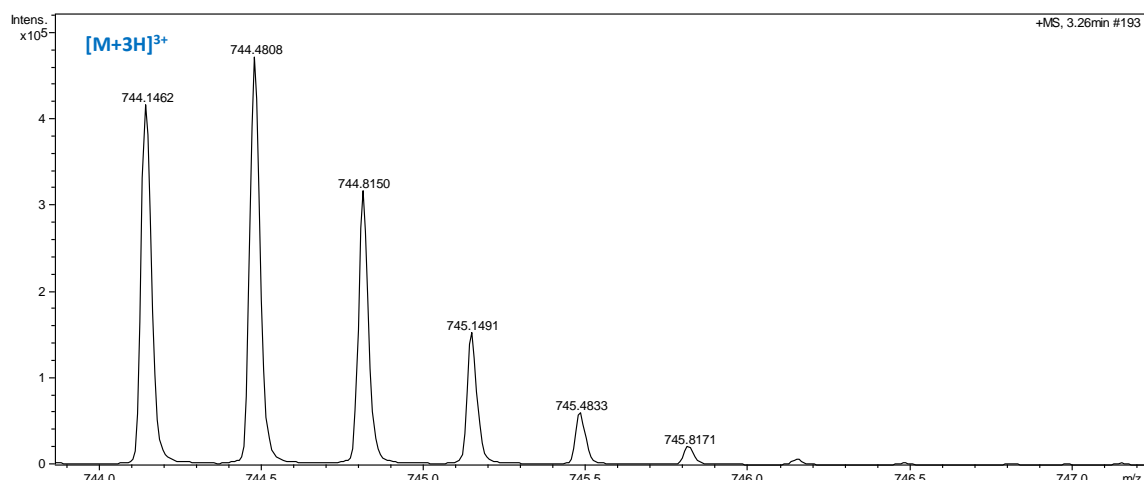
a) LC-UV-HRMS chromatogram (UV 210 nm: pink trace; MS+: blue trace) for **2**



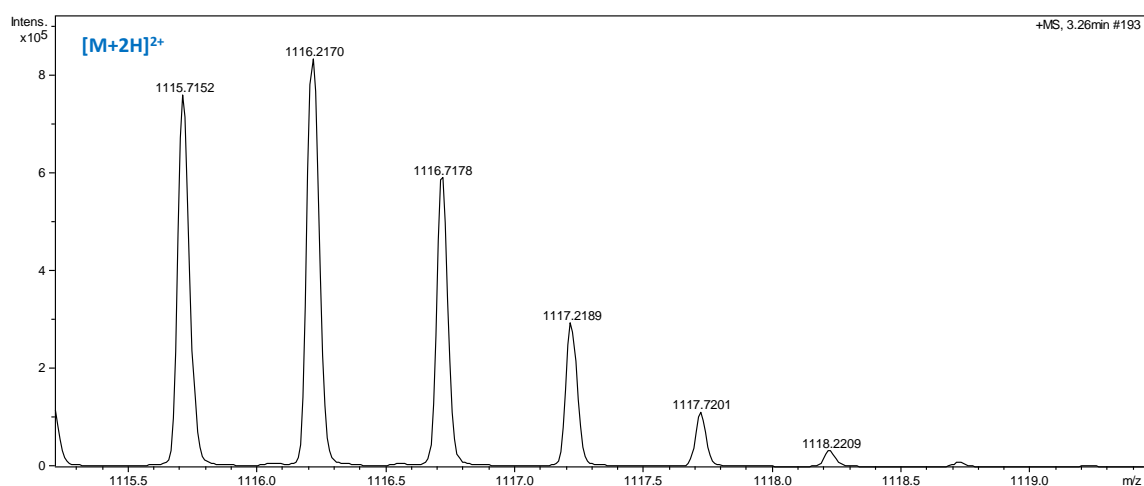
b) UV spectrum of **2**



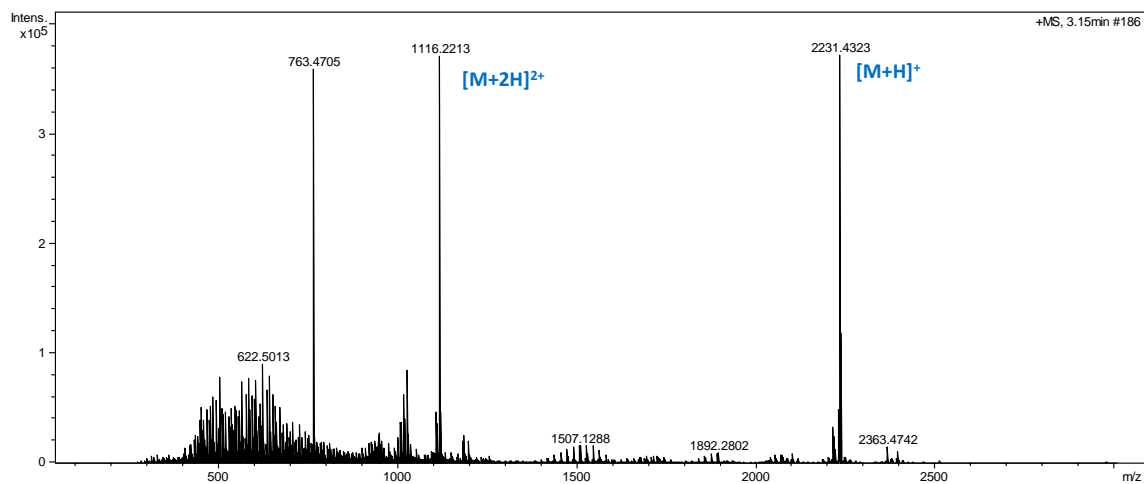
c) HRESIMS(+) -TOF spectra (ISCID 0 eV) of **2** (overview)



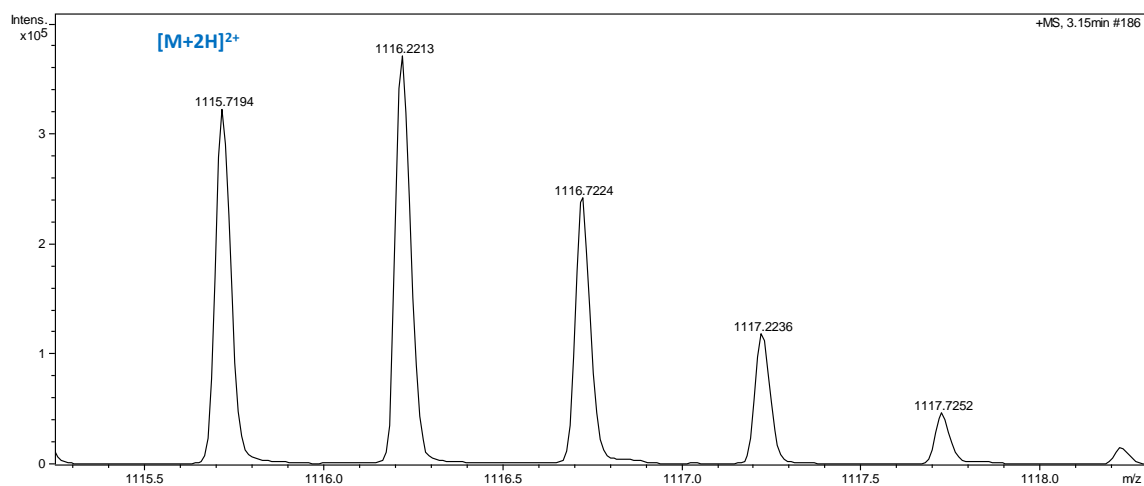
d) HRESIMS(+) -TOF spectra (ISCID 0 eV) of **1**. Triply-charged adducts (zoom in region)



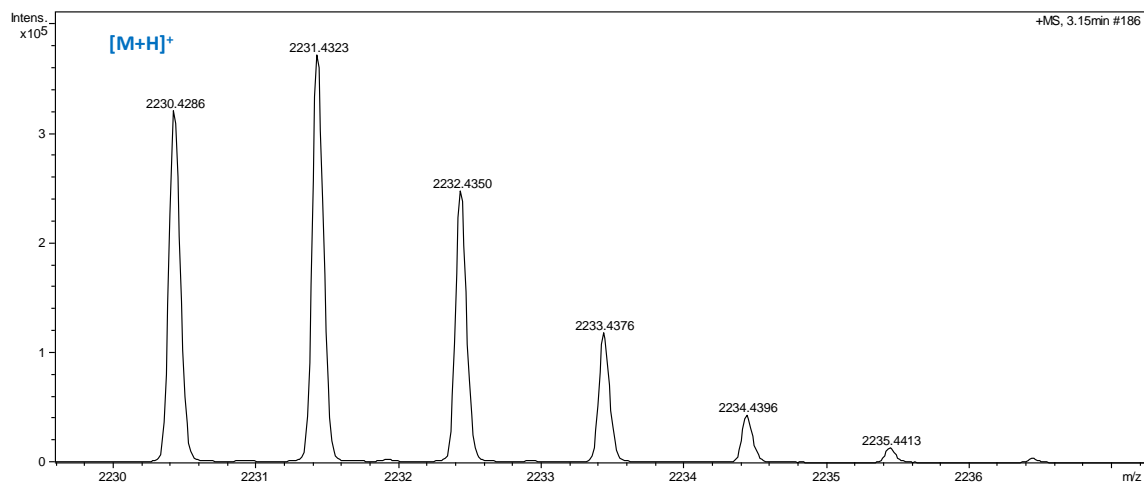
e) HRESIMS(+) -TOF spectra (ISCID 0 eV) of **1**. Doubly-charged adducts (zoom in region)



f) HRESIMS(+)TOF spectra (ISCID 75 eV) of **2** (overview)



g) HRESIMS(+)TOF spectra (ISCID 75 eV) of **2**. [M+H]⁺ adduct (zoom in region)



h) HRESIMS(+)TOF spectra (ISCID 75 eV) of **2**. [M+2H]²⁺ adduct (zoom in region)

Table S1. NMR spectroscopic data (CD_3OD) of **1** and **2**.

Gargantulide B (1)			Gargantulide C (2)		
nº	δ ^{13}C	δ ^1H (mult, J, Hz)	nº	δ ^{13}C	δ ^1H (mult, J, Hz)
1	175.3, C		1	175.3, C	
2	35.5, CH_2	2.36, m	2	35.6, CH_2	2.36, m
3	26.9, CH_2	1.61 ^a , m	3	26.9, CH_2	1.62 ^a , m
4	28.5 ^a , CH_2	1.32 ^a , m 1.43 ^a , m	4	28.5 ^a , CH_2	1.33 ^a , m 1.43 ^a , m
5	34.4 ^b , CH_2	1.19, m 1.50 ^a , m	5	34.4 ^a , CH_2	1.19, m 1.50 ^a , m
6	39.9, CH	1.48 ^a , m	6	39.9, CH	1.48 ^a , m
Me-6	14.6, CH_3	0.88 ^a , d (6.7)	Me-6	14.6, CH_3	0.89 ^a , d (6.7)
7	76.2, CH	3.42, m	7	76.2, CH	3.42, m
8	32.9, CH_2	1.46 ^a , m	8	32.9, CH_2	1.47 ^a , m
9	32.5, CH_2	1.38 ^a , m 1.46 ^a , m	9	32.5, CH_2	1.38 ^a , m 1.47 ^a , m
10	36.2, CH	1.65 ^a , m	10	36.2, CH	1.65 ^a , m
Me-10	13.4, CH_3	0.86 ^a , d (6.7)	Me-10	13.3, CH_3	0.86 ^a , d (6.7)
11	79.9, CH	3.12, dd (8.2, 3.2)	11	79.9, CH	3.12, dd (8.3, 3.2)
12	37.6, CH	1.55 ^a , m	12	37.6, CH	1.55, m
Me-12	16.8, CH_3	0.86 ^a , d (6.7)	Me-12	16.8, CH_3	0.86 ^a , d (6.8)
13	34.0, CH_2	1.10 ^a , m 1.75, m	13	34.1, CH_2	1.10 ^a , m 1.75, m
14	28.5 ^a , CH_2	1.48 ^a , m 1.22, m	14	28.5 ^a , CH_2	1.48 ^a , m 1.22, m
15	27.2, CH_2	1.33 ^a , m 1.57 ^a , m	15	27.1, CH_2	1.32 ^a , m 1.57 ^a , m
16	35.6, CH_2	1.35 ^a , m 1.57 ^a , m	16	35.9, CH_2	1.35 ^a , m 1.57 ^a , m
17	74.8, CH	3.67 ^a , m	17	74.8, CH	3.60 ^a , m
18	54.1, CH	2.69, dq (8.6, 6.9)	18	53.9, CH	2.68, dq (8.6, 7.0)
Me-18	13.5, CH_3	1.00, d (6.9)	Me-18	13.7, CH_3	0.99, d (6.8)
19	214.6, C		19	214.6, C	
20	49.9, CH_2	2.72, dd (17.2, 5.1) 2.89, dd (17.2, 7.8)	20	49.9, CH_2	2.80, dd (17.6, 6.9) 2.87, dd (17.6, 6.8)
21	74.1, CH	4.49, dd (7.8, 5.1)	21	74.1, CH	4.47, dd (6.9, 6.8)
22	146.8, C		22	146.7, C	
Me-22	12.6, CH_3	1.81 ^a , s	Me-22	11.9, CH_3	1.78 ^a , s
23	123.2, CH	5.21, d (10.3)	23	123.5, CH	5.22, d (10.3)
24	76.1, CH	4.76, dd (10.3, 8.1)	24	75.8, CH	4.81, dd (10.3, 8.0)
25	80.6, CH	3.56, dd (8.1, 3.5)	25	80.4, CH	3.64, dd (8.0, 2.8)
26	39.3, CH	1.69 ^a , m	26	39.4, CH	1.74 ^a , m
Me-26	11.9, CH_3	1.06, d (7.0)	Me-26	11.8, CH_3	1.06, d (7.2)
27	68.6, CH	4.22 ^a , m	27	68.8 ^a , CH	4.20 ^a , m
28	43.9, CH_2	1.27, m 1.59 ^a , m	28	43.9, CH_2	1.27, m 1.59 ^a , m
29	68.6 ^a , CH	3.64 ^a , m	29	68.8 ^a , CH	3.61 ^a , m
30	39.2 ^a , CH_2	1.40 ^a , m 1.44 ^a , m	30	39.2 ^a , CH_2	1.41 ^a , m 1.44 ^a , m
31	23.1, CH_2	1.53 ^a , m	31	23.2, CH_2	1.51 ^a , m
32	39.2 ^a , CH_2	1.48 ^a , m 1.52 ^a , m	32	39.2 ^a , CH_2	1.48 ^a , m 1.52 ^a , m
33	69.4, CH	3.84 ^a , m	33	69.4, CH	3.84 ^a , m

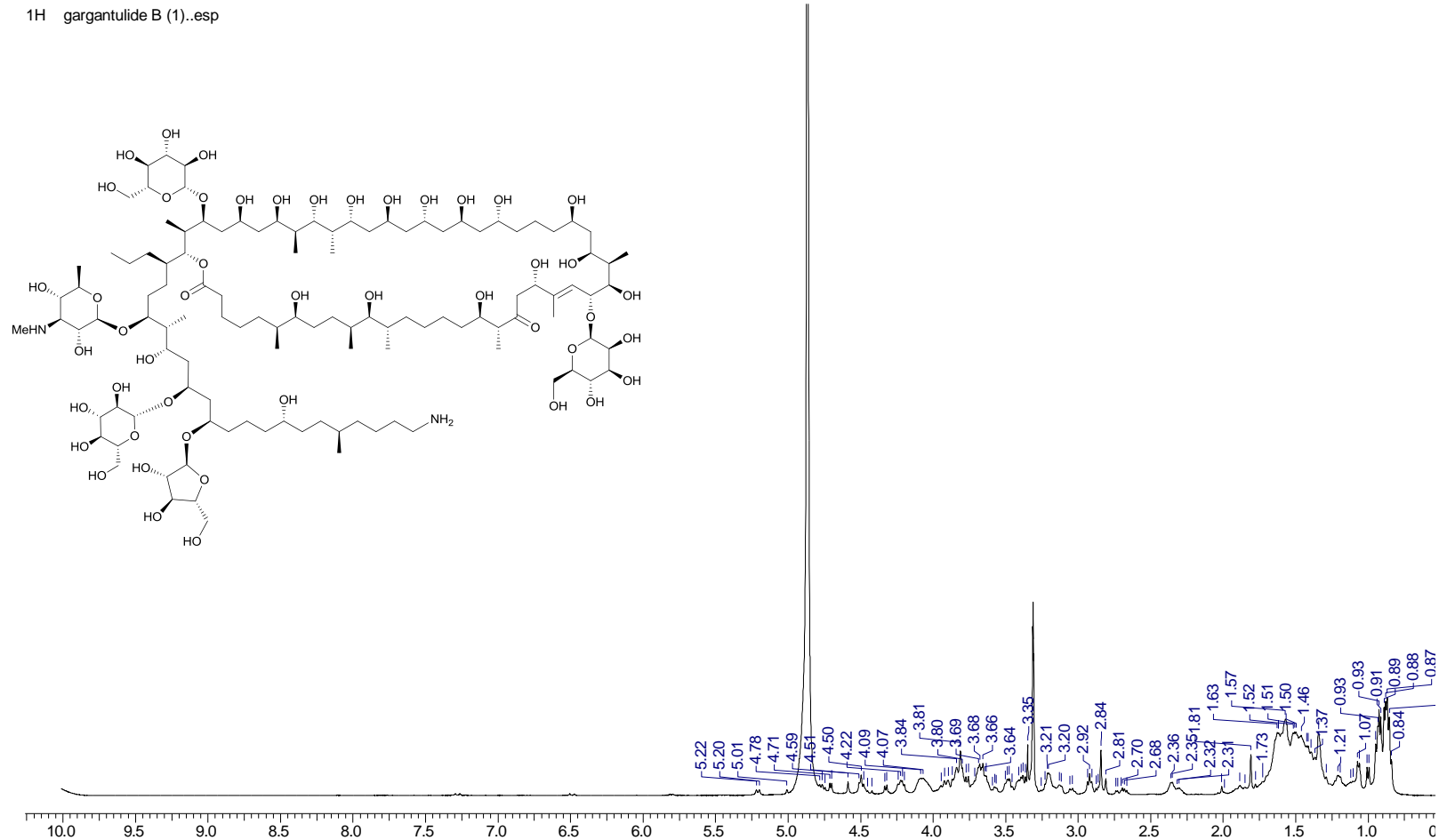
34	46.0 ^a , CH ₂	1.51 ^a , m 1.59 ^a , m	34	46.3 ^a , CH ₂	1.51 ^a , m 1.59 ^a , m
35	66.6, CH	4.10 ^a , m	35	66.6, CH	4.10 ^a , m
36	46.9 ^a , CH ₂	1.57 ^a , m	36	46.9 ^a , CH ₂	1.58 ^a , m
37	66.6 ^a , CH	4.10 ^a , m	37	66.6, CH	4.10 ^a , m
38	46.9 ^a , CH ₂	1.58 ^a , m	38	46.9 ^a , CH ₂	1.58 ^a , m
39	66.6 ^a , CH	4.08 ^a , m	39	66.6 ^a , CH	4.08 ^a , m
40	44.1, CH ₂	1.57 ^a , m 1.61 ^a , m	40	44.2, CH ₂	1.57 ^a , m 1.61 ^a , m
41	73.8, CH	4.04, m	41	73.8, CH	4.03, m
42	41.1, CH	1.63 ^a , m	42	40.9, CH	1.63 ^a , m
Me-42	6.9, CH ₃	0.95 ^a , d (6.8)	Me-42	6.8, CH ₃	0.95 ^a , d (6.9)
43	77.5, CH	3.80 ^a , m	43	77.5, CH	3.80 ^a , m
44	41.9, CH	1.67 ^a , m	44	41.9, CH	1.67 ^a , m
Me-44	10.8, CH ₃	0.84, d (6.9)	Me-44	10.8, CH ₃	0.84, d (6.8)
45	72.4, CH	4.23 ^a , m	45	72.4, CH	4.22 ^a , m
46	40.8, CH ₂	1.58 ^a , m	46	40.7, CH ₂	1.57 ^a , m
47	71.6, CH	4.06, m	47	71.6, CH	4.05, m
48	38.2, CH ₂	1.58 ^a , m 1.67 ^a , m	48	38.3, CH ₂	1.57 ^a , m 1.66 ^a , m
49	77.1, CH	3.69 ^a , m	49	77.1, CH	3.69 ^y , m
50	38.5, CH	2.30, m	50	38.5, CH	2.30, m
Me-50	10.8, CH ₃	0.93 ^a , d (6.9)	Me-50	10.7, CH ₃	0.93 ^a , d (6.9)
51	76.9, CH	4.88, m	51	77.0, CH	4.88, m
52	41.1, CH	1.52 ^a , m	52	41.1, CH	1.52 ^a , m
53	24.7, CH ₂	1.20 ^a , m 1.78 ^a , m	53	24.6, CH ₂	1.20 ^a , m 1.78 ^a , m
54	31.9, CH ₂	1.44 ^a , m 1.89, m	54	31.8, CH ₂	1.45 ^a , m 1.89, m
55	83.9, CH	3.68 ^a , m	55	83.8, CH	3.67 ^a , m
56	43.4, CH	1.73, m	56	43.3, CH	1.73, m
Me-56	10.7, CH ₃	0.94 ^a , d (6.9)	Me-56	10.8, CH ₃	0.94 ^a , d (7.0)
57	68.8, CH	4.19 ^a , m	57	68.8, CH	4.19 ^a , m
58	44.2, CH ₂	1.39 ^a , m 1.67 ^a , m	58	44.6, CH ₂	1.41 ^a , m 1.67 ^a , m
59	77.0 ^a , CH	3.84 ^a , m	59	68.8, CH	3.61, m
60	46.0 ^a , CH ₂	1.58 ^a , m 1.63 ^a , m	60	46.0 ^a , CH ₂	1.58 ^a , m 1.63 ^a , m
61	77.0 ^a , CH	3.84 ^a , m	61	76.9, CH	3.83, m
62	38.7, CH ₂	1.53, m 1.41 ^a , m	62	38.7, CH ₂	1.53, m 1.41 ^a , m
63	22.6, CH ₂	1.41 ^a , m 1.61 ^a , m	63	22.5, CH ₂	1.41 ^a , m 1.61 ^a , m
64	38.6, CH ₂	1.40 ^a , m 1.49 ^a , m	64	38.5, CH ₂	1.40 ^a , m 1.49 ^a , m
65	73.1 ^a , CH	3.50 ^a , m	65	72.9 ^a , CH	3.50 ^a , m
66	36.1, CH ₂	1.36, m 1.51 ^a , m	66	36.1, CH ₂	1.35 ^a , m 1.51 ^a , m
67	34.2 ^a , CH ₂	1.10 ^a , m 1.50 ^a , m	67	34.2 ^a , CH ₂	1.11 ^a , m 1.50 ^a , m
68	34.2 ^a , CH	1.42 ^a , m	68	34.2 ^a , CH	1.43 ^a , m
Me-68	20.2, CH ₃	0.92 ^a , d (6.5)	Me-68	20.2, CH ₃	0.92 ^a , d (6.5)
69	37.7, CH ₂	1.20 ^a , m 1.39 ^a , m	69	37.7, CH ₂	1.19 ^a , m 1.38 ^a , m
70	25.1, CH ₂	1.39 ^a , m	70	25.1, CH ₂	1.39 ^a , m

		1.45 ^a , m			1.44 ^a , m
71	29.1, CH ₂	1.64 ^a , m	71	29.1, CH ₂	1.64 ^a , m
72	40.9, CH ₂	2.92, t (7.7)	72	40.9, CH ₂	2.92, t (7.7)
1'	34.4 ^b , CH ₂	1.09, m	1'	34.4 ^a , CH ₂	1.10, m
		1.36 ^a , m			1.35 ^a , m
2'	21.6, CH ₂	1.29, m	2'	21.6, CH ₂	1.28, m
		1.48 ^a , m			1.48 ^a , m
3'	14.9, CH ₃	0.89 ^a , t (7.2)	3'	14.9, CH ₃	0.89 ^a , t (7.2)
Man-1	97.1, CH	4.58, br s	Man-1	96.9, CH	4.58, br s
Man-2	73.1 ^a , CH	3.81 ^a , m	Man-2	73.1 ^a , CH	3.81 ^a , m
Man-3	75.4, CH	3.47, dd (9.5, 3.2)	Man-3	75.4, CH	3.47, dd (9.5, 3.2)
Man-4	68.6 ^a , CH	3.67 ^a , t (9.5)	Man-4	68.8 ^a , CH	3.61 ^a , t (9.5)
Man-5	78.5, CH	3.17, m	Man-5	78.6, CH	3.15, m
Man-6	62.8 ^a , CH ₂	3.75 ^{m'} , m	Man-6	62.9 ^a , CH ₂	3.74 ^{m'} , m
		3.87 ^a , m			3.87 ^a , m
Glc-1	102.4, CH	4.20 ^a , d (7.8)	Glc-1	102.4, CH	4.22 ^a , d (7.8)
Glc-2	74.9, CH	3.20 ^a , m	Glc-2	74.9, CH	3.20 ^a , m
Glc-3	78.2, CH	3.33 ^a , m	Glc-3	78.2, CH	3.33 ^a , m
Glc-4	71.8, CH	3.32 ^a , m	Glc-4	71.7, CH	3.33 ^a , m
Glc-5	78.3 ^a , CH	3.21 ^a , m	Glc-5	78.3 ^a , CH	3.21 ^a , m
Glc-6	62.8 ^a , CH ₂	3.68 ^a , m	Glc-6	62.9 ^a , CH ₂	3.68 ^a , m
		3.84 ^a , m			3.85 ^a , m
maG-1	104.4, CH	4.46, d (7.5)	maG-1	104.7, CH	4.45, d (7.4)
maG-2	70.5, CH	3.50 ^a , dd (10.4, 7.5)	maG-2	70.6, CH	3.49 ^a , dd (10.6, 7.4)
maG-3	66.1, CH	3.06, t (10.4)	maG-3	66.0, CH	3.05, t (10.6)
maG-4	71.5, CH	3.39 ^a , dd (10.4, 8.7)	maG-4	71.5, CH	3.38 ^a , dd (10.6, 8.8)
maG-5	74.4, CH	3.40, dq (8.7, 6.2)	maG-5	74.3, CH	3.41, dq (8.8, 6.1)
maG-6	18.4, CH ₃	1.34 ^a , d (6.2)	maG-6	18.4, CH ₃	1.33 ^a , d (6.1)
N-Me	31.1, CH ₃	2.81, br s	N-Me	31.1, CH ₃	2.81, br s
Ara-1	108.3, CH	5.01, d (1.6)	Ara-1	108.2, CH	5.01, d (1.5)
Ara-2	83.9, CH	3.96, dd (3.9, 1.6)	Ara-2	83.9, CH	3.96, dd (3.9, 1.5)
Ara-3	78.7, CH	3.86 ^a , m	Ara-3	78.6, CH	3.85 ^a , m
Ara-4	85.4, CH	3.98, m	Ara-4	85.4, CH	3.98, m
Ara-5	63.2, CH ₂	3.64 ^a , m	Ara-5	63.2, CH ₂	3.64 ^a , m
		3.74 ^a , m			3.75 ^a , m
Glc'-1	103.9, CH	4.33, d (7.6)			
Glc'-2	75.2, CH	3.21 ^a , m			
Glc'-3	78.3 ^a , CH	3.37 ^a , m			
Glc'-4	72.5, CH	3.23 ^a , m			
Glc'-5	78.3 ^a , CH	3.21 ^a , m			
Glc'-6	63.4, CH ₂	3.93, m			
		3.70 ^a , m			

^a Overlapping with other isochronous ¹³C-NMR / ¹H-NMR signals.

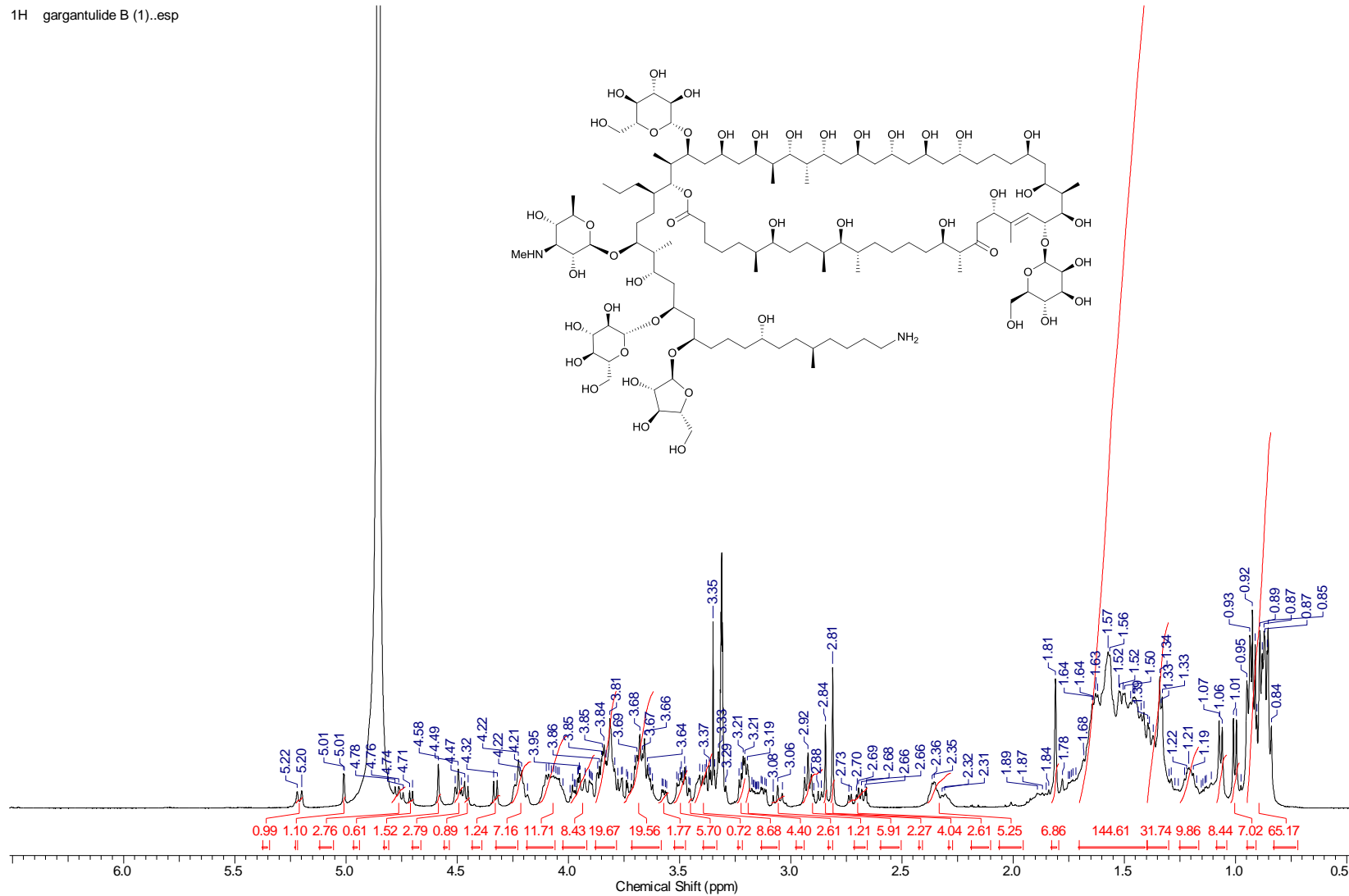
* No multiplicity is given (m) for ¹H-NMR signals for which coupling constants (*J*s) could not be measured directly in ¹H or JRES spectra nor determined from HSQC traces. The assignments were supported by HSQC, HMBC, TOCSY and HSQC-TOCSY.

Figure S4. 1D/2D NMR spectra of gargantulide B (**1**)



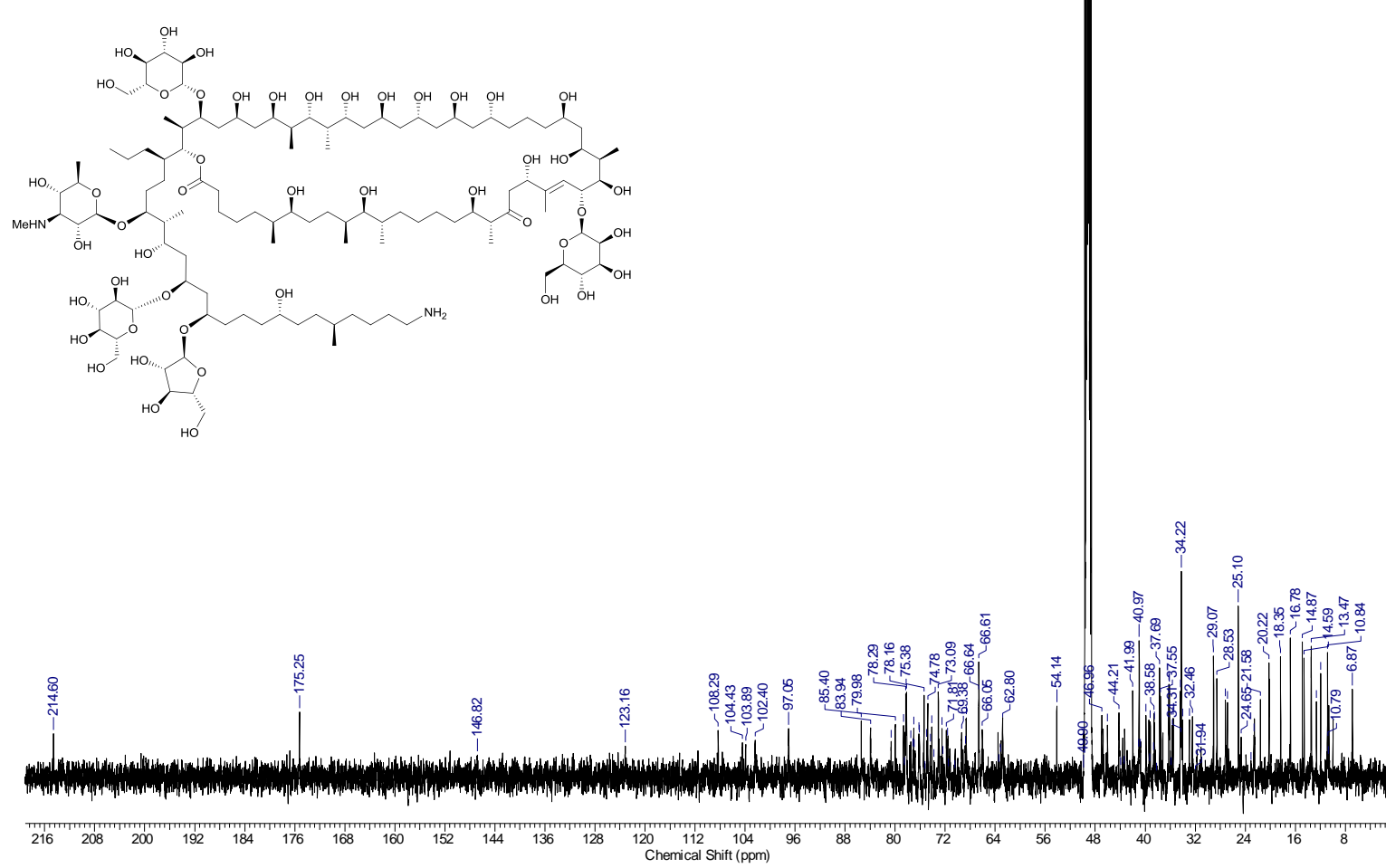
a) ¹H NMR spectrum (CD₃OD, 500 MHz) of **1**. Full scale (0-10 ppm)

1H gargantulide B (1)..esp



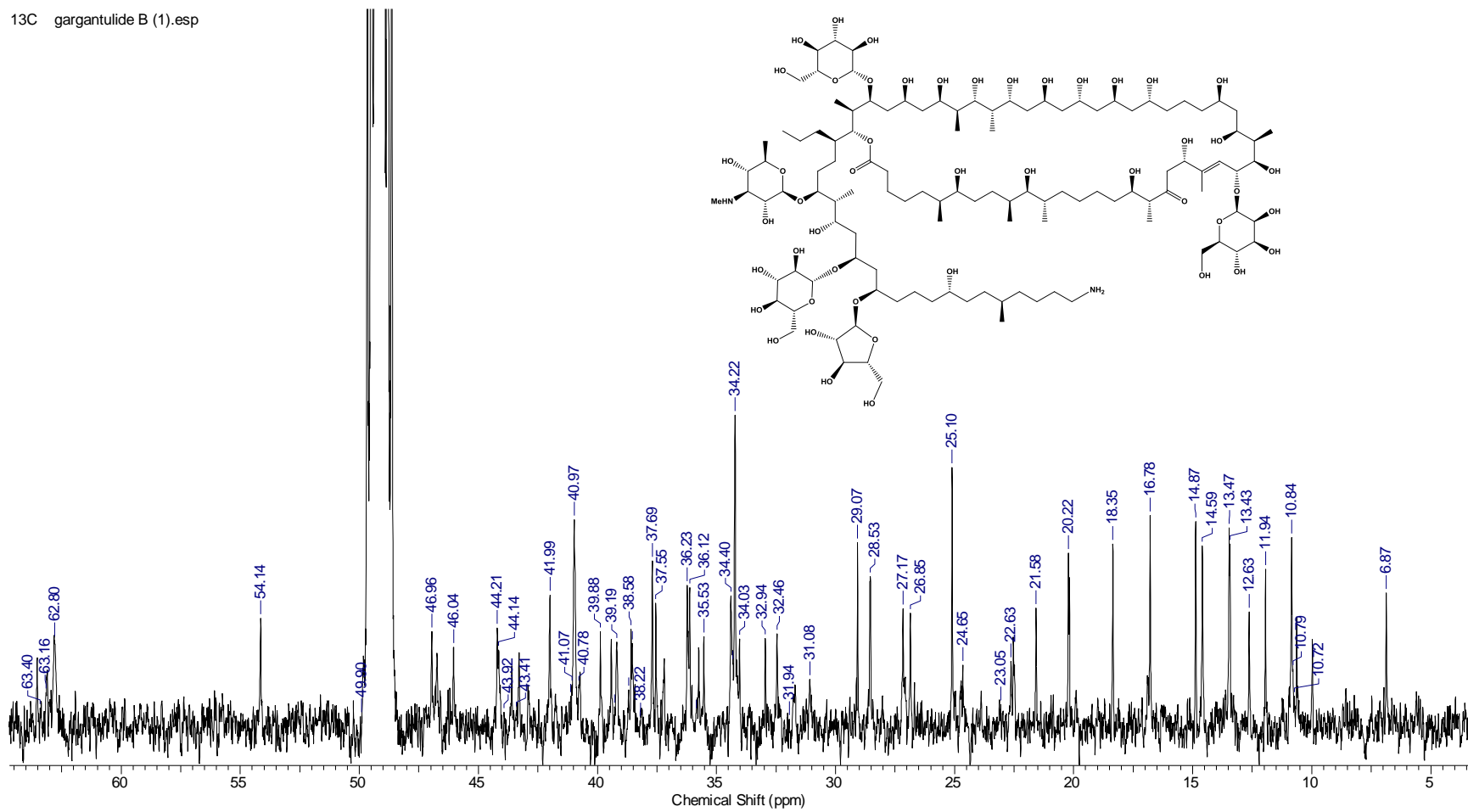
b) ^1H NMR spectrum (CD_3OD , 500 MHz) of **1**. Expansion between 0 and 7 ppm showing integral values

13C gargantulide B (1).esp



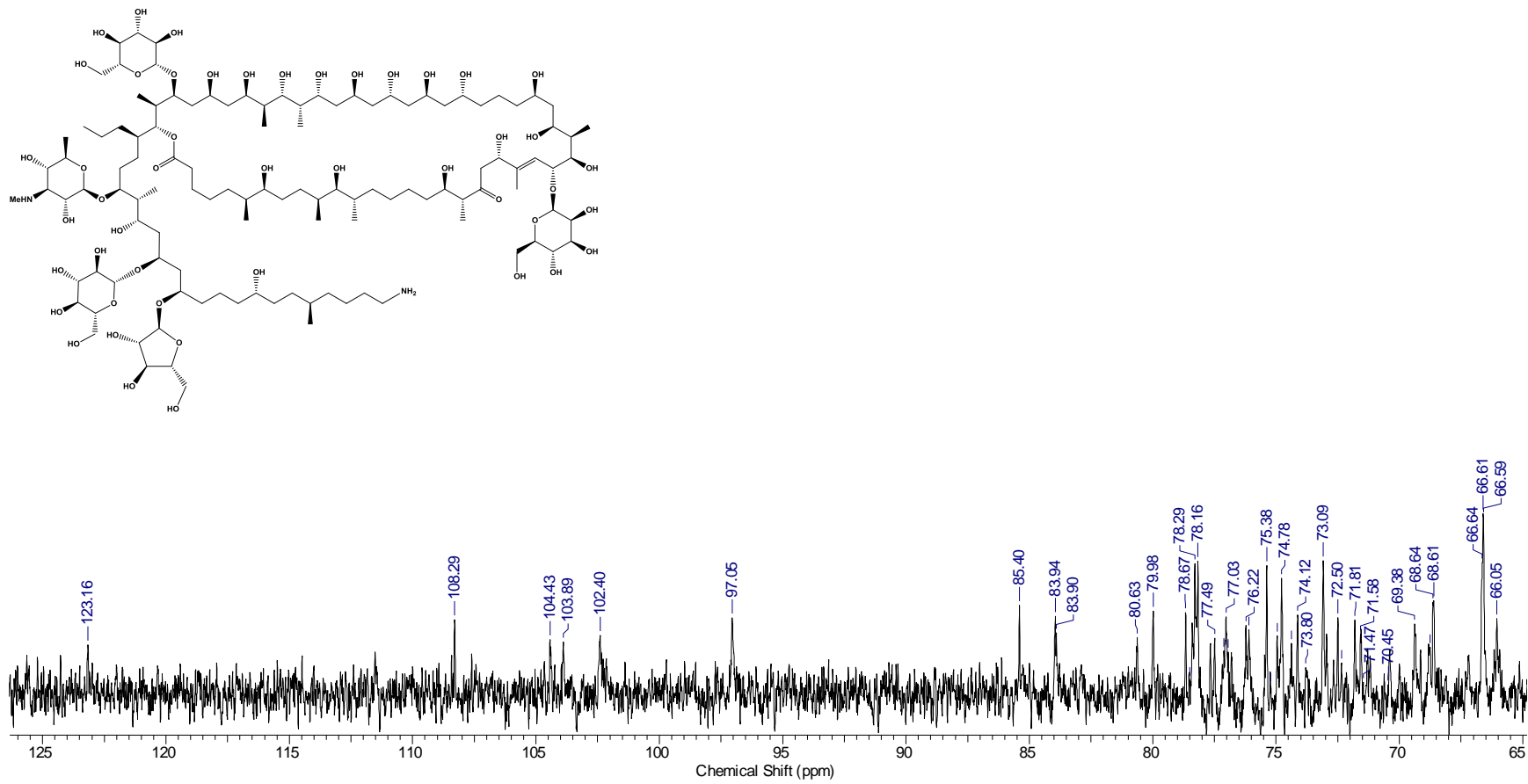
c) ^{13}C NMR spectrum (CD_3OD , 125 MHz) of 1

13C gargantulide B (1).esp

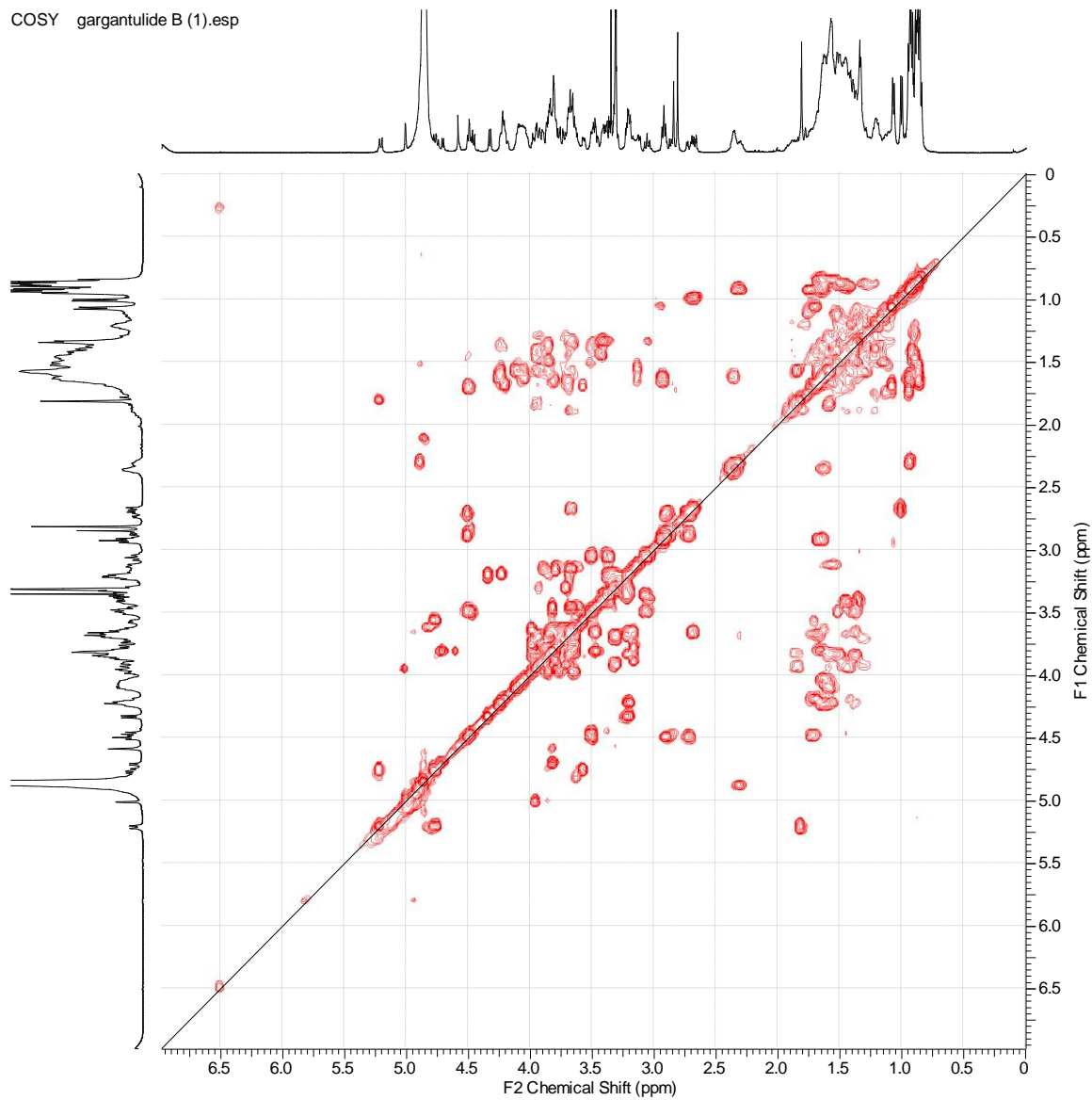


d) ¹³C NMR spectrum (CD₃OD, 125 MHz) of **1**. Expansion between 0 and 65 ppm

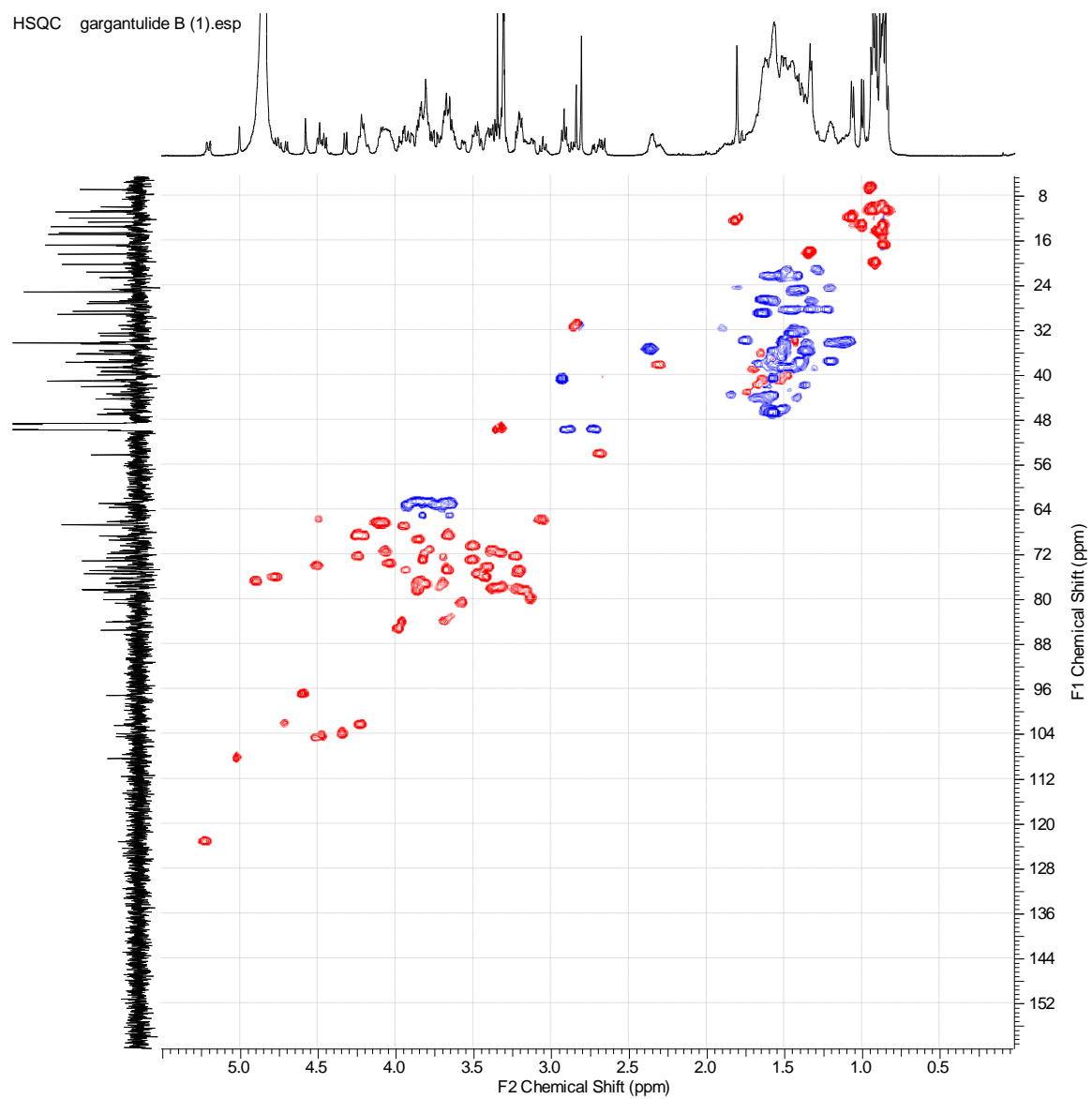
13C gargantulide B (1).esp



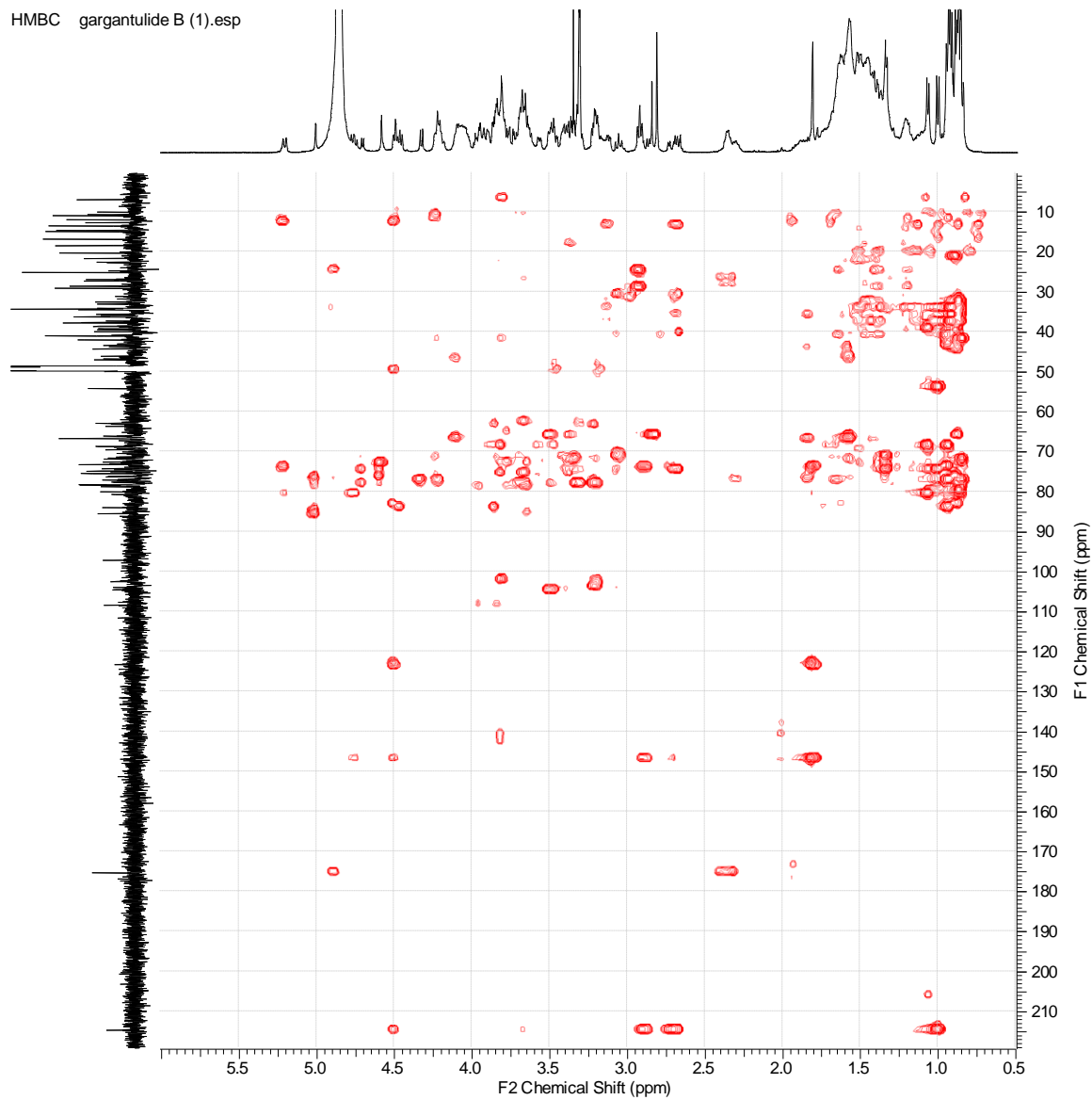
e) ^{13}C NMR spectrum (CD_3OD , 125 MHz) of **1**. Expansion between 65 and 125 ppm



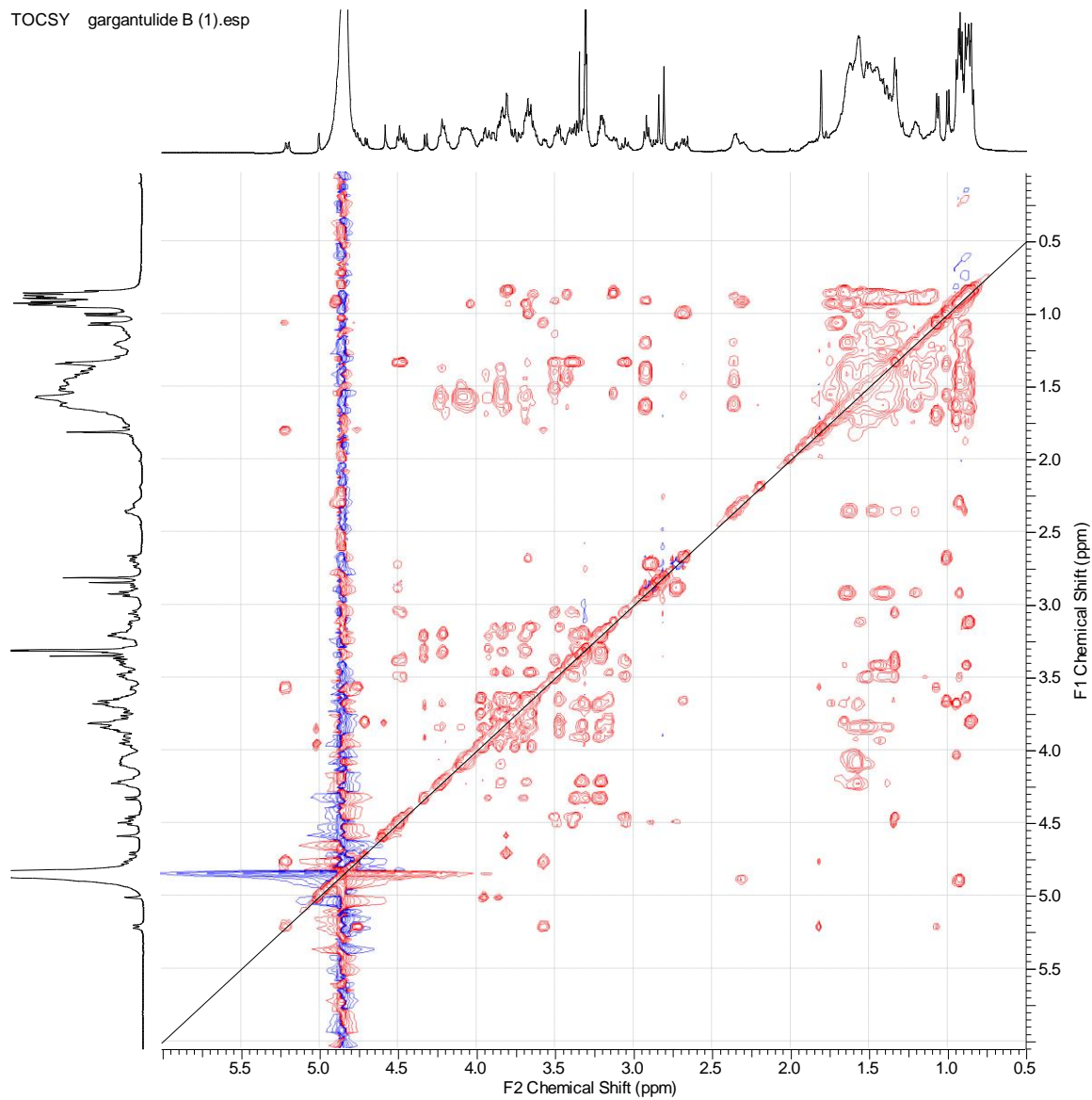
f) COSY spectrum of **1**



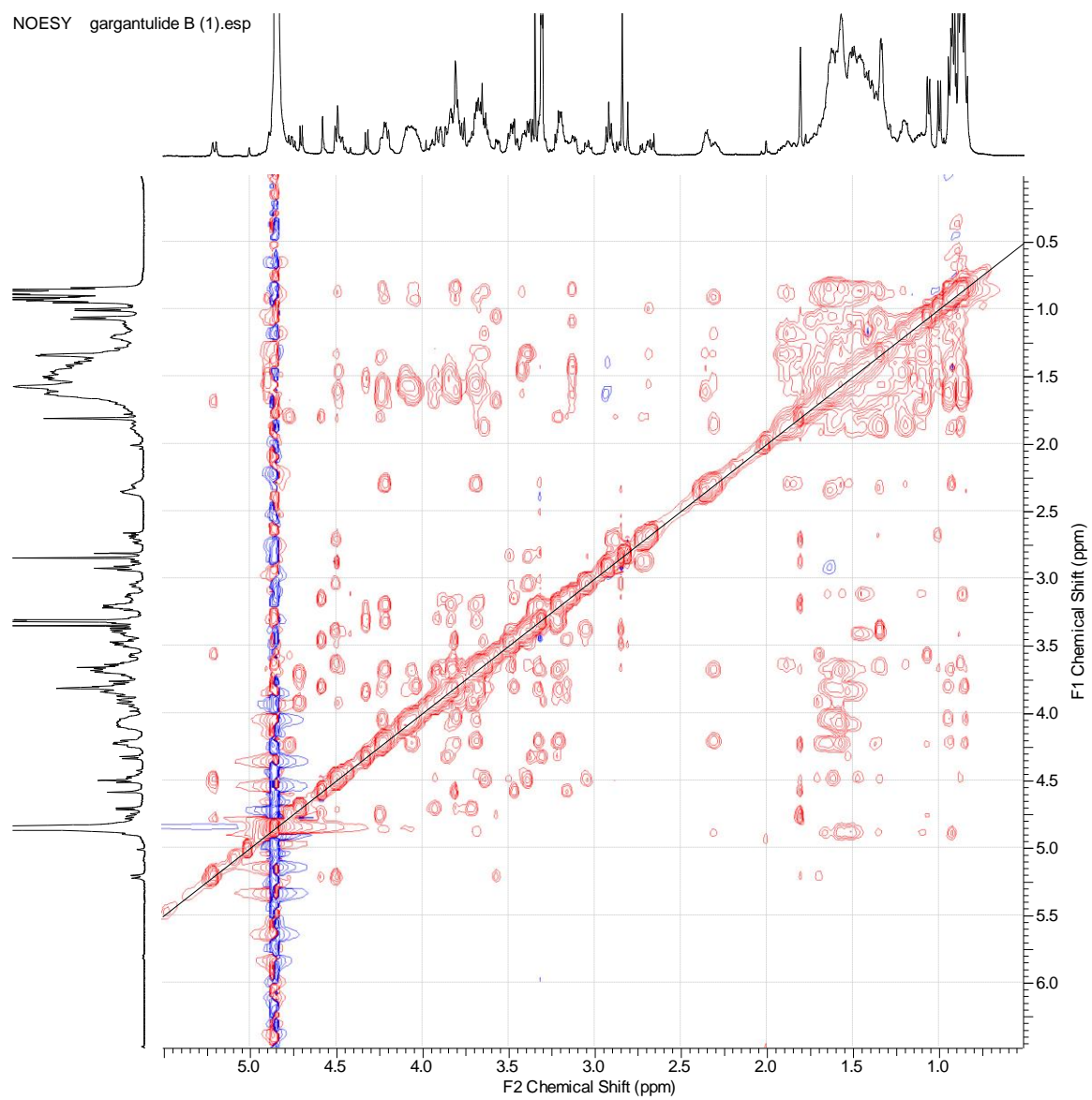
g) HSQC spectrum of **1**



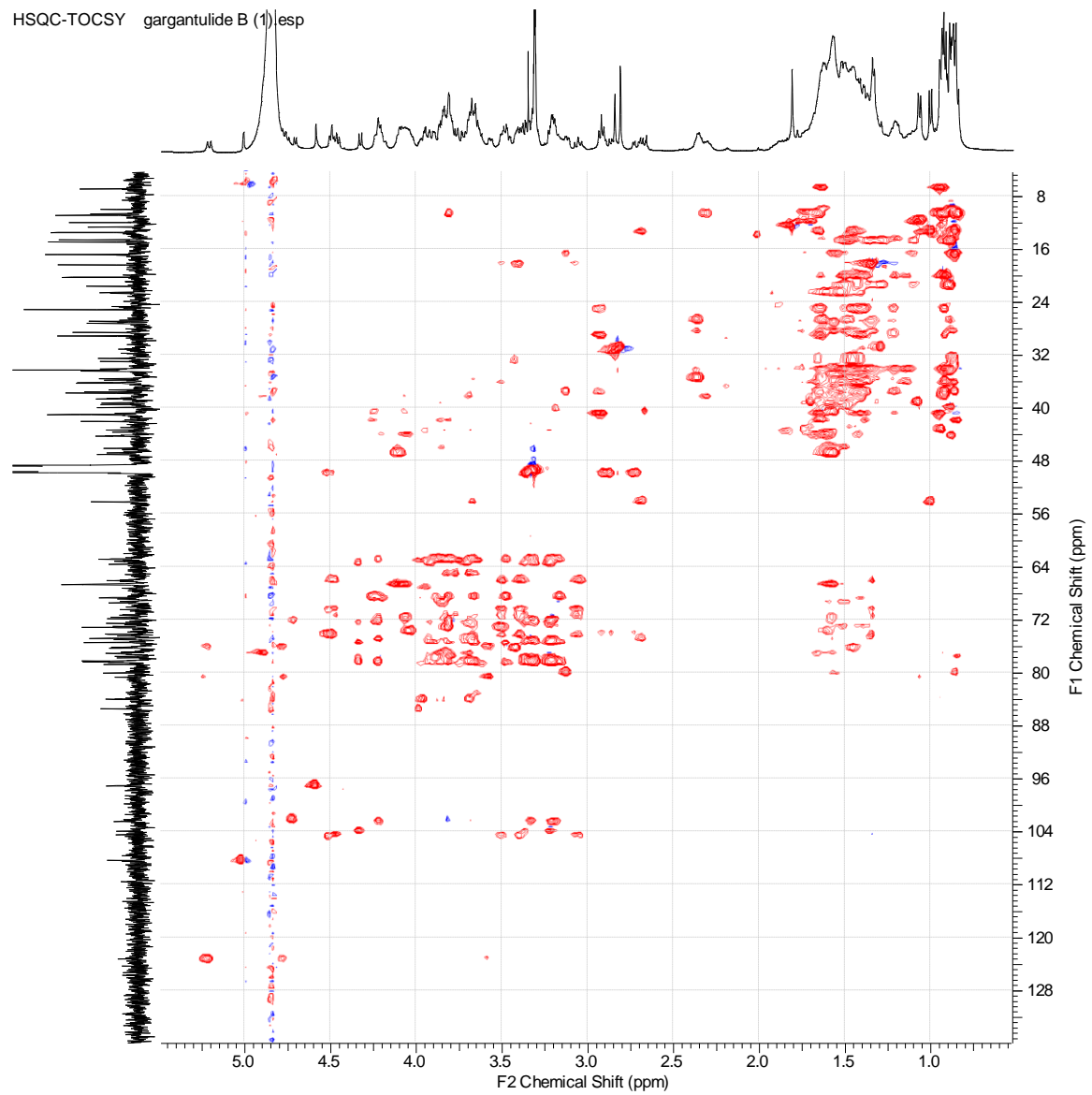
h) HMBC spectrum of **1**



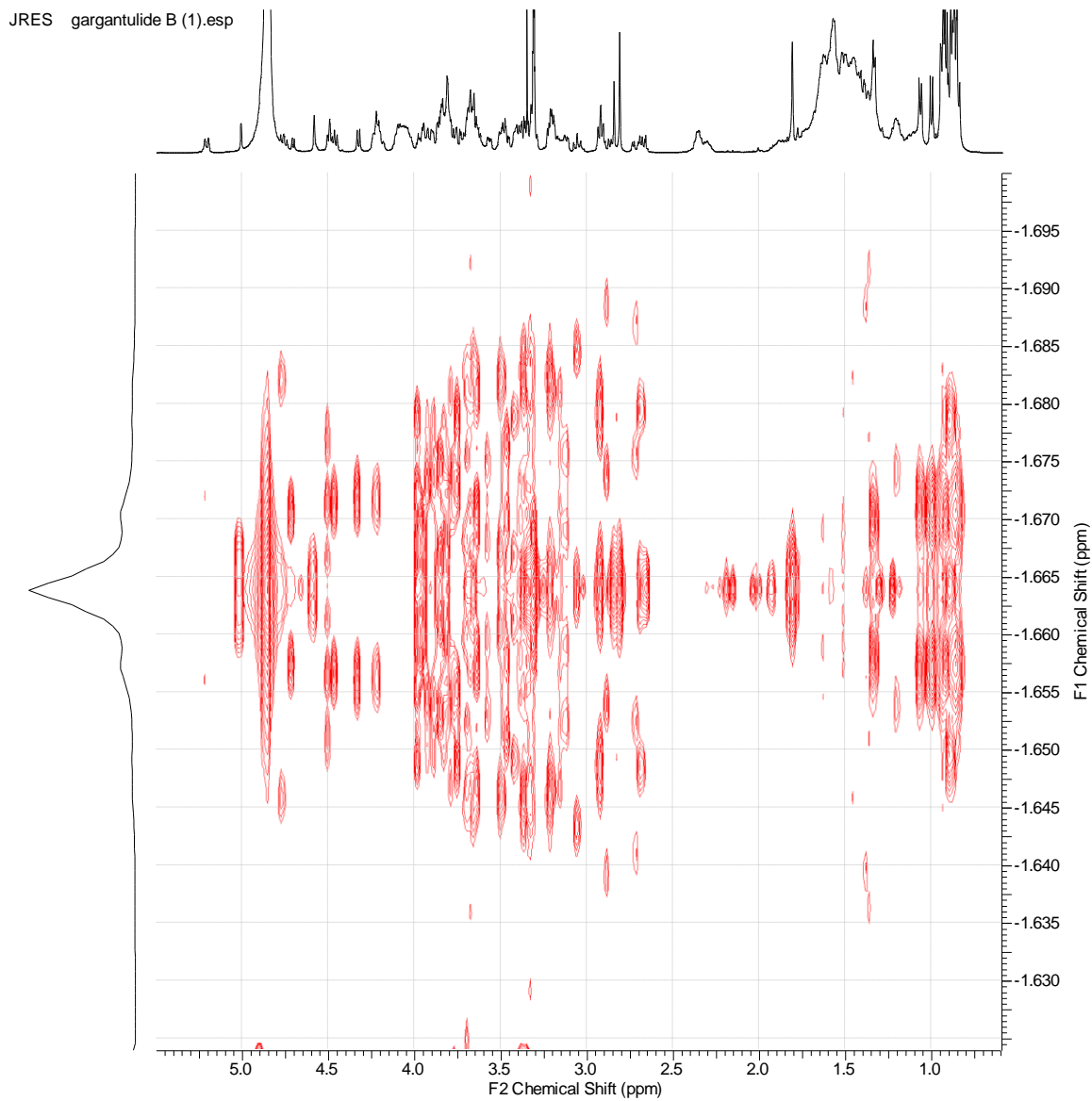
i) TOCSY spectrum of **1**



j) NOESY spectrum of **1**

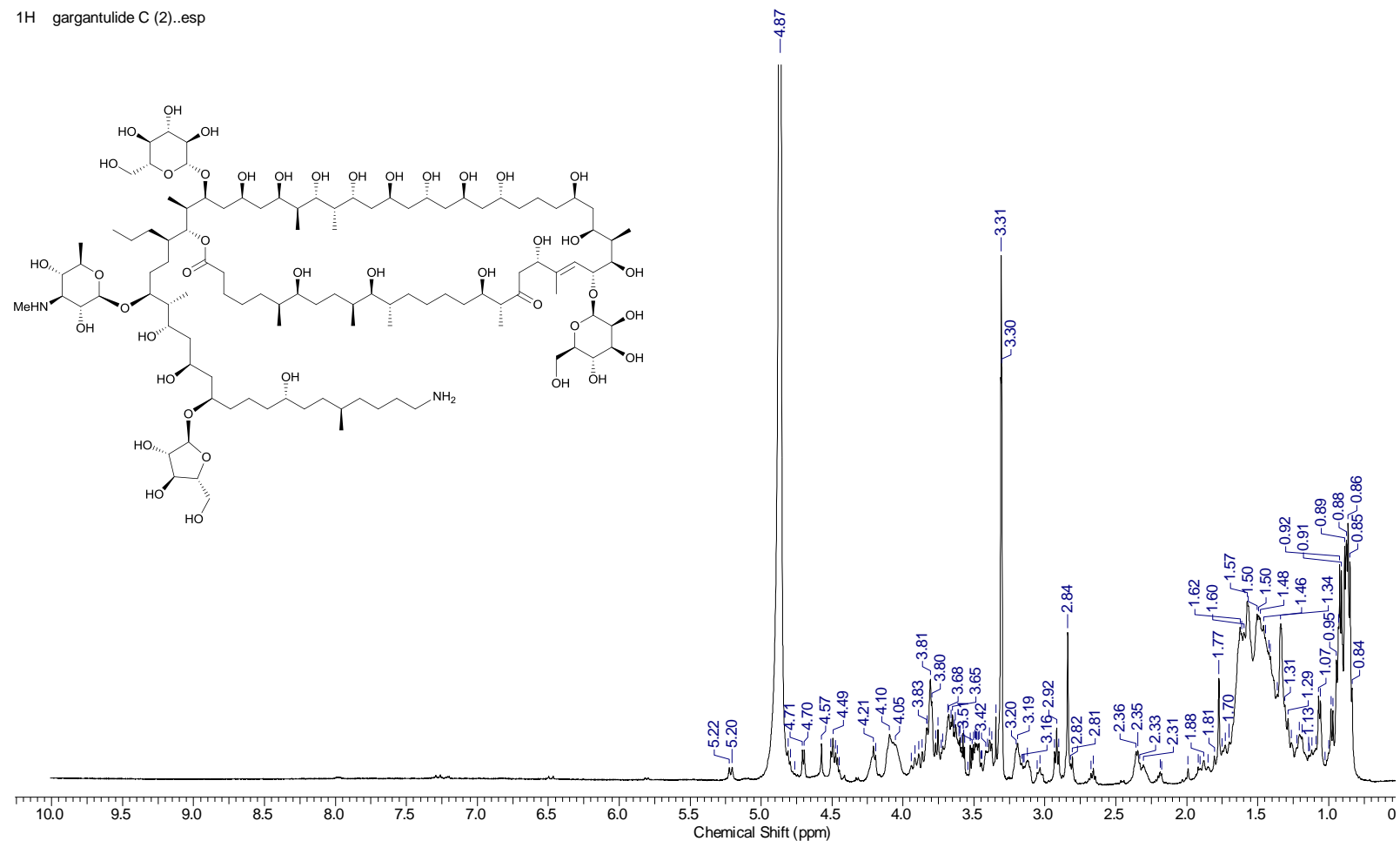


k) HSQC-TOCSY spectrum of **1**



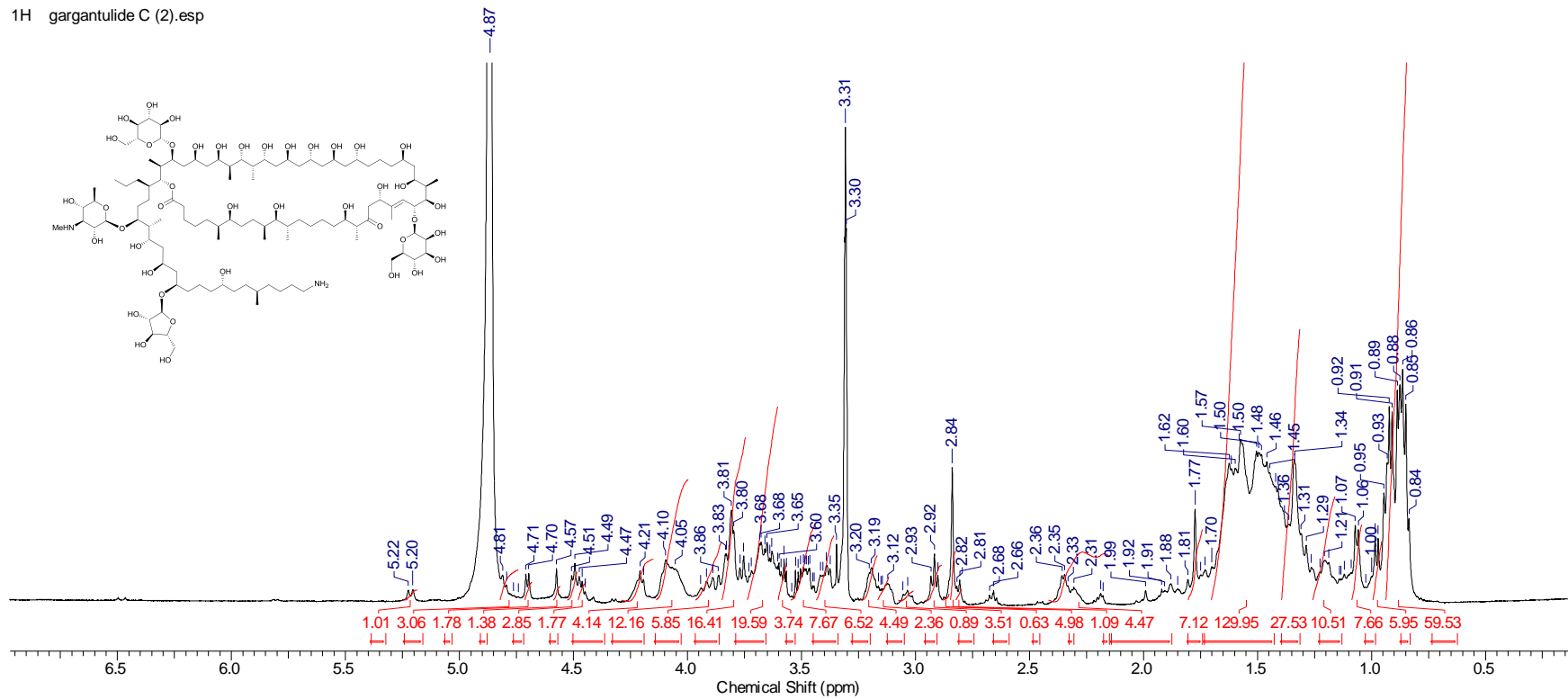
I) JRES spectrum of **1**

Figure S5. 1D/2D NMR spectra of gargantulide C (**2**)



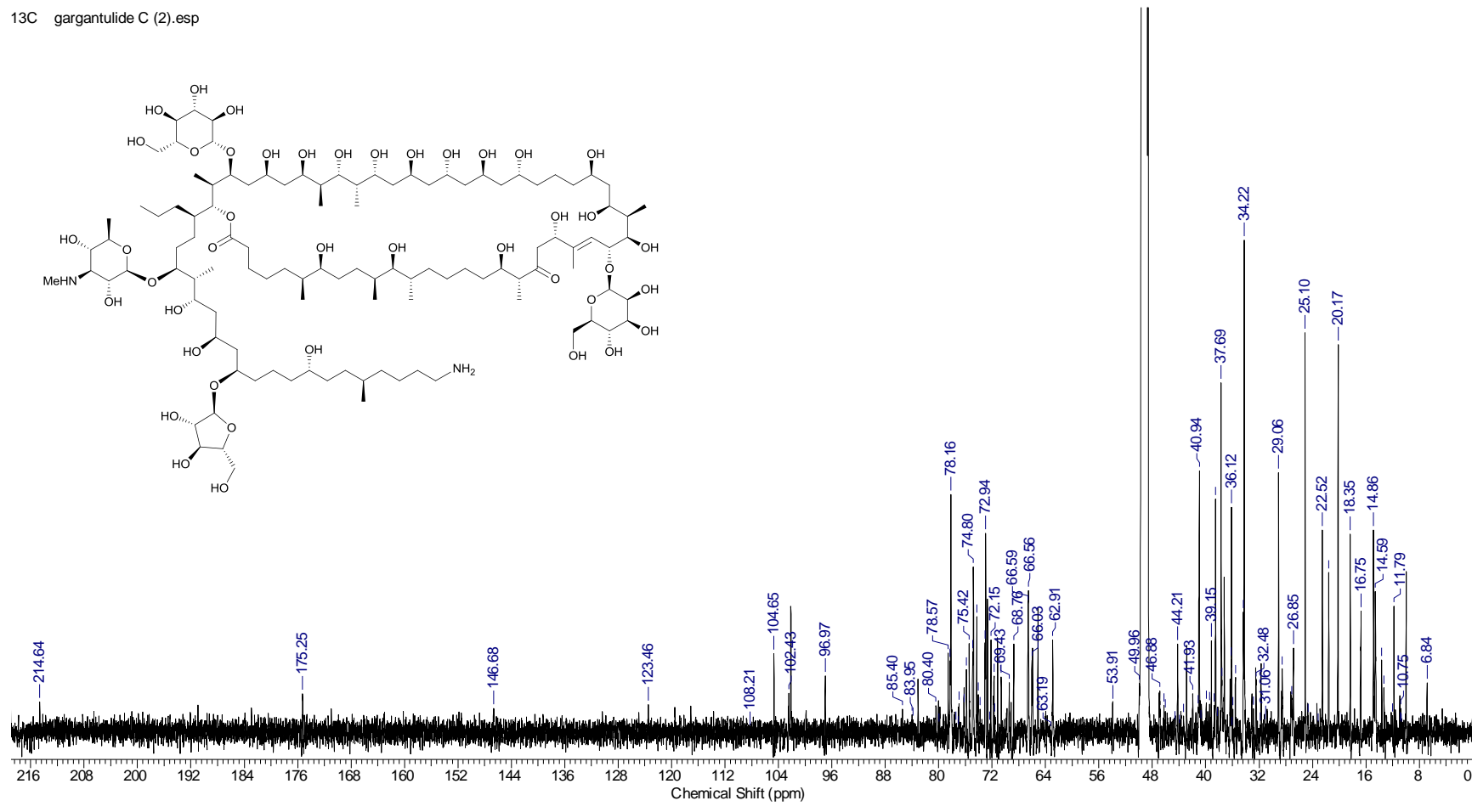
a) ¹H NMR spectrum (CD₃OD, 500 MHz) of **2**. Full scale (0-10 ppm)

¹H gargantulide C (2).esp



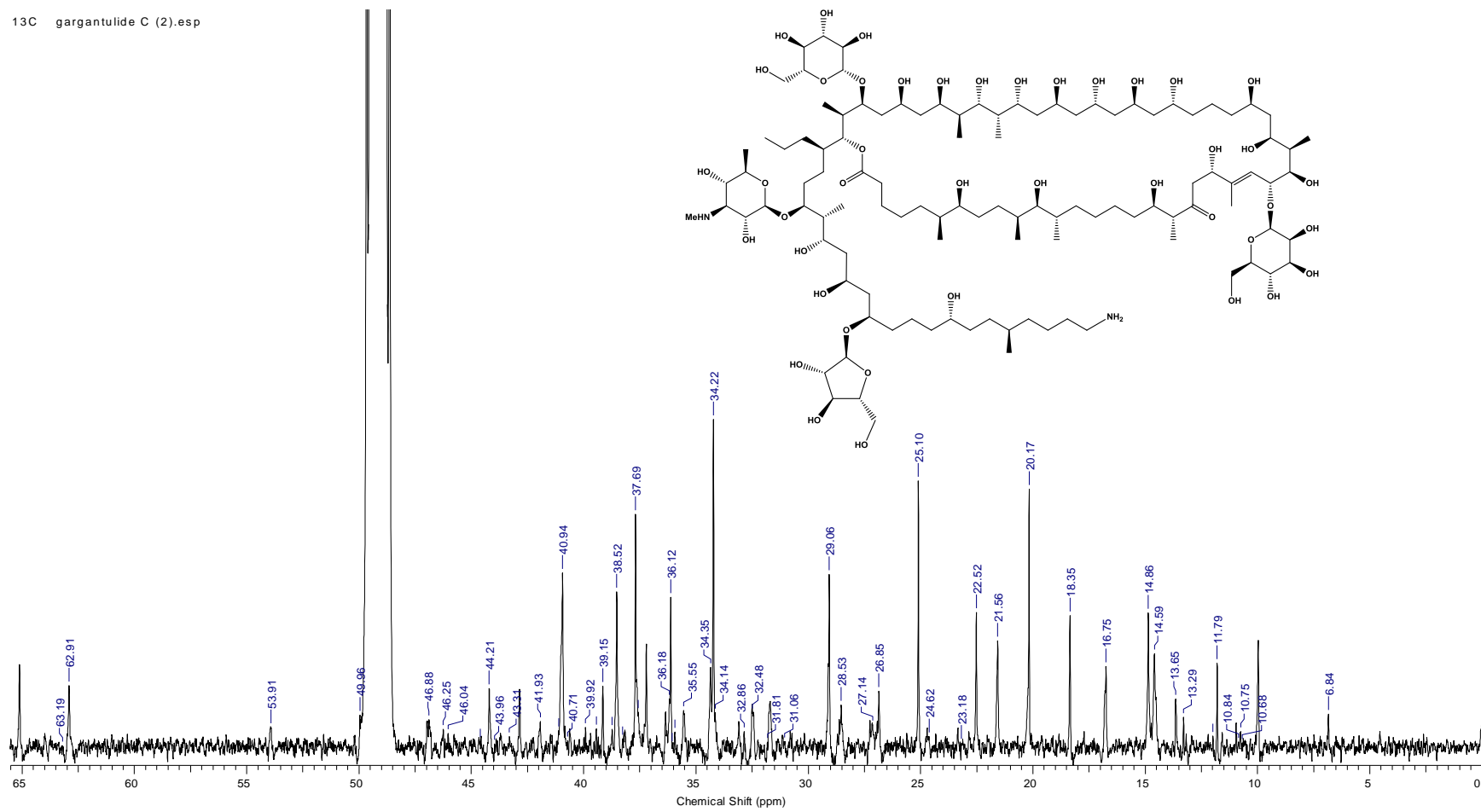
b) ¹H NMR spectrum (CD₃OD, 500 MHz) of 2. Expansion between 0 and 7 ppm showing integral values

13C gargantulide C (2).esp



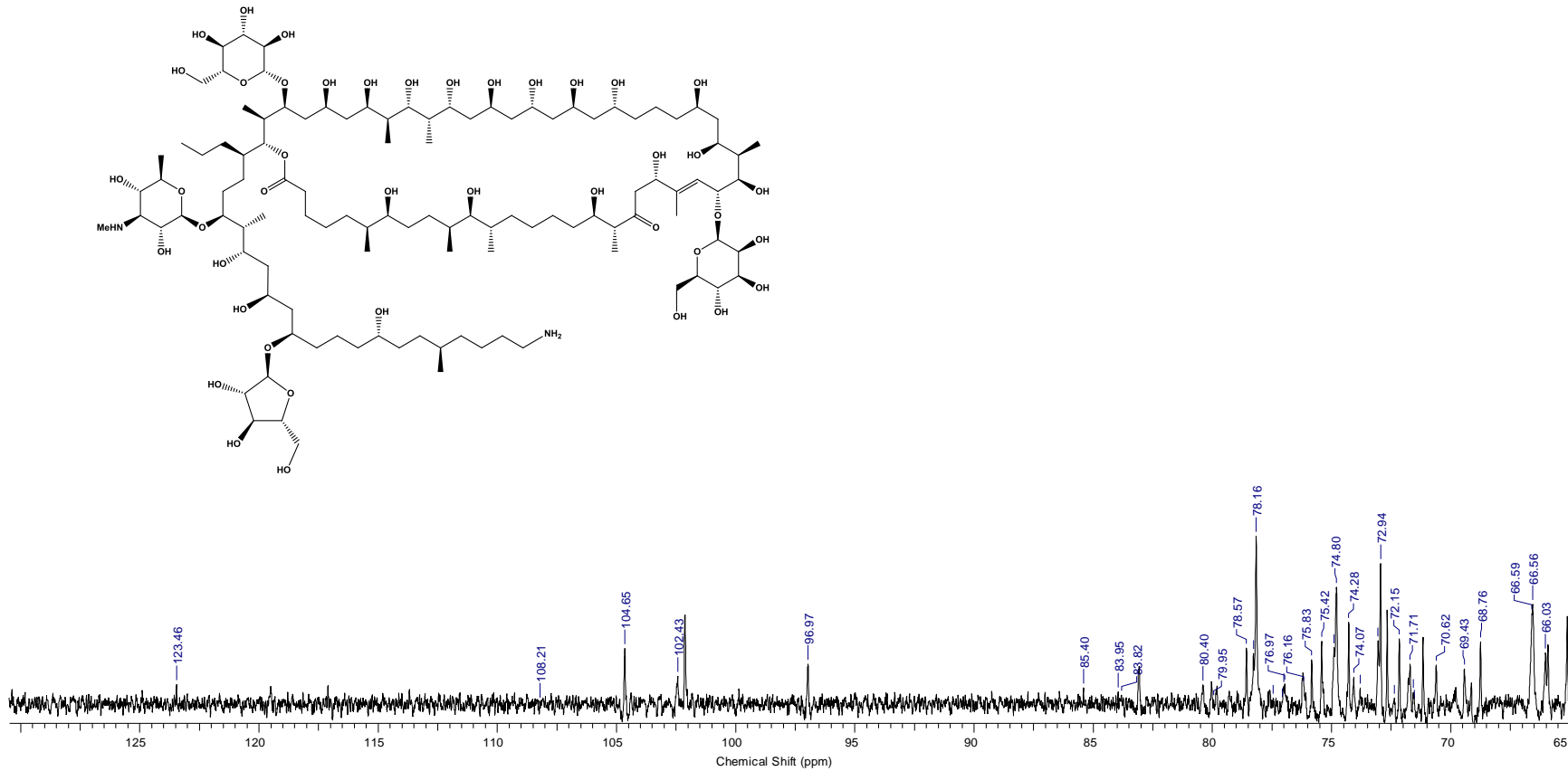
c) ^{13}C NMR spectrum (CD_3OD , 125 MHz) of **2**

¹³C gargantulide C (2).esp



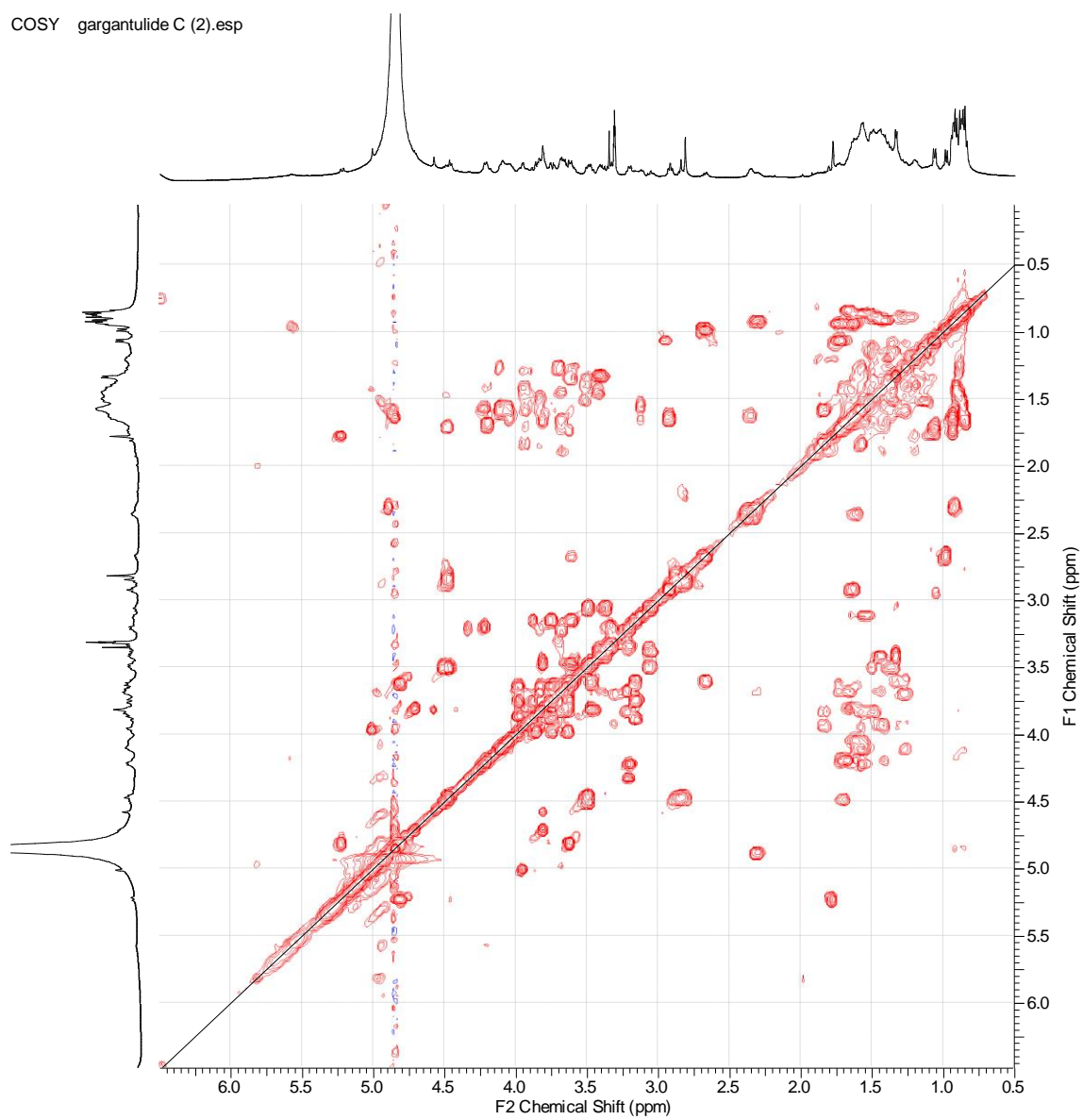
d) ¹³C NMR spectrum (CD₃OD, 125 MHz) of **2**. Expansion between 0 and 65 ppm

¹³C gargantulide C (2).esp

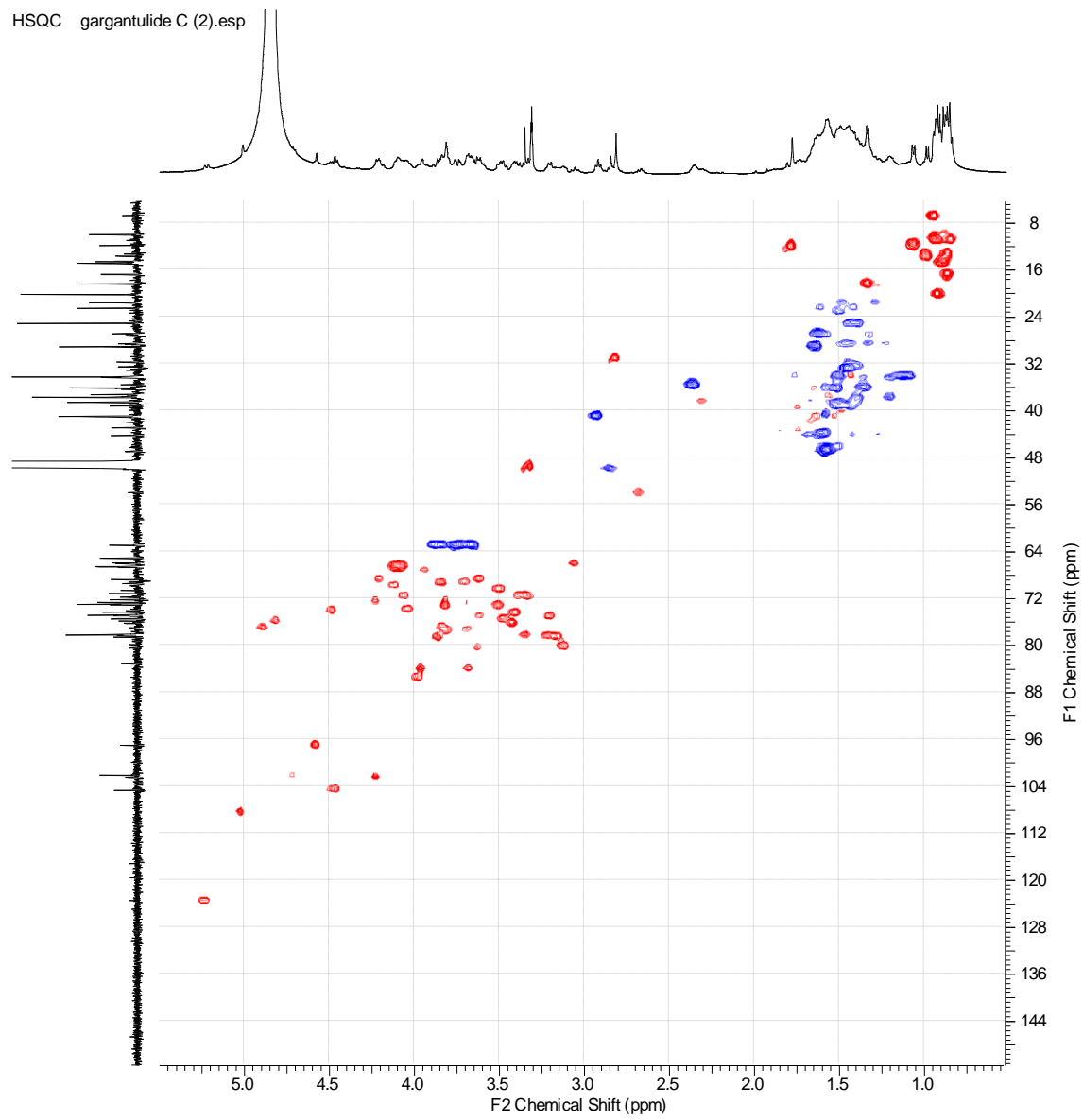


e) ¹³C NMR spectrum (CD₃OD, 125 MHz) of **2**. Expansion between 65 and 130 ppm

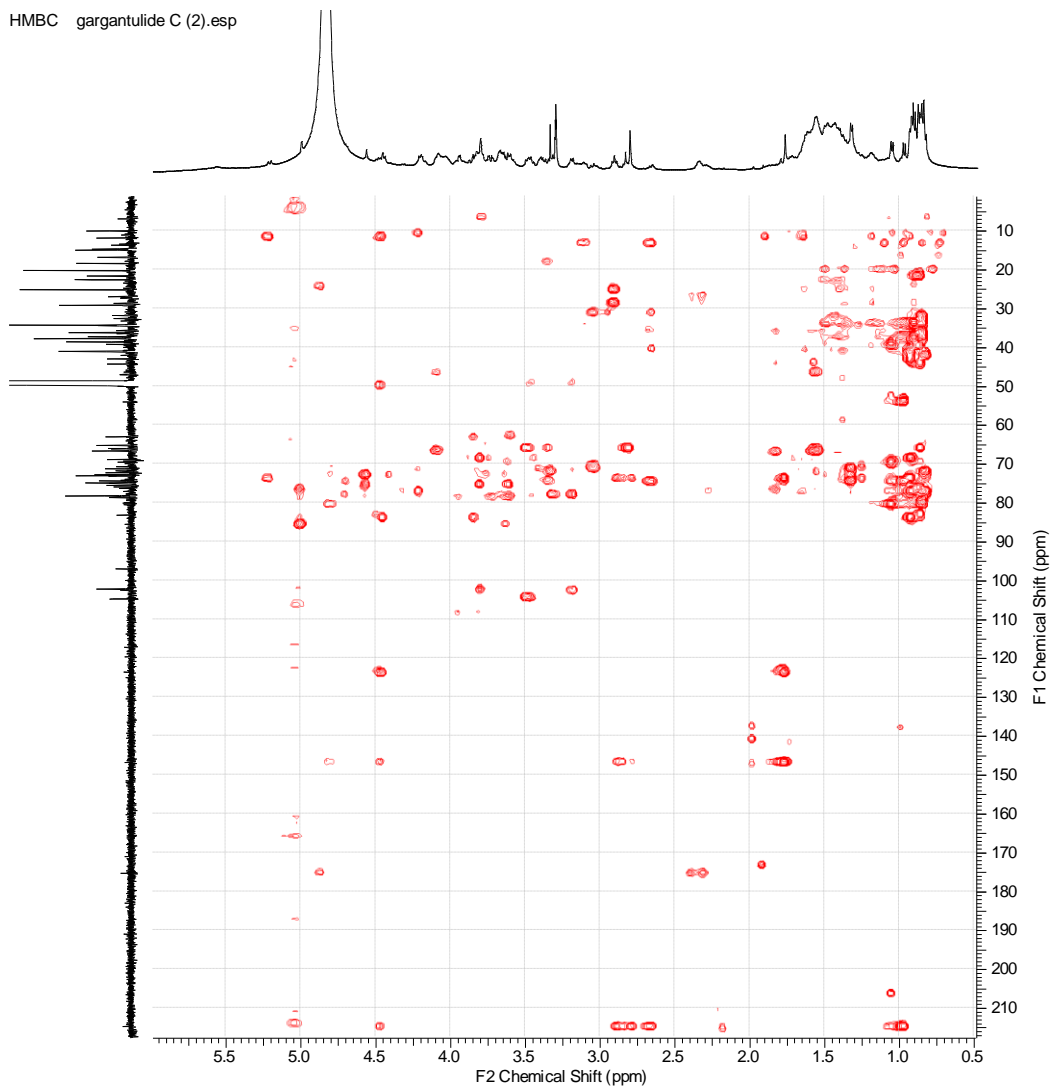
COSY gargantulide C (2).esp



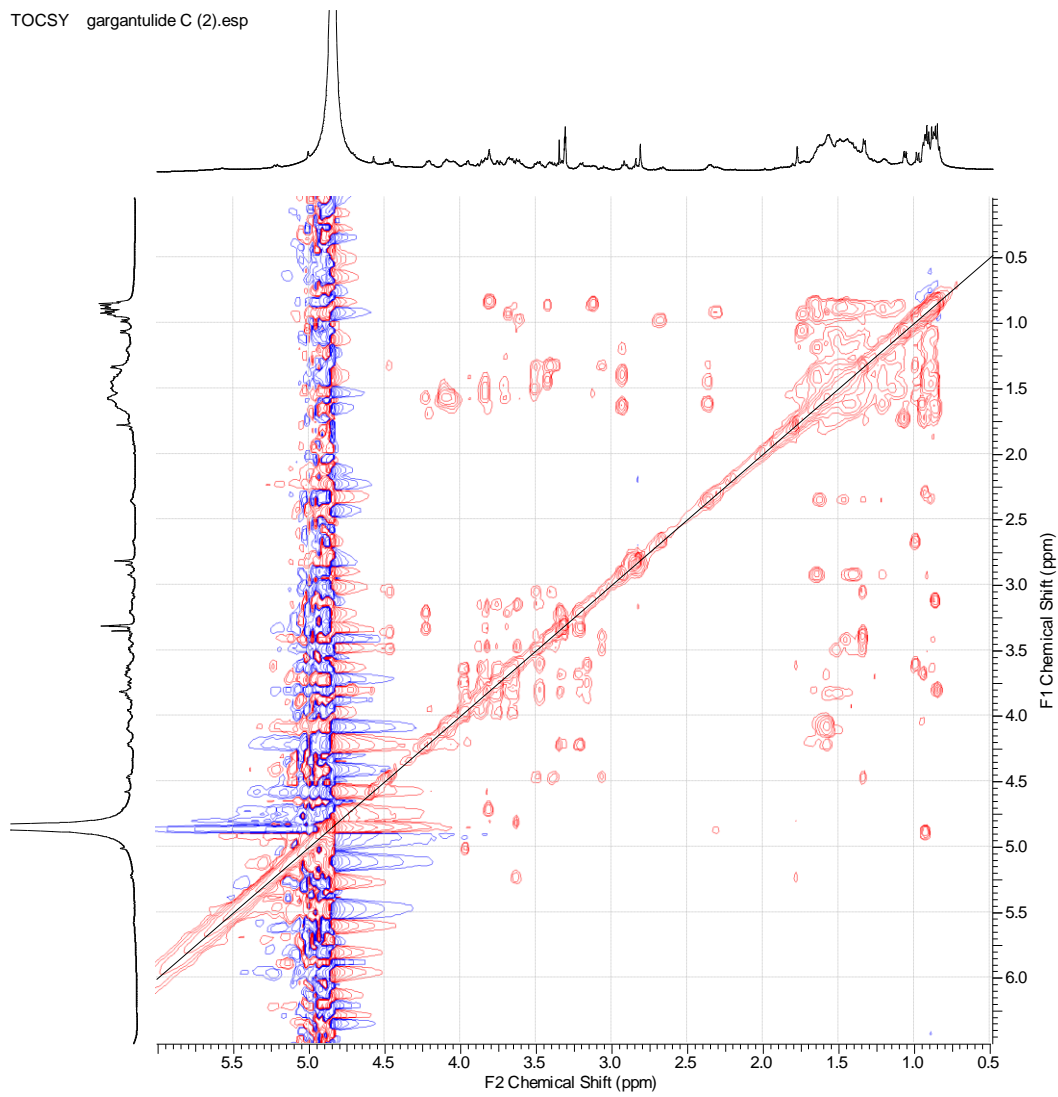
f) COSY spectrum of **2**



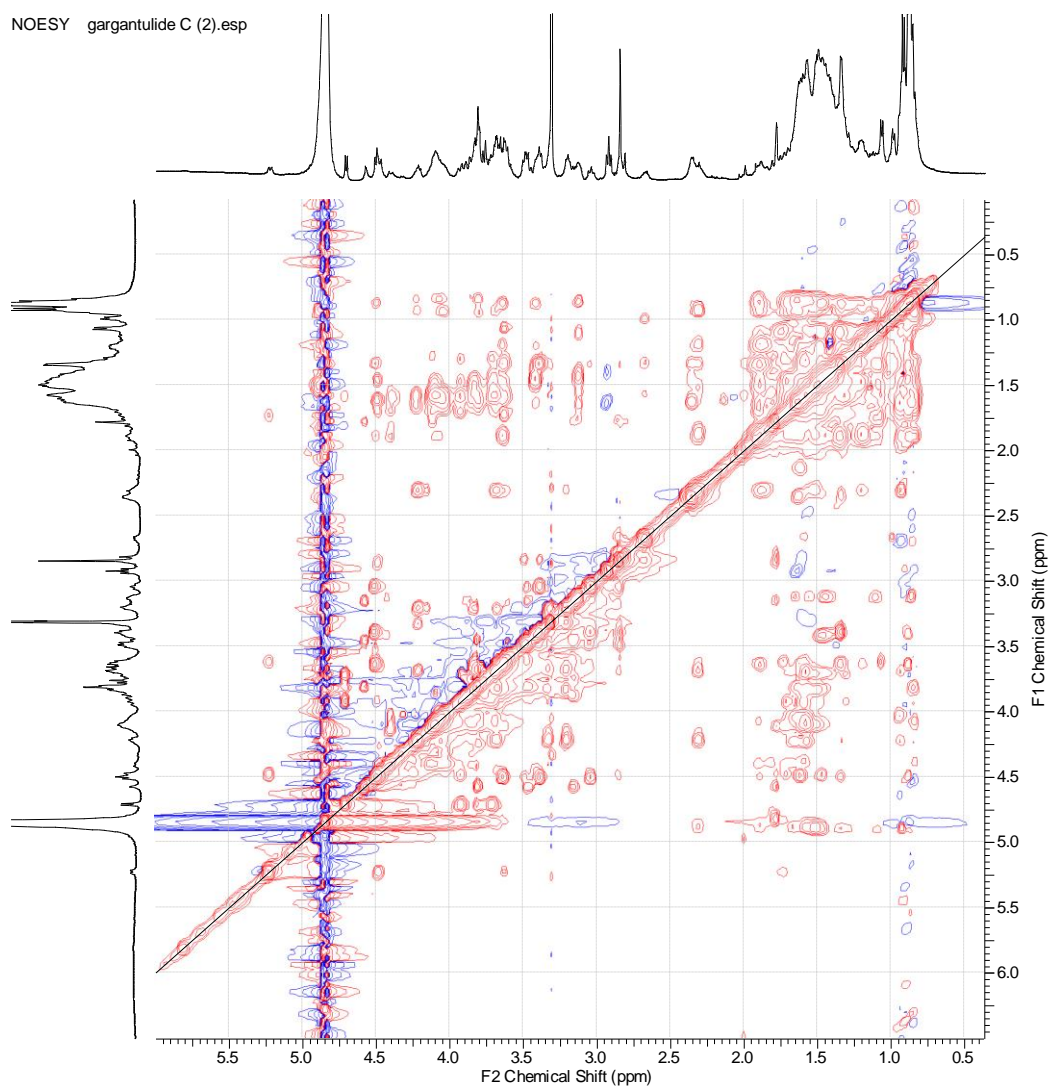
g) HSQC spectrum of **2**



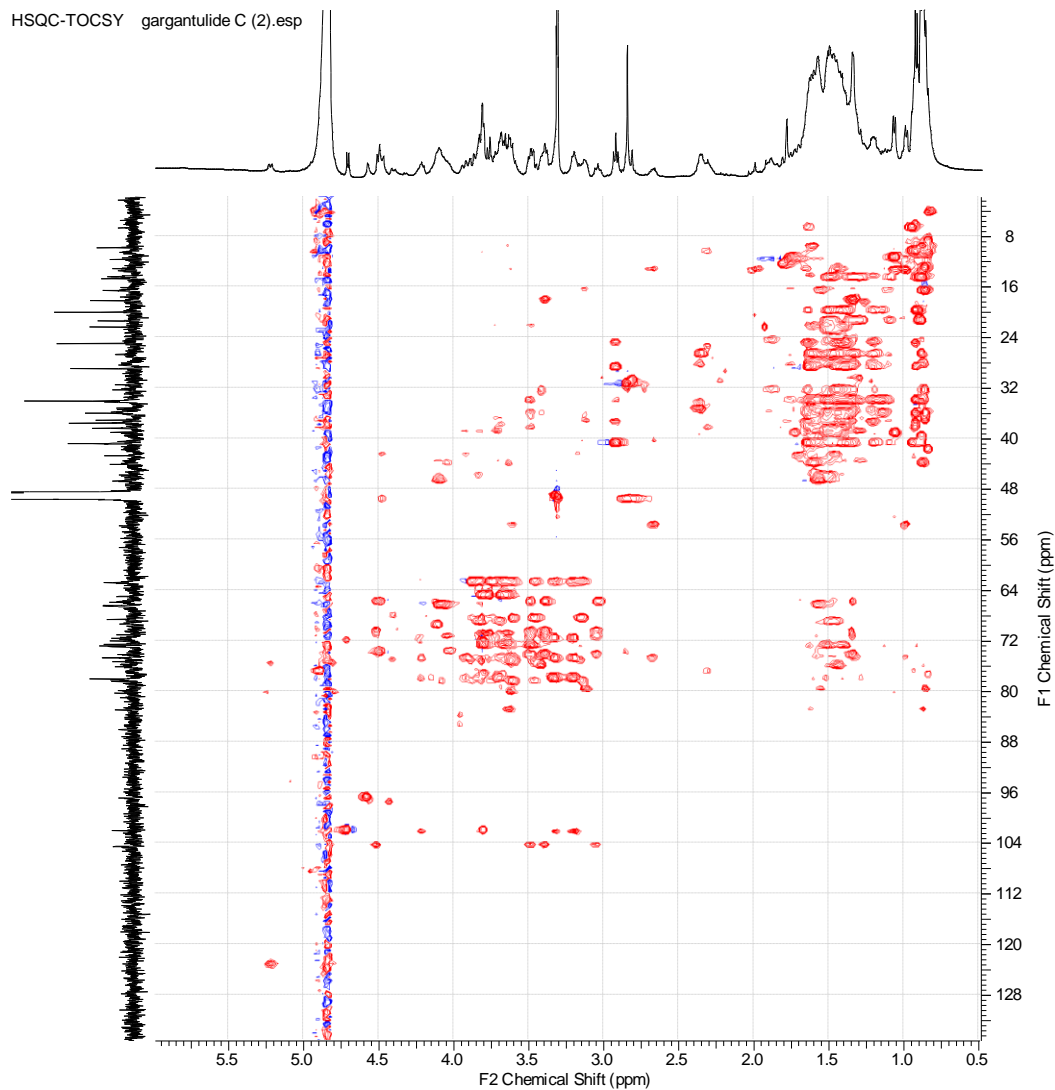
h) HMBC spectrum of **2**



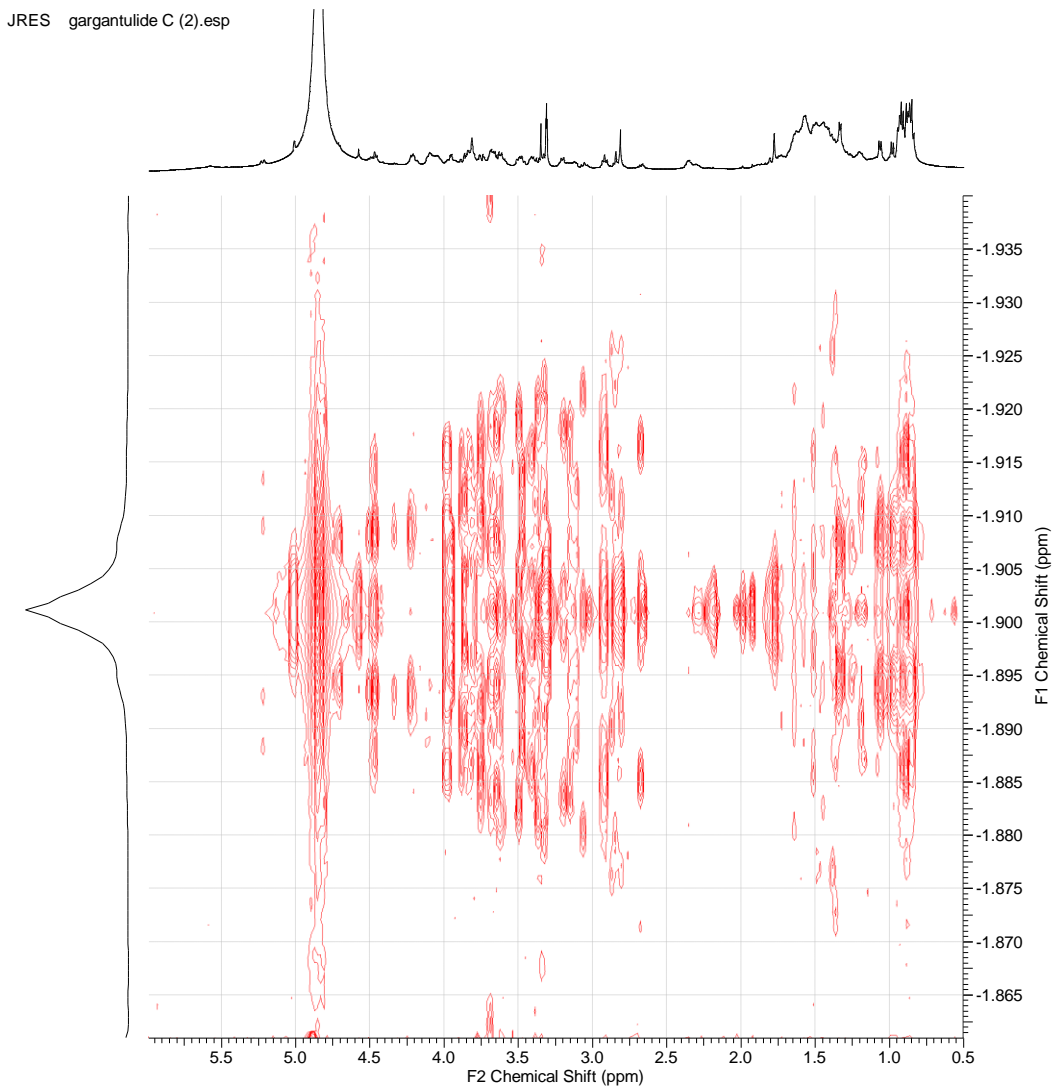
i) TOCSY spectrum of **2**



j) NOESY spectrum of **2**



k) HSQC-TOCSY spectrum of **2**



I) JRES spectrum of **2**

Figure S6. Key COSY, TOCSY, HSQC-TOCSY and HMBC correlations observed for **2**

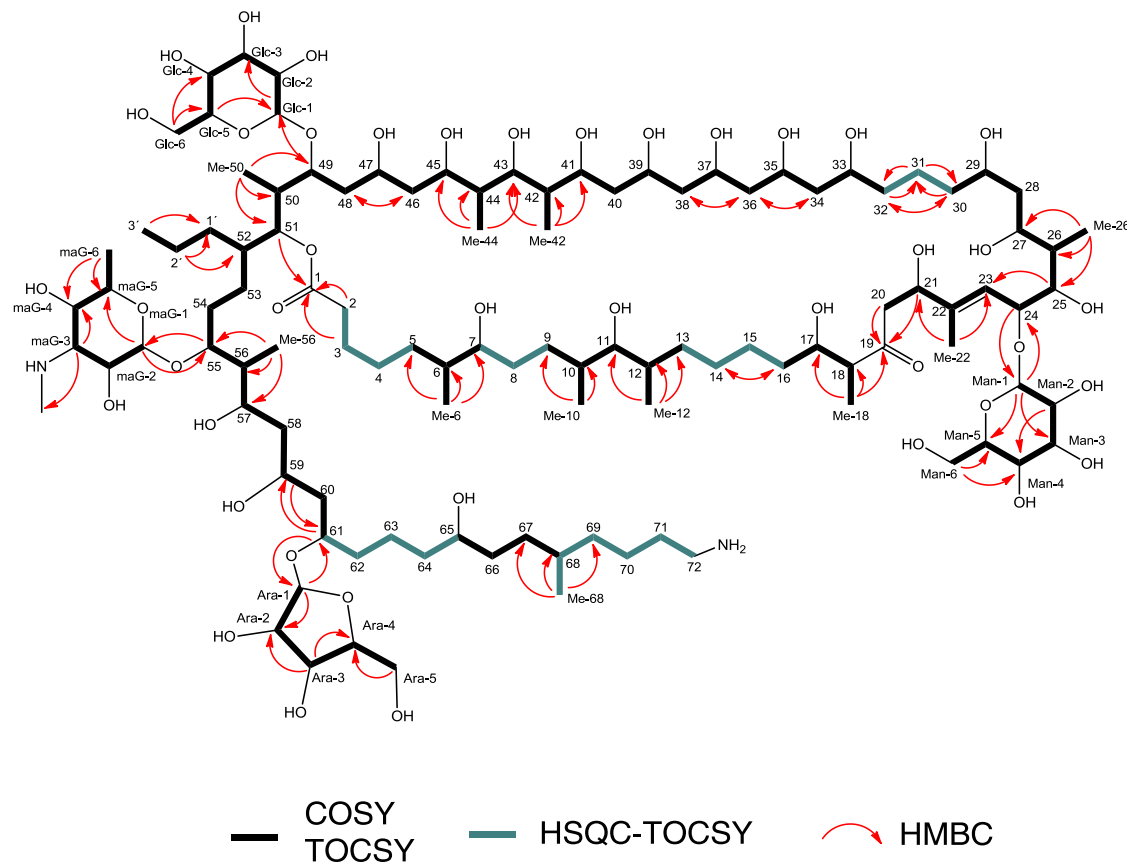


Figure S7. LC-HRMS co-detection of gargantulides A (**3**), B (**1**) and C (**2**) in the acetone crude extract of a micro-scale fermentation. (UV 210 nm: pink trace; MS+: blue trace) HRESIMS(+)-TOF spectra (ISCID 0 eV) of gargantulides A (triply and doubly-charged adducts) B and C (doubly-charged ions)

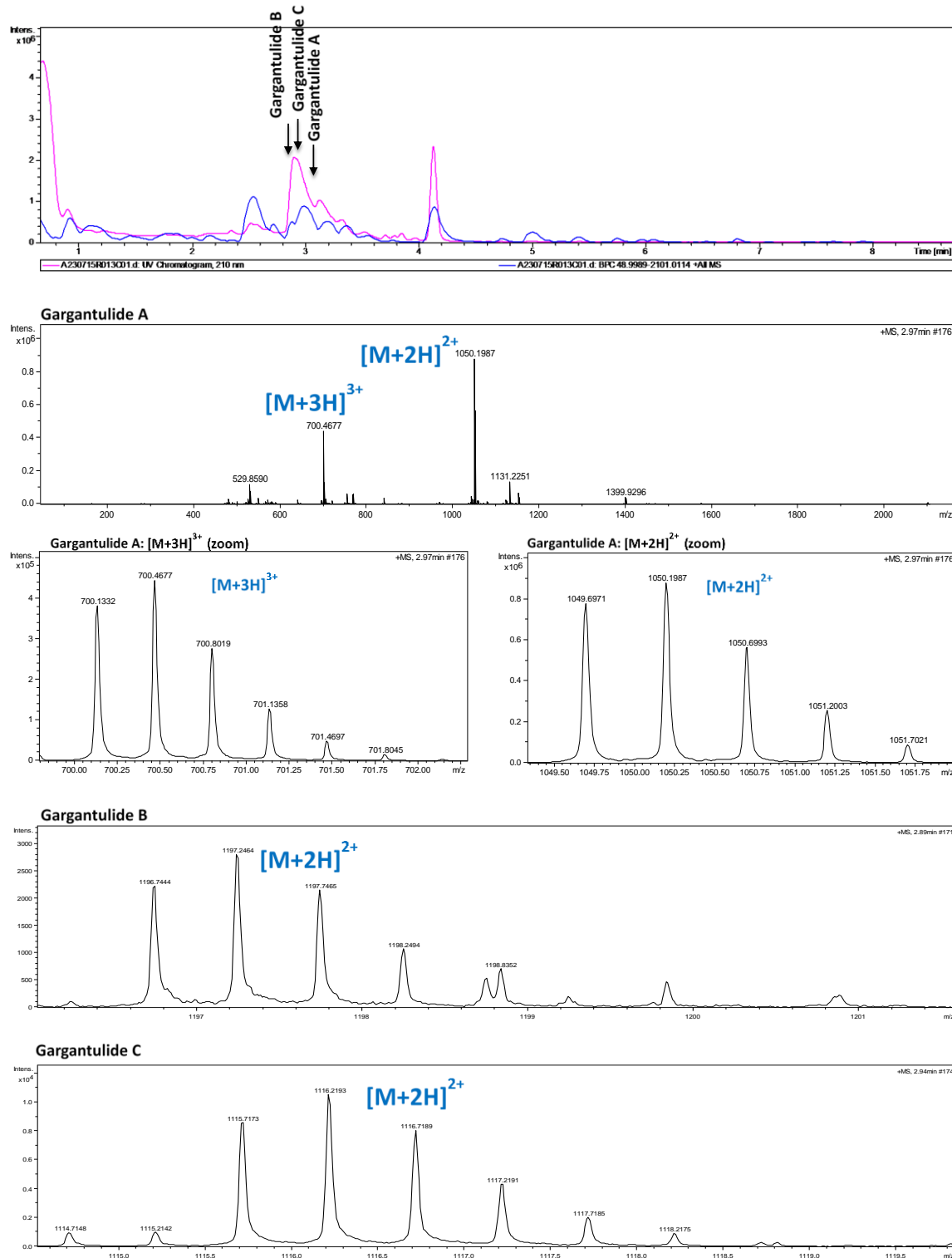


Table S2. antiSMASH results (bacterial version, relaxed mode). All types of BGCs are listed as detected by antiSMASH

Region number	Type	Approx. size, kbp	Most similar known cluster	Remarks
1	PKS-like	40,855	No hits	
2	NRPS	44,211	Daptomycin (4%)	
3	Siderophore	11,832	Macrotetrolide (33%)	
4	RIPP-like	9,971	Enduracidin (4%)	
5	LAP, thiopeptide	27,977	No hits	
6	Terpene	21,678	Geosmin (100%)	
7	NRPS-like, terpene	42,088	Isorenieratene (42%)	Possibly two clusters
8	T1PKS	45,457	EDHA (33%)	
9	Terpene	19,827	Lipopeptide 8D1-1 (6%)	
10	T1PKS	45,036	Sch-47554/Sch-47555 (3%)	
11	T1PKS, oligosaccharide	216,516	Funisamine (30%)	Putative cluster, coding for gargantulide compounds
12	LAP, ladderane, thioamide-NRP, NRPS	76,620	Ishigamide (72%)	Possibly several clusters
13	Other, thiopeptide, terpene, lantipeptide clas II	72,243	2-methylisoborneol (100%)	
14	NAPAA	31,640	Himastatin (8%)	
15	NRPS	62,803	Albachelin (70%)	
16	CDPS	20,683	No hits	
17	PKS-like	40,596	No hits	
18	Lantipeptide class I	25,334	No hits	
19	Lantipeptide class III	22,579	Ery-9 / Ery-6 / Ery-8 / Ery-7 / Ery-5 / Ery-4 / Ery-3 (100%)	
20	Arylpolyene	40,340	Ibomycin (5%)	
21	Ectoine	8,532	Ectoine (100%)	
22	NRPS, T1PKS	73,041	Ecumicin (10%)	
23	thiopeptide, LAP	30,258	No hits	

24	redox-cofactor	22,025	Lankacidin C (20%)	
25	cyanobactin, PKS-like, NRPS, T1PKS, lantipeptide class V, linaridin	85,858	prenylagaramide B / prenylagaramide C (8%)	
26	Lantipeptide class V	40,587	Arginomycin (13%)	
27	Linaridin	20,557	Legonaridin (25%)	
28	Lantipeptide class V	41,924	Ashimides (8%)	
29	Lantipeptide class II	23,053	No hits	
30	NAPAA	32,569	No hits	
31	hgIE-KS, T1PKS	49,901	Rifamorpholine A/B/C/D/E (4%)	
32	NRPS	57,957	Telomycin (5%)	
33	NRPS, ectoine, T1PKS	80,296	Kosinostatin (16%)	
34	NRPS, NRPS-like	74,191	WS9326 (10%)	
35	NAPAA	32,384	No hits	
36	Terpene	21,115	SF2575 (6%)	
37	Ladderane, NRPS, T1PKS	173,101	Spiramycin (22%)	Possibly three clusters
38	NRPS, arylpolyene	130,298	Kedarcidin (14%)	
39	T1PKS	67,639	Meilingmycin (5%)	
40	Lassopeptide	24,502	No hits	
41	ladderane,NRPS,NRPS-like,transAT-PKS,T1PKS,NAPAA	245,836	Incednine (13%)	Possibly several clusters
42	NRPS, RIPP-like	49,672	Capreomycin IA/IB (6%)	
43	Furan	20,998	No hits	
44	NRPS, thioamitides	80,729	Mannopeptimycin (44%)	
45	Betalactone	25,210	No hits	

Table S3. Putative functions of genes in *gar* BGC

Protein (NCBI accession)	a.a.	Proposed function	BLAST hit protein	Query coverage/Per. identity/ E value	Accession number of BLAST hit
GarR1 (HUW46_01962)	938	Putative Malt family HTH-containing regulator	Helix-turn-helix transcriptional regulator (<i>Kutzneria albida</i>)	99% / 49.58% / 0.0	WP_025354824.1
GarR2 (HUW46_01961)	414	Putative sensor histidine kinase	Sensor histidine kinase (<i>Asanoa ferruginea</i>)	95% / 51.23% / 3e-110	WP_116067603.1
GarT1 (HUW46_01960)	240	Putative ABC-type multidrug transport system, ATPase component	ATP-binding cassette domain-containing protein (<i>Micromonospora pattaloongensis</i>)	96% / 51.95% / 1e-62	WP_091558576.1
GarA (HUW46_01959)	467	Acyl-CoA ligase	Acyl-CoA ligase (<i>Kibdelosporangium aridum</i>)	99% / 73.18% / 0.0	WP_084424151.1
Orf1 (HUW46_01958)	180	PH domain-containing protein	PH domain-containing protein (<i>Pseudonocardiaceae bacterium</i>)	91% / 59.76% / 3e-56	MPZ66135.1
Orf2 (HUW46_01957)	524	PH domain-containing protein	PH domain-containing protein (<i>Kutzneria albida</i>)	95% / 52.08 / 6e-169	WP_025356057.1
GarR3 (HUW46_01956)	228	TetR family transcriptional regulator	TetR/AcrR family transcriptional regulator [<i>Kutzneria albida</i>]	81% / 48.92% / 4e-55	WP_025359812.1
GarT2 (HUW46_01955)	615	Putative ABC-type multidrug transport system, ATPase component	ATP-binding cassette domain-containing protein [<i>Amycolatopsis</i> sp. EGI 650086]	95% / 63.27 / 0.0	WP_158888982.1
GarG1 (HUW46_01954)	396	Putative glycosyltransferase of MGT family	glycosyltransferase MGT family protein [<i>Mycolicibacterium thermoresistibile</i>]	98% / 57.11% / 6e-142	WP_003926533.1
Orf3 (HUW46_01953)	84	Hypothetical protein	hypothetical protein [<i>Scisionella</i> sp. SE31]	91% / 53.25% / 7e-17	WP_031470089.1
GarG2 (HUW46_01952)	457	Putative glycosyltransferase of MGT family	glycosyltransferase family 1 protein [<i>Amycolatopsis</i> sp. SID8362]	92% / 43.88% / 5e-115	WP_160698909.1

GarG3 (HUW46_01951)	421	Putative glycosyltransferase of MGT family	glycosyltransferase family 1 protein [<i>Allokutzneria albata</i>]	97% / 46.12% / 1e-115	WP_030432743.1
GarG4 (HUW46_01950)	419	Putative glycosyltransferase of MGT family	glycosyltransferase family 1 protein [<i>Allokutzneria albata</i>]	98% / 43.06% / 1e-104	WP_030432743.1
GarP1 (HUW46_01949)	4568	Modular polyketide synthase	type I polyketide synthase [<i>Actinophytocola oryzae</i>]	97% / 55.09% / 0.0	WP_133901401.1
GarP2 (HUW46_01948)	9791	Modular polyketide synthase	modular polyketide synthase [<i>Streptomyces</i> sp. RK95-74]	96% / 56.64% / 0.0	BAW35608.1
GarP3 (HUW46_01947)	5411	Modular polyketide synthase	PKS I [<i>Kutzneria albida</i> DSM 43870]	99% / 56.34% / 0.0	AHH99926.1
GarP4 (HUW46_01946)	6168	Modular polyketide synthase	type I polyketide synthase [<i>Streptomyces</i> sp. LamerLS-31b]	98% / 55.92% / 0.0	WP_093893008.1
GarP5 (HUW46_01945)	8075	Modular polyketide synthase	beta-ketoacyl synthase [<i>Streptomyces hygroscopicus</i>]	99% / 54.13% / 0.0	AQW47576.1
GarP6 (HUW46_01944)	4542	Modular polyketide synthase	type I polyketide synthase [<i>Streptomyces cinnamoneus</i>]	99% / 62.72% / 0.0	WP_099199035.1
GarP7 (HUW46_01943)	5347	Modular polyketide synthase	type I polyketide synthase [<i>Amycolatopsis orientalis</i>]	100% / 54.65% / 0.0	WP_051173827.1
GarP8 (HUW46_01942)	3617	Modular polyketide synthase	type I polyketide synthase [<i>Streptomyces cinnamoneus</i>]	99% / 59.56% / 0.0	WP_099199033.1
GarP9 (HUW46_01941)	5662	Modular polyketide synthase	PKS I [<i>Kutzneria albida</i> DSM 43870]	99% / 58.65% / 0.0	AHH99926.1
GarP10 (HUW46_01940)	5910	Modular polyketide synthase	type I polyketide synthase [<i>Streptomyces cinnamoneus</i>]	95% / 61.75% / 0.0	WP_104650952.1
GarB (HUW46_01939)	314	AT domain containing protein	ACP S-malonyltransferase [unclassified <i>Kitasatospora</i>]	96% / 53.77% / 5e-111	WP_057230119.1
GarC (HUW46_01938)	421	Putative cytochrome p450	cytochrome P450 [<i>Streptomyces cinnamoneus</i>]	99% / 56.87 / 1e-165	WP_099199030.1
GarR4 (HUW46_01937)	222	Putative response regulator	response regulator [<i>Propionibacteriales bacterium</i>]	92% / 69.42% / 1e-94	MPZ63410.1
GarR5 (HUW46_01936)	452	Sensor histidine kinase	sensor histidine kinase [<i>Propionibacteriales bacterium</i>]	87% / 51.87% / 1e-103	MPZ96507.1

GarD (HUW46_01935)	156	Putative TDP-4-keto-6-deoxy-D-glucose 3,4-isomerase	WxcM-like domain-containing protein [<i>Amycolatopsis antarctica</i>]	88% / 74.64% / 4e-71	WP_094863117.1
GarE (HUW46_01934)	367	Putative aminotransferase	DegT/DnrJ/EryC1/StrS family aminotransferase [<i>Actinoalloteichus</i>]	100% / 68.39% / 0.0	WP_075741202.1
GarG5 (HUW46_01933)	513	Putative glycosyltransferase	glycosyltransferase, family 39 [<i>Streptomyces cinnamoneus</i>]	100% / 60.23% / 0.0	WP_099199029.1
GarF (HUW46_01932)	450	Putative crotonyl-CoA reductase	crotonyl-CoA carboxylase/reductase [<i>Actinomadura macra</i>]	99% / 79.15% / 0.0	WP_067467652.1
GarH (HUW46_01931)	338	Putative <i>fabH</i>	ketoacyl-ACP synthase III [<i>Micromonospora pisi</i>]	97% / 77.2 % / 2e-175	WP_121159999.1
GarI (HUW46_01930)	291	Putative 3-hydroxybutyryl-CoA dehydrogenase	3-hydroxybutyryl-CoA dehydrogenase [<i>Micromonospora pisi</i>]	92% / 74.72% / 3e-138	WP_121160000.1
GarR6 (HUW46_01929)	956	Putative HTH transcriptional regulator	helix-turn-helix transcriptional regulator [<i>Kutzneria albida</i>]	97% / 49.89% / 0.0	WP_025354824.1
Orf4 (HUW46_01928)	369	Putative IS4-like element	IS4-like element ISMfl1 family transposase [Mycobacteriaceae]	98% / 36.22% / 3e-52	WP_011891513.1
Orf5 (HUW46_01927)	73	Hypothetical protein	hypothetical protein [<i>Streptomyces kasugaensis</i>]	100% / 60.27% /	WP_131126254.1
GarR7 (HUW46_01926)	222	DNA-binding response regulator	DNA-binding response regulator, NarL/FixJ family, contains REC and HTH domains [<i>Sinosporangium album</i>]	98% / 62.39 / 1e-86	SDG85138.1
Orf6 (HUW46_01925)	370	Putative IS256 family element	IS256 family transposase [<i>Actinopolymorpha alba</i>]	66% / 30.26% / 5e-36	WP_040420563.1

Table S4. Prediction of activity and stereochemistry of AT, KR, ER and DH domains from bioinformatics analysis. Stereochemical outcomes for gargantulides B and C.

Protein	Module	Substrate of AT domain	KR domain	DH domain	ER domain	Predicted stereochemistry (Keatinge-Clay) ^a	Predicted stereochemistry (fully assembled linear polyketides) ^b	Stereochemical outcome for gargantulides B and C ^c
GarP1	1	Mmal-CoA	B1	Active	R	"R" (C-68)	R (C-68)	R (C-68)
	2	Mal-CoA	B1	Active	R	-	-	-
GarP2	3	Mal-CoA	B1	-	-	"R" (C-65)	S (C-65)	S (C-65)
	4	Mal-CoA	B1	Active	S	-	-	-
	5	Mal-CoA	B1	-	-	"R" (C-61)	R (C-61)	R (C-61)
	6	Mal-CoA	B1	-	-	"R" (C-59)	R (C-59)	S (C-59) ^d
	7	Mmal-coA	A1	-	-	"R,S" (C-56,57)	S,S (C-56,57)	R,S (C-56,57) ^e
	8	Mal-CoA	B1	n.d.	-	"R" (C-55)	S (C-55)	S (C-55)
GarP3	9	Pmal-CoA ^f	B1	Active	R	"R" (C-52)	R (C-52)	R (C-52)
	10	Mmal-CoA	B1	-	-	"R,R" (C-50,51)	S,R (C-50,51)	S,R (C-50,51)
	11	Mal-CoA	B1	Inactive	-	"R" (C-49)	S (C-49)	S (C-49)
GarP4	12	Mal-CoA	B1	-	-	"R" (C-47)	R (C-47)	S (C-47) ^g
	13	Mmal-CoA	B2	-	-	"S,R" (C-44,45)	S,R (C-44,45)	S,R (C-44,45)
	14	Mmal-CoA	A1	-	-	"R,S" (C-42,43)	S,R (C-42,43)	S,R (C-42,43)
	15	Mal-CoA	A1	-	-	"S" (C-41)	R (C-41)	R (C-41)
GarP5	16	Mal-CoA	B1	-	-	"R" (C-39)	S (C-39)	S (C-39)
	17	Mal-CoA	A1	-	-	"S" (C-37)	R (C-37)	R (C-37)
	18	Mal-CoA	B1	-	-	"R" (C-35)	S (C-35)	S (C-35)
	19	Mal-CoA	A1	-	-	"S" (C-33)	R (C-33)	R (C-33)
	20	Mal-CoA	B1	Active	S	-	-	-
GarP6	21	Mal-CoA	B1	-	-	"R" (C-29)	R (C-29)	R (C-29)
	22	Mmal-CoA	A1	-	-	"R,S" (C-26,27)	S,S (C-26,27)	R,S (C-26,27) ^h
	23	Mal-CoA	B1	-	-	"R" (C-25)	S (C-25)	R (C-25) ^h
GarP7	24	Mmal-CoA	B1	Active	-	"E" double bond	E double bond	E double bond
	25	Mal-CoA	B1	-	-	"R" (C-21)	S (C-21)	S (C-21)
	26	Mmal-CoA	C1 ⁱ	n.d.	n.d.	"R" (C-18)	S (C-18)	R (C-18) ⁱ
GarP8	27	Mal-CoA	A1	-	-	"S" (C-17)	R (C-17)	R (C-17)
	28	Mal-CoA	B1	Active	S	-	-	-
GarP9	29	Mmal-CoA	B1	Active	S	"S" (C-12)	S (C-12)	S (C-12)
	30	Mmal-CoA	A1	-	-	"R,S" (C-10,11)	S,S (C-10,11)	S,S (C-10,11)
	31	Mal-CoA	B1	Active	S	-	-	-
GarP10	32	Mmal-CoA	A1	-	-	"R,S" (C-6,7)	S,S (C-6,7)	S,S (C-6,7)
	33	Mal-CoA	B1	Active	S	-	-	-
	34	Mal-CoA	B1	Active	S	-	-	-

^a Bioinformatics prediction for each separate module

^b See Fig SX (fully assembled linear polyketides)

^c Stereochemistry determined by a combination of NMR and bioinformatics gene cluster analysis for gargantulides B and C (and extrapolated to gargantulide A, revised in this work)

^d The Cahn-Ingold-Prelog descriptor in gargantulides B and C for C-59 is inverted to S due to the glycosylation at C-61

^e The Cahn-Ingold-Prelog descriptor in gargantulides A-C for C-56 is inverted to R due to the glycosylation at C-55

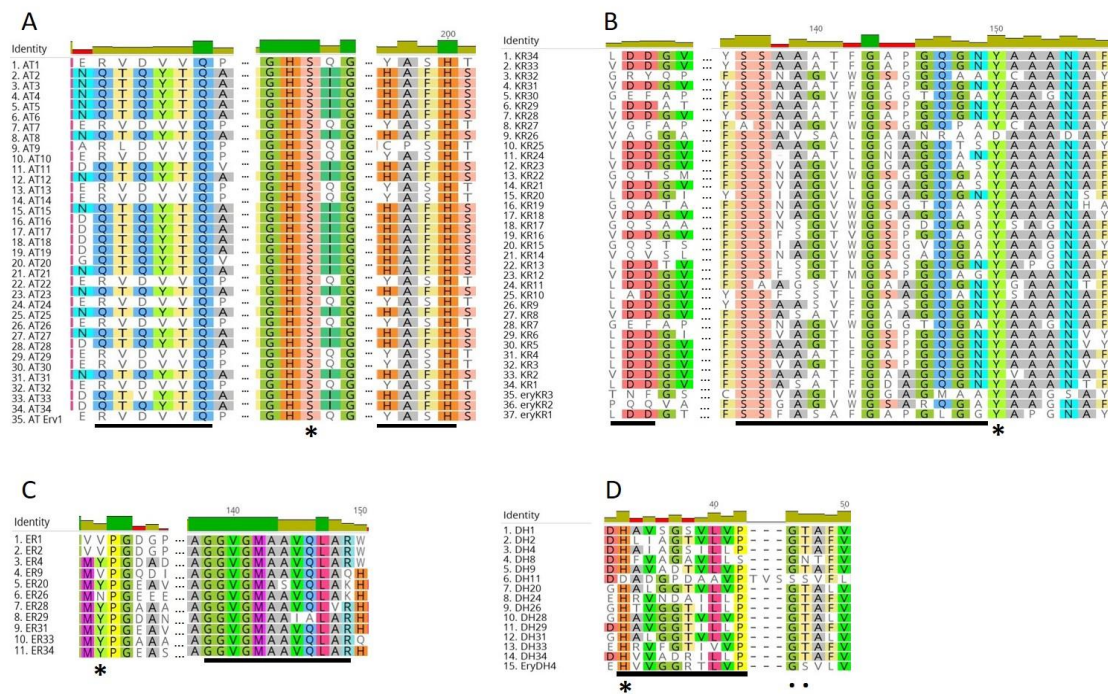
^f Propyl malonyl-CoA established by NMR analysis

^g The Cahn-Ingold-Prelog descriptor in gargantulides A-C for C-47 is inverted to S due to macrolactone cyclization and glycosylation at C-49.

^h The Cahn-Ingold-Prelog descriptor in gargantulides A-C for both C-25 and C-26 is inverted to R due to the post-PKS hydroxylation at C-24

ⁱ Redox-inactive, methyl-epimerizing KR; (module 26)

Figure S8. Extracted amino acid sequence alignments of AT, KR, DH and ER domains



A - amino acid sequence alignment of AT domains. Characteristic residues for substrate recognition are underlined with black bars. The catalytic residue is identified with asterisk; **B** - amino acid sequence alignment of KR domains. Two motifs, responsible for determination of A/B/C type of KRs are underlined with black bars; the catalytic tyrosine residue is identified with an asterisk; **C** - amino acid sequence alignment of ER domains. The amino acid related to the stereochemistry of reduced residue is identified with an asterisk. NADPH binding site is identified with a black bar; **D** - amino acid sequence alignment of DH domains. The conserved motif "HXXXGXXXXP" is identified with a black bar. The catalytic residue is identified with an asterisk. Two supporting catalytic residues are identified with filled black spots. The assignment of characteristic residues for substrate recognition and catalytic residues for ATs, KRs, DHs and ERs was done as described in previous works.³⁻⁶

Supplementary note: Biosynthesis of amino sugar maG

Within the *gar* BGC, *garD* codes for a protein with high level of similarity (51% identity, 64% similarity) to Tyl1a from the mycaminose biosynthetic pathway in the tylosin BGC,^{12,13} suggesting it could function as a TDP-4-keto-6-deoxy-D-glucose 3,4-isomerase. *garE* encodes a PLP-dependent aminotransferase with high homology (62% identity, 73% similarity) to the biochemically characterized aminotransferase TylB from mycaminose biosynthesis.¹⁴ Thus, GarE is proposed to catalyze a C-3 transamination to afford TDP-3-amino-3,6-dideoxy-D-glucose. Surprisingly, the *gar* cluster lacks a gene coding for a putative *N*-methyltransferase to convert TDP-3-amino-3,6-dideoxy-D-glucose into *N*-demethyl-mycaminose (i.e., maG). To look for a candidate gene responsible for the *N*-methylation, we employed the amino acid sequences of some known methyltransferases found in the mycaminose, desosamine, L-ossamine and D-forosamine pathways from different microorganisms. The best candidate was HUW46_03188, located just outside of the boundaries of the BGC 15, which encodes for a putative S-adenosylmethionine-dependent methyltransferase with high similarity (51% / 65% amino acid identity / similarity) to DesVI, the biochemically characterized *N,N*-dimethyltransferase from desosamine biosynthesis¹⁵ (Table S5). Interestingly, other DesVI homologous proteins, such as TylM1 (tylosin gene cluster) or SpnS (spinosyns BGC), have been shown to catalyze *N*-methylation in a stepwise manner, involving the release of the monomethylated product from the active site.^{15,16} This could explain the formation of the monomethylated amino sugar maG in gargantulides A-C. Additionally, genes encoding for a putative glucose-1-phosphate thymidyltransferase and dTDP-glucose 4,6-dehydratase, required in the first two steps to afford the intermediate TDP-4-keto-2,6-dideoxy-D-glucose, are also found elsewhere in the genome (Table S6). Based on these findings, a biosynthetic pathway to maG from glucose-1-phosphate can be proposed (Fig. S9)

Table S5. Levels of identity and similarity of the putative *N*-Methyltransferase HUW46_03188 from CA-230715 with other known *N*-Methyltransferases.

Protein	Microorganism	% Identity to HUW46_03188	% Similarity to HUW46_03188
TyIM1	<i>Streptomyces fradiae</i>	43	61
DesVI	<i>Streptomyces venezuelae</i>	51	65
SpnS	<i>Saccharopolyspora spinosa</i>	42	58
Ossl	<i>Streptomyces ossamyceticus</i>	43	59
Orf1C	<i>Streptomyces ambofaciens</i>	44	62
Orf9c	<i>Streptomyces ambofaciens</i>	44	57

Table S6. Identified genes encoding for putative glucose-1-phosphate thymidyltransferase and dTDP-glucose 4,6-dehydratase in the genome of CA-230715.

CA-230715 ORF	Protein a. a.	Putative function	Best match accession number	% Identity / Similarity
HUW46_03193	293	glucose-1-phosphate thymidyltransferase	WP_020668504.1	87 / 93
HUW46_02674	330	dTDP-glucose 4,6- dehydratase	WP_144591396.1	88 / 92
HUW46_09296	335	dTDP-glucose 4,6- dehydratase	WP_125677294.1	72 / 83

Figure S9. Proposed biosynthetic pathway for the amino sugar 3,6-deoxy-3-methylamino D-glucose (maG)

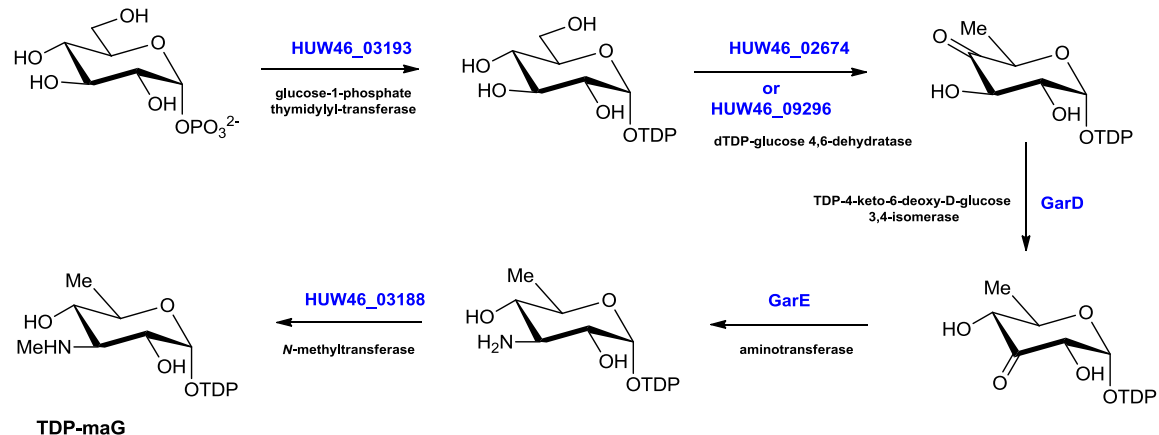
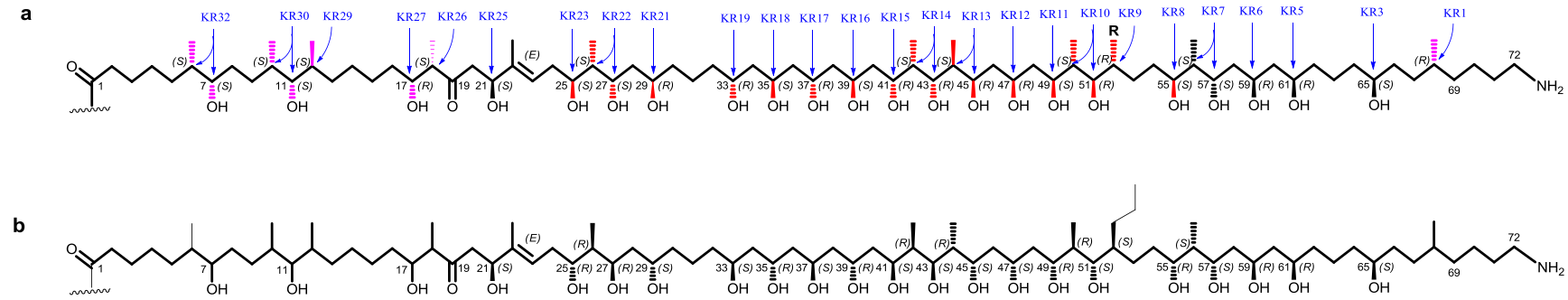
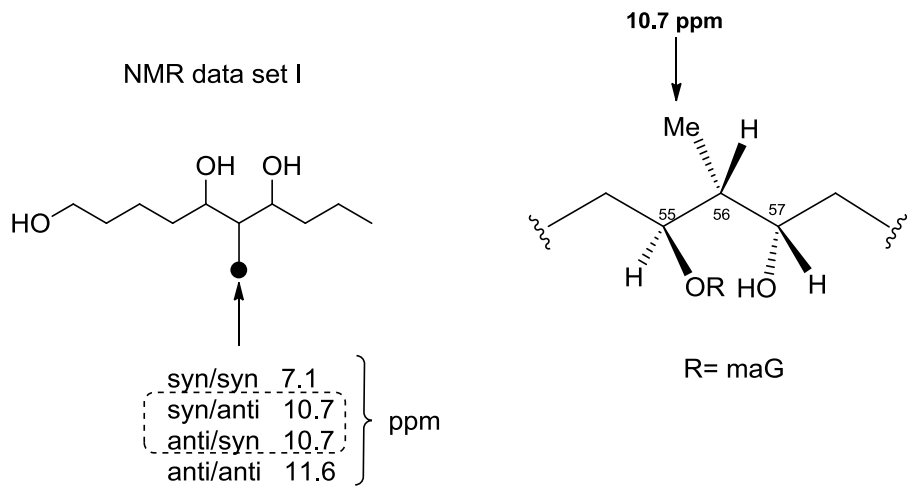


Figure S10. Bioinformatics assignments (*gar* BGC analysis) of the absolute configurations for the gargantulides polyketide aglycon (a). Comparison with the absolute configurations previously reported for gargantulide A (b)¹⁷



KR domains determining the stereochemical outcome are indicated in blue color. Chiral centers showing disagreement between the *in silico* prediction and the previously reported NMR-based structure for gargantulide A, are highlighted in red color. Undetermined chiral centers for gargantulide A in the original work, which have been now assigned by bioinformatic analysis, are highlighted in pink color.

Figure S11. Determination of the relative configuration of the C-55 to C-57 stereocluster for gargantulide B (**1**)



a) Kishi's NMR data set I for 2-methyl-1,3-diols¹⁸ (left) and chemical shift value of Me-56 (right)



$$^3J_{H55-H56} = \text{ca. } 9 \text{ Hz}$$

$$^3J_{C54-H56} = \text{ca. small}$$

$$^3J_{C57-H55} = \text{ca. small}$$

$$^3J_{Me56-H55} = \text{ca. small}$$

$$^2J_{C56-H55} = \text{ca. small}$$

$$^2J_{C55-H56} = \text{ca. large}$$

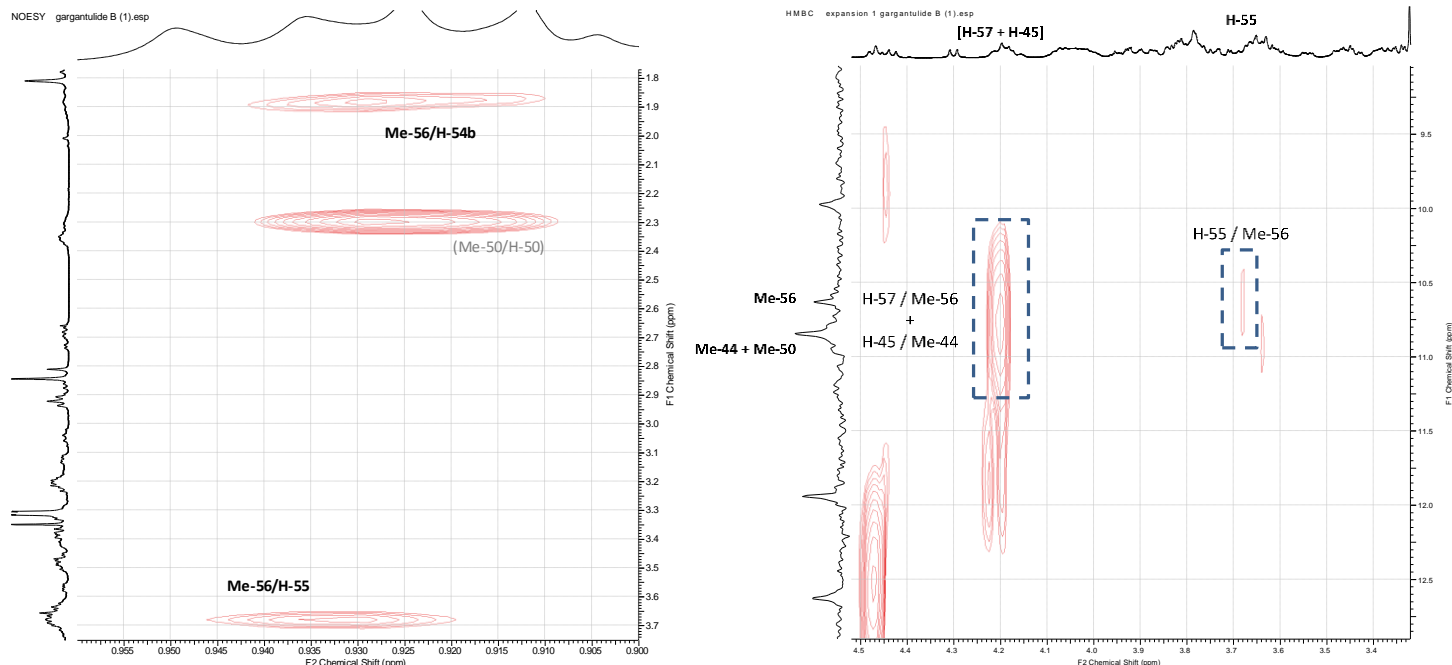
$$^3J_{H56-H57} = \text{ca. } 2 \text{ Hz}$$

$$^3J_{C55-H57} = \text{ca. small}$$

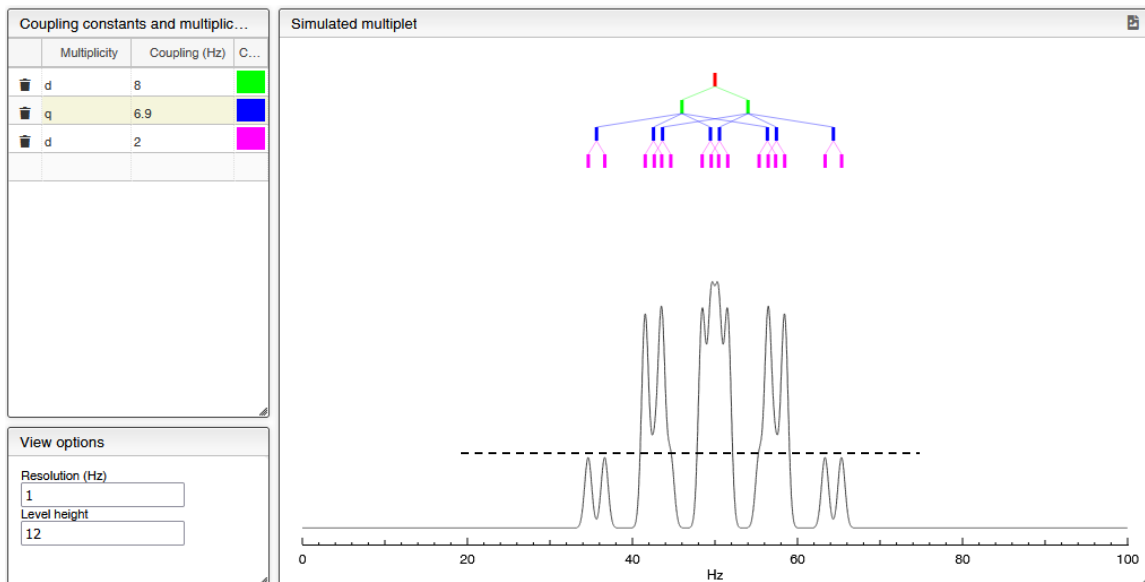
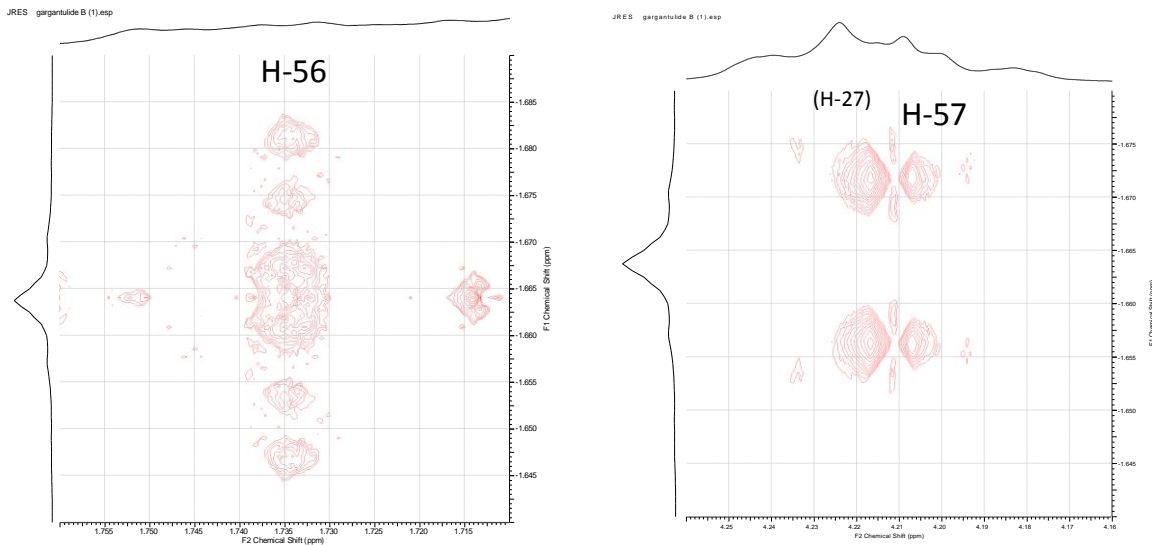
$$^3J_{C58-H56} = \text{ca. small}$$

$$^3J_{Me56-H57} = \text{ca. large}$$

b) Qualitative $^3J_{C,H}$ -based configuration analysis of the C-55 to C-57 stereocluster. Other $^2J_{C,H}$ constants are classified as “small” or “large” according to Murata’s method.¹⁹ Key NOESY correlations are also indicated (NOESY correlation Me-56/H-58 partially overlapped with other nOe cross-peaks).

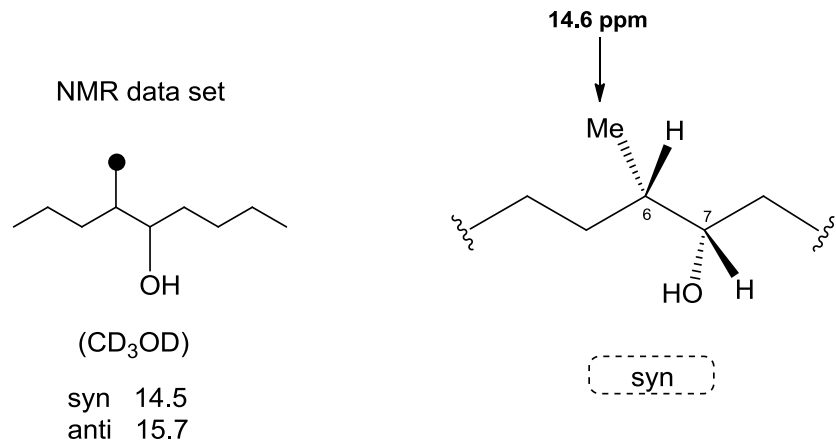


c) NOESY (left) and HMBC (right) expansion supporting the *anti/syn* configuration for C-55/C-56/C-57.



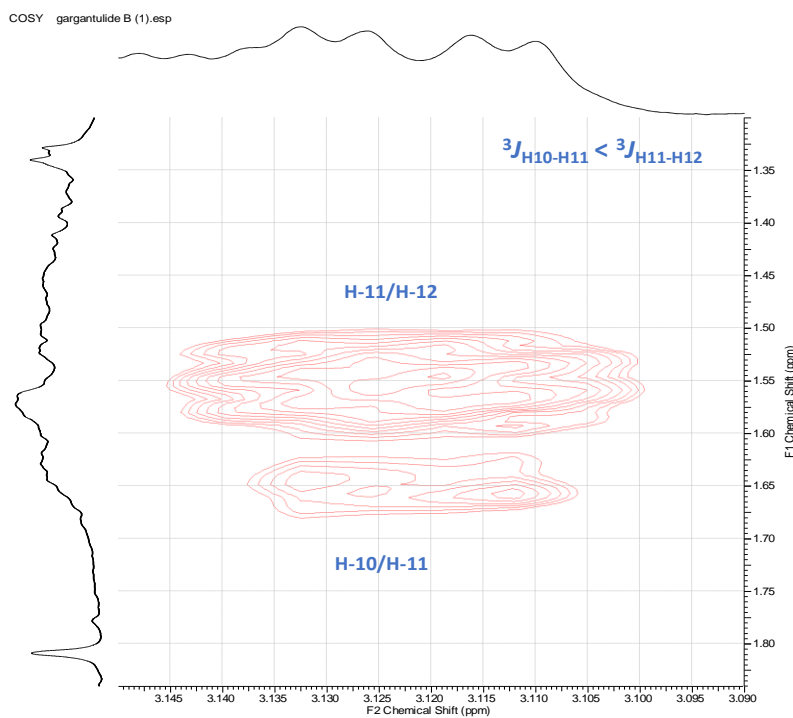
d) Expansions of the JRES spectrum of **1** showing the higher multiplicity of H-56 compared to that of H-57 (top). Multiplet simulation²⁰ for H-56 (applied values for ^1H - ^1H coupling constants are indicated) showing good fitting with the multiplicity experimentally observed (bottom).

Figure S12. Determination of the relative configuration of the C-6–C-7 stereocluster for gargantulide B (**1**)

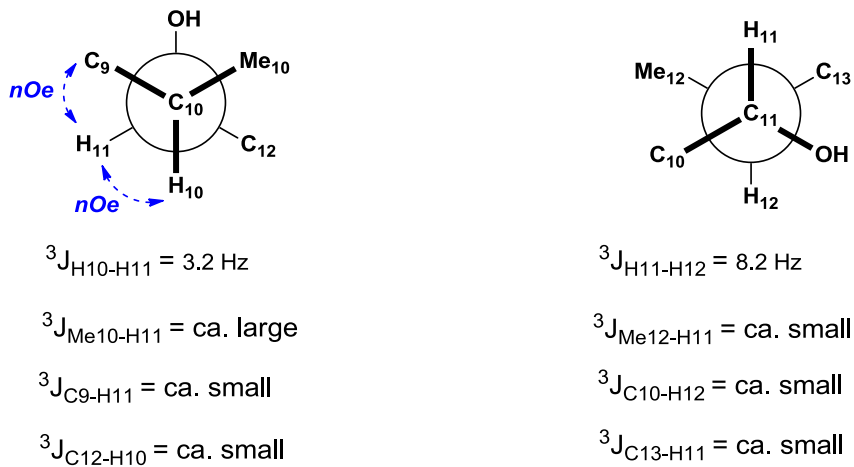


Application of Kishi's NMR data set for 4-methylnonan-5-ol isomers ²¹.

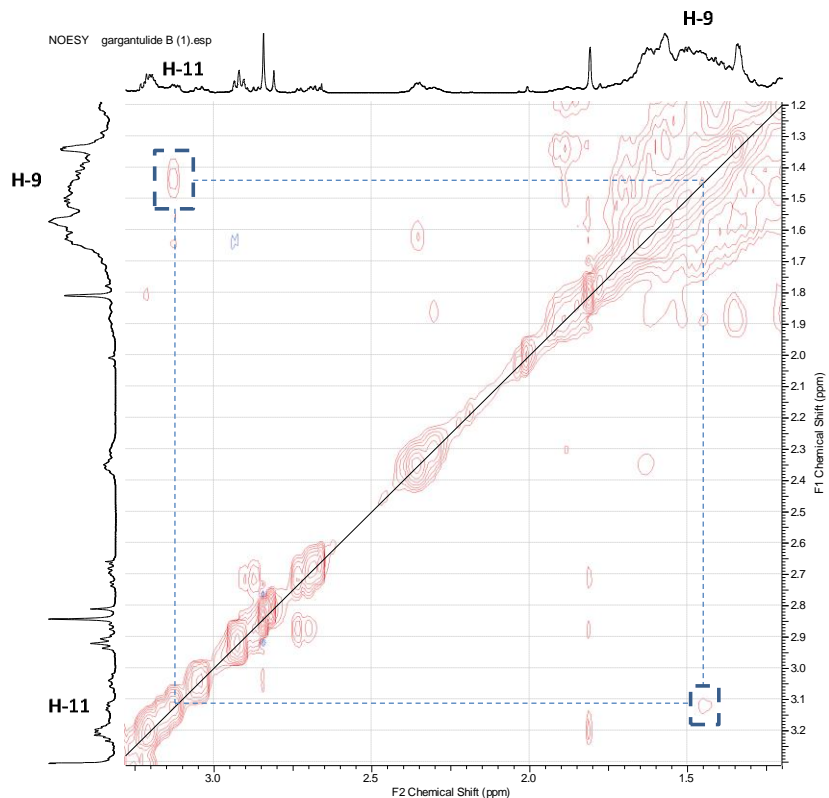
Figure S13. Determination of the relative configuration of the C-10–C-12 stereocluster for gargantulide B (**1**)



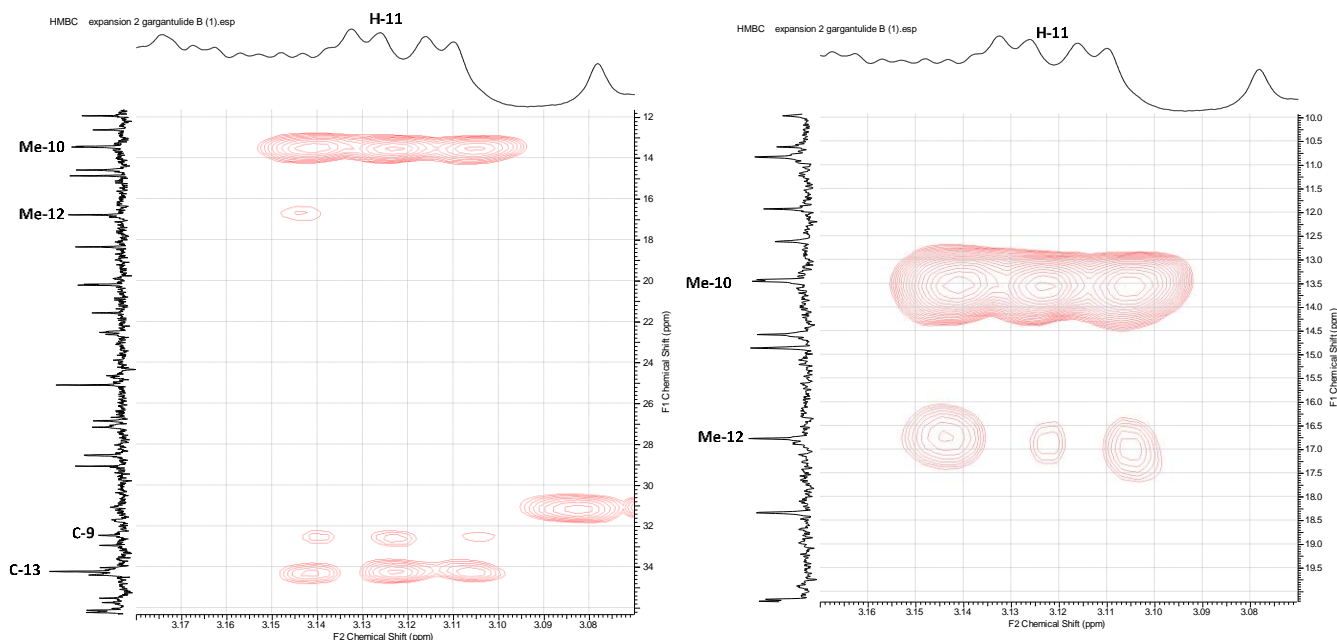
a) Key COSY correlations supporting the *syn/anti* configuration for C-10/C-11/C-12



b) Qualitative $^3J_{\text{C},\text{H}}$ -based configuration analysis of the C-10 to C-12 stereocluster. Key NOESY correlations are also indicated (although critical overlapping of proton NMR signals corresponding to Me-10 and Me-12 make impossible to distinguish the key NOESY correlation H-10/Me-12 from the genuine cross-peak H-10/Me-10, the clear absence of NOESY correlations between H-10 and both H-13 further supports the configurational proposal)



c) Key NOESY correlation supporting the *anti* configuration for C-10–C-12 stereocluster



d) HMBC correlations supporting the *anti* configuration for C-10–C-12 stereocluster

Figure S14. Determination of the relative configuration of the C-17(R)–C-18(R) stereocluster for gargantulide B (**1**)



anti relative configuration

17(R), 18(R) abs. configuration

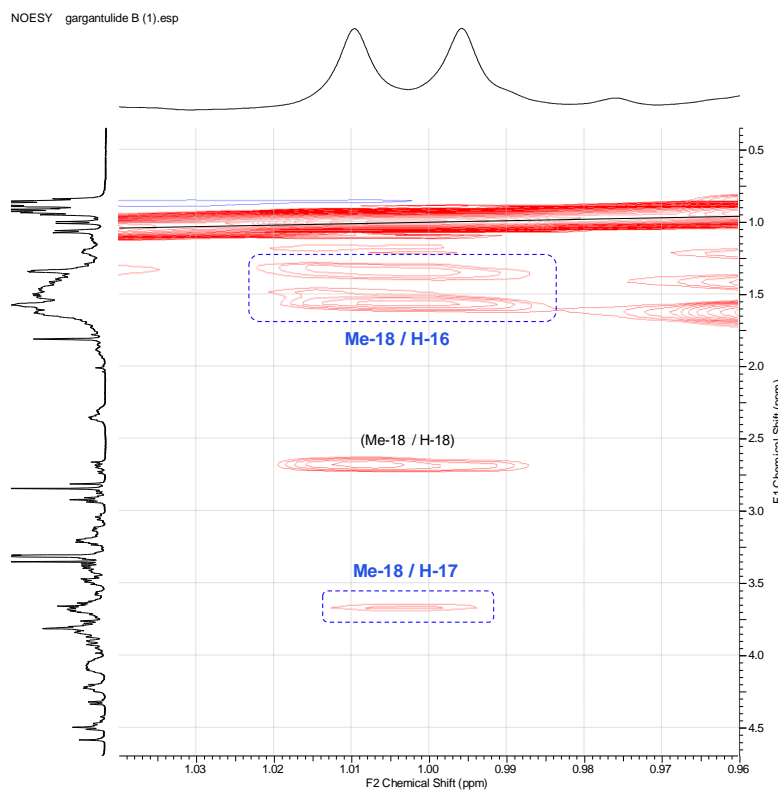
$$^3J_{H17-H18} = 8.6 \text{ Hz}$$

$$^3J_{Me18-H17} = \text{ca. small}$$

$$^3J_{C16-H18} = \text{ca. small}$$

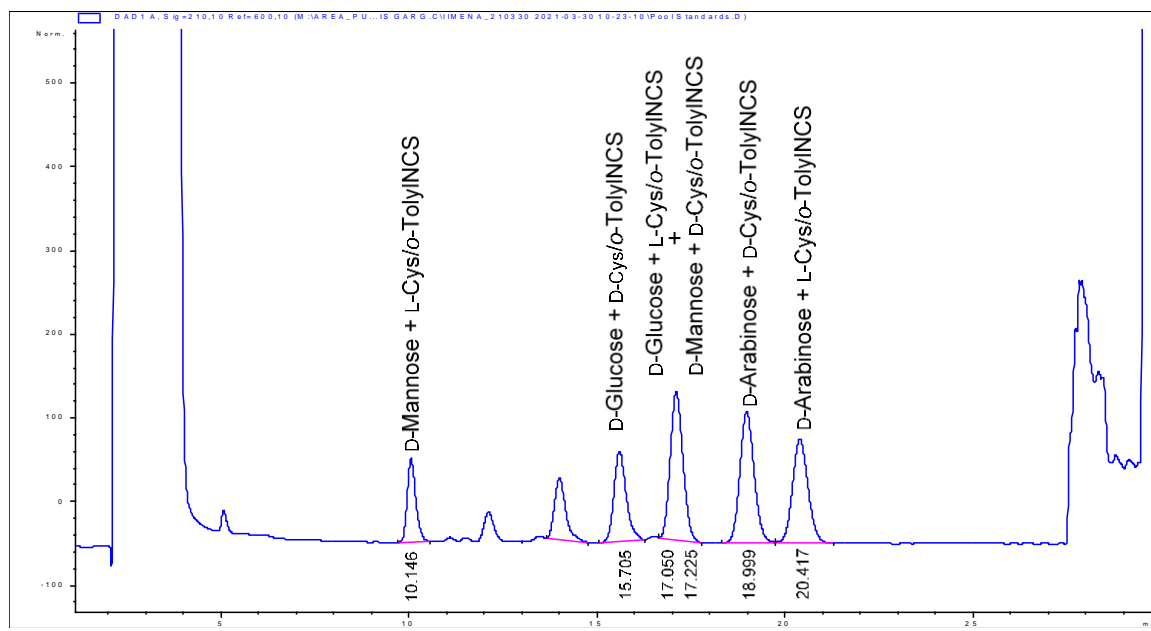
$$^3J_{C19-H17} = \text{ca. small}$$

a) Qualitative $^3J_{C,H}$ -based configuration analysis of the C-17–C-18 stereocluster

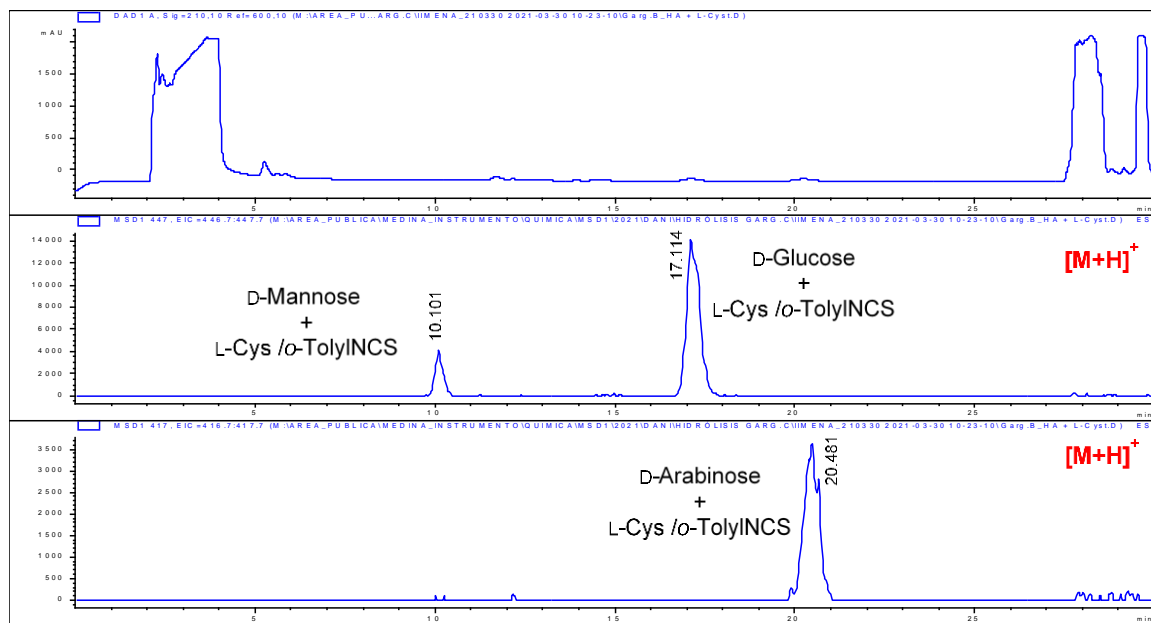


b) Key NOESY correlations supporting the anti configuration for C-17–C-18 stereocluster

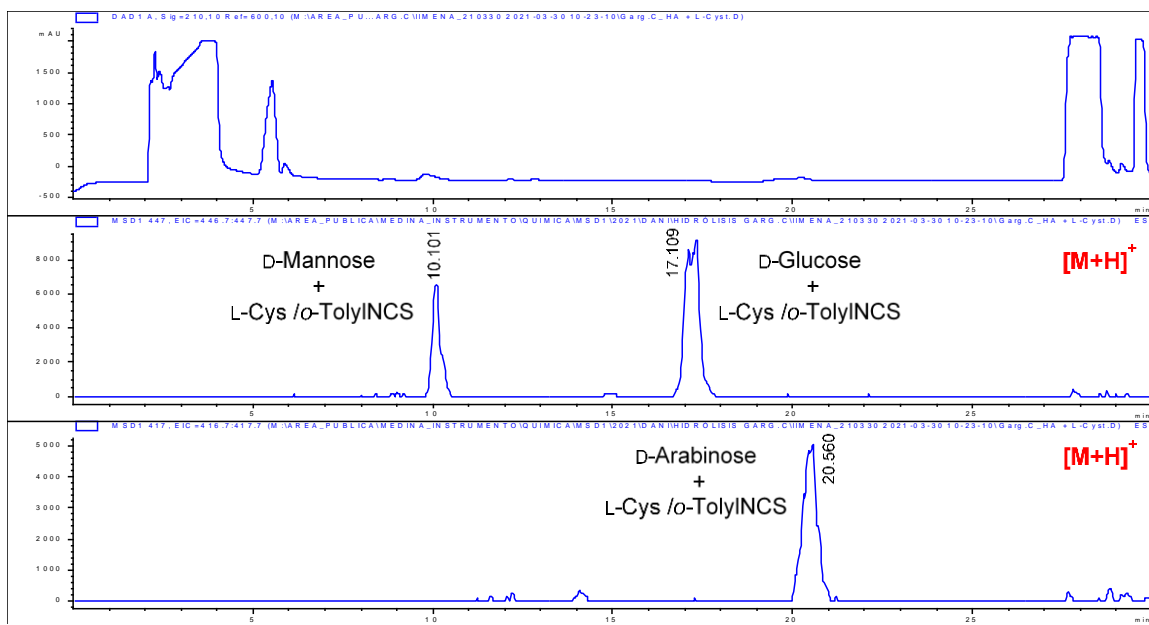
Figure S15. Determination of the absolute configuration of the non-amino sugars present in gargantulides B (**1**) and C (**2**)



a) LC-UV chromatogram of a mixture of both L- and D-cysteine methyl ester hydrochloride / *o*-tolyl isothiocyanate derivatization reactions of D-Mannose / D-Glucose / D-arabinose standard monosaccharides.



b) LC-UV and extracted-ion chromatograms (EIC) of L-cysteine methyl ester hydrochloride / *o*-tolyl isothiocyanate derivatized hydrolysate of **1** with HCl. D-Mannose, D-Glucose and D-Arabinose were found in **1**



c) LC-UV and extracted-ion chromatograms (EIC) of L-cysteine methyl ester hydrochloride / *o*-tolyl isothiocyanate derivatized hydrolysate of **2** with HCl. D-Mannose, D-Glucose and D-Arabinose were found in **2**

Table S9. Antibacterial and antifungal activities of compounds **1** and **2**.

Microbial strain	Strain number	MIC ($\mu\text{g/mL}$)					
		(1)	(2)	R	A	Am	V
<i>A. baumannii</i>	MB5973	16-32	16-32	2-4			
<i>P. aeruginosa</i>	MB5919	>128	>128		1		
<i>E. coli</i>	ATCC 25922	>128	>128		0.5-0.25		
<i>K. pneumoniae</i>	ATCC 700603	>128	>128		>16		
MRSA		4-8	2-4			2-4	
MSSA		2-4	2-4			1	
VRE		2-4	1-2			>128	
<i>A. fumigatus</i>	ATCC46645	32-64	32-64			4	
<i>C. albicans</i>	ATCC64124	>128	>128			4	

*Positive controls: R Rifampicin, A Aztreonam, Am Amphotericin B, V Vancomycin

Supplementary references

- 1 I. Pérez-Victoria, J. Martín and F. Reyes, Combined LC/UV/MS and NMR Strategies for the Dereplication of Marine Natural Products, *Planta Med.*, 2016, **82**, 857–871.
<https://www.geneious.com>, <https://www.geneious.com>.
- 2 A. T. Keatinge-Clay, A Tylosin Ketoreductase Reveals How Chirality Is Determined in Polyketides, *Chem. Biol.*, 2007, **14**, 898–908.
- 3 A. Keatinge-Clay, Crystal Structure of the Erythromycin Polyketide Synthase Dehydratase, *J. Mol. Biol.*, 2008, **384**, 941–953.
- 4 D. H. Kwan and F. Schulz, The stereochemistry of complex polyketide biosynthesis by modular polyketide synthases, *Molecules*, 2011, **16**, 6092–6115.
- 5 E. M. Musiol-Kroll and W. Wohlleben, Acyltransferases as tools for polyketide synthase engineering, *Antibiotics*, DOI:10.3390/antibiotics7030062.
- 6 R. C. Edgar, MUSCLE: A multiple sequence alignment method with reduced time and space complexity, *BMC Bioinformatics*, 2004, **5**, 1–19.
- 7 M. C. Monteiro, M. De La Cruz, J. Cantizani, C. Moreno, J. R. Tormo, E. Mellado, J. R. De Lucas, F. Asensio, V. Valiante, A. A. Brakhage, J. P. Latgé, O. Genilloud and F. Vicente, A new approach to drug discovery: High-throughput screening of microbial natural extracts against *Aspergillus fumigatus* using resazurin, *J. Biomol. Screen.*, 2012, **17**, 542–549.
- 8 J. Martín, T. S. Da Sousa, G. Crespo, S. Palomo, I. González, J. R. Tormo, M. De La Cruz, M. Anderson, R. T. Hill, F. Vicente, O. Genilloud and F. Reyes, Kocurin, the true structure of PM181104, an anti-methicillin-resistant *Staphylococcus aureus* (MRSA) thiazolyl peptide from the marine-derived bacterium *Kocuria palustris*, *Mar. Drugs*, 2013, **11**, 387–398.
- 9 L. Zhang, A. S. Ravipati, S. R. Koyyalamudi, S. C. Jeong, N. Reddy, J. Bartlett, P. T. Smith, M. de la Cruz, M. C. Monteiro, Á. Melguizo, E. Jiménez and F. Vicente, Anti-fungal and anti-bacterial activities of ethanol extracts of selected traditional Chinese medicinal herbs, *Asian Pac. J. Trop. Med.*, 2013, **6**, 673–681.
- 10 J. H. Zhang, T. D. Y. Chung and K. R. Oldenburg, A simple statistical parameter for use in evaluation and validation of high throughput screening assays, *J. Biomol. Screen.*, 1999, **4**, 67–73.
- 11 C. E. Melançon, L. Hong, J. A. White, Y. N. Liu and H. W. Liu, Characterization of TDP-4-keto-6-deoxy-D-glucose-3,4-ketosomerase from the D-mycaminose biosynthetic pathway of *Streptomyces fradiae*: In vitro activity and substrate specificity studies, *Biochemistry*, 2007, **46**, 577–590.
- 12 M. Tello, M. Rejzek, B. Wilkinson, D. M. Lawson and R. A. Field, Tyl1a, a TDP-6-deoxy-D-xylo-4-hexulose 3,4-isomerase from *Streptomyces fradiae*: Structure prediction, mutagenesis and solvent isotope incorporation experiments to investigate reaction mechanism, *ChemBioChem*, 2008, **9**, 1295–1302.
- 13 H. Chen, S. M. Yeung, N. L. S. Que, T. Müller, R. R. Schmidt and H. W. Liu, Expression, purification, and characterization of Ty1B, an aminotransferase involved in the biosynthesis of mycaminose [9], *J. Am. Chem. Soc.*, 1999, **121**, 7166–7167.
- 14 H. Chen, H. Yamase, K. Murakami, C. wei Chang, L. Zhao, Z. Zhao and H. wen Liu, Expression, purification, and characterization of two N,N-dimethyltransferases, Ty1M1 and DesVI, involved in the biosynthesis of mycaminose and desosamine, *Biochemistry*, 2002, **41**, 9165–9183.
- 15 L. Hong, Z. Zhao, C. E. Melançon, H. Zhang and H. W. Liu, In vitro characterization of the enzymes involved in TDP-D-forosamine biosynthesis in the spinosyn pathway of *Saccharopolyspora spinosa*, *J. Am. Chem. Soc.*, 2008, **130**, 4954–4967.
- 16 J. R. Rho, G. Subramaniam, H. Choi, E. H. Kim, S. P. Ng, K. Yoganathan, S. Ng, A. D. Buss, M. S. Butler and W. H. Gerwick, Gargantulide A, a complex 52-membered macrolactone showing antibacterial activity from *streptomyces* sp., *Org. Lett.*, 2015, **17**, 1377–1380.
- 17 Y. Kobayashi, C.-H. Tan and Y. Kishi, Toward Creation of a Universal NMR Database for Stereochemical Assignment: Complete Structure of the Desertomycin/Oasomycin Class of Natural Products, *J. Am. Chem. Soc.*, 2001, **123**, 2076–2078.
- 18 N. Matsumori, D. Kaneno, M. Murata, H. Nakamura and K. Tachibana, Stereochemical

- Determination of Acyclic Structures Based on Carbon–Proton Spin-Coupling Constants. A Method of Configuration Analysis for Natural Products, *J. Org. Chem.*, 1999, **64**, 866–876.
20 http://www.cheminfo.org/Spectra/NMR/Tools/Multiplet_simulator/index.html, .
21 K. Takada, Y. Imae, Y. Ise, S. Ohtsuka, A. Ito, S. Okada, M. Yoshida and S. Matsunaga, Yakushinamides, Polyoxygenated Fatty Acid Amides That Inhibit HDACs and SIRTs, from the Marine Sponge *Theonella swinhoei*, *J. Nat. Prod.*, 2016, **79**, 2384–2390.